POLYTECHNIQUE MONTRÉAL

affiliée à l'Université de Montréal

Development of a New Building Integrated PV-Thermal Solar Module

AUSTIN SAMSON MYLES

Département de génie métallurgique

Thèse présentée en vue de l'obtention du diplôme de *Philosophiae Doctor*

Génie métallurgique

Août 2019

POLYTECHNIQUE MONTRÉAL

affiliée à l'Université de Montréal

Cette thèse intitulée :

Development of a New Building Integrated PV-Thermal Solar Module

présentée par **Austin Samson MYLES**

en vue de l'obtention du diplôme de *Philosophiae Doctor*

a été dûment acceptée par le jury d'examen constitué de :

Sylvain TURENNE, président

Oumarou SAVADOGO, membre et directeur de recherche

Mureithi NJUKI, membre

Kamal AL-HADDAD, membre externe

DEDICATION

My humble effort I dedicate to my late parents who provided me good basic education, values and upbringing in difficult times to achieve success in life. I am fulfilling their dreams to go for higher education.

ACKNOWLEDGEMENTS

Firstly, I would like to express my sincere gratitude to my advisor Prof. Oumarou Savadogo for his continuous support and motivation during my Ph.D. study and related research. His guidance was invaluable for my research, fabrication, BIPV-T prototype testing, and authoring this thesis. I could not have imagined having a better advisor and mentor for my Ph.D. study. Prof. Savadogo made himself available even on weekends and holidays for any clarifications I needed.

I am also very grateful to Prof. Sylvain Turenne, Professor, Polytechnic Montreal, President of Jury; Kamal Haddad, Ph.D., Professor, ETS, External Member of Jury; and Jean Koclas, Professor, Polytechnic Montreal, Member of Jury for their constructive advice, insightful discussions and suggestions during my pre-doctoral presentation.

I would like to express my special appreciation to Mr. Ajoy Das, Owner of the Centennial Group of companies, for sponsoring my PhD study at Polytechnic, and providing the photovoltaic panels for fabricating the BIPV-T module and the outdoor testing equipment. He also paid for the fabrication and any required travel.

Besides my advisor and sponsor, I would like to thank my fellow colleagues Daniel Kalufya Mukalayi, Pengyu Chen, Ulrich Compaore, Fabrice Kabore and Diego Garcia who helped me to set up the outdoor test facility and test the BIPV-T prototype on many sunny days. My gratitude to my newest colleague Mina Dadvand for making a 3D autocad drawing for my project.

My sincere thanks also go to Kentaro, Research Associate in my department, for helping me procure raw material, software, and other equipment. I also thank him for getting approval for suitable indoor laboratory space and outdoor sunny space for testing.

I also thank Ms. Veronique Delisle, Research Officer at Canmet Energy, Varennes, for providing me support in using TRNSYS software and sending me clarifications when required.

I will forever be thankful to my former colleague Prakash Magal from Bangalore India who helped me fabricate my second working model – the improved BIPV-T module.

RÉSUMÉ

Les caractéristiques des modules solaires PV sont déterminées dans les conditions normales d'essai (STC) avec une température ambiante de 25°C. Toutefois, dans les conditions de fonctionnement, la température normale d'opération de la cellule (NOCT) est généralement supérieure de 20°C au-dessus de cette température ambiante. Ceci fait que dans les conditions réelles le module délivre une puissance inférieure à sa valeur nominale. Cette diminution est généralement de - 0,4% par °C au-dessus des conditions STC. Dans les climats chauds, les températures des cellules solaires sont encore plus élevées, réduisant ainsi plus significativement l'énergie électrique de sortie des modules PV.

Lorsqu'un module photovoltaïque est en contact direct avec le toit ou le mur d'un bâtiment, le refroidissement naturel par son revêtement arrière est impossible; ce qui engendre une augmentation de sa température. Dans ce cas, lorsque la température ambiante est de 25°C, la température d'opération de la cellule est de 45°C (NOCT) et le fait que les cellules soient en contact direct avec le toit ou le mur fait de plus augmenter leur température de 18°C. Ainsi la température totale de la cellule est : 45 +18 = 63°C. Dans les climats plus chauds, la température de la cellule sera encore plus élevée, réduisant sensiblement la puissance de sortie.

Dans le passé, les chercheurs ont essayé de nombreuses matrices différentes pour refroidir les modules PV. Malheureusement, chacune de ces configurations provoque des températures non uniformes par cellule à travers le module PV, ce qui permet d'obtenir moins d'avantages sur la performance du module. Comme l'eau traverse le tuyau de refroidissement, il ramasse la chaleur cellule par cellule. Par conséquent, la température des cellules près de l'entrée est inférieure à celle des cellules près de la sortie du tuyau.de refroidissement. La répartition précise de la chaleur dépend de la configuration du tuyau de refroidissement. Des températures plus élevées à une cellule conduisent à la fois à une diminution de la tension à la cellule et à une augmentation beaucoup plus faible du courant généré à cette cellule. Ceci est dû au fait que toutes les cellules sont connectées en série; et de ce fait, la cellule ayant la température la plus basse détermine le courant de sortie final du module. Cela réduit donc l'efficacité énergétique de l'ensemble du module solaire.

Le nouveau concept de refroidissement discuté ici vise à maximiser la puissance de sortie d'un panneau PV en refroidissant uniformément les cellules. La chaleur extraite sous forme d'eau

chaude est limitée au refroidissement par passage unique dans chaque cellule solaire, car la recirculation augmentera la température des cellules solaires.

Le concept de photovoltaïque intégré au bâtiment (BIPV-T) thermique (PV-T) n'est pas nouveau, mais ces dernières années ses applications pratiques deviennent populaires. Les modules cristallins demeurent la technologie photovoltaïque dominante, représentant plus de 90% de la production et de l'utilisation dans le monde entier. Malgré une augmentation massive de la capacité de production, les prix des modules photovoltaïques pour les consommateurs demeurent élevés. De plus, au cours des 40 dernières années, l'efficacité commerciale des cellules photovoltaïques cristallines les plus largement produites a augmenté à un rythme lent, passant de 13% en 1979 à 22% en 2018, soit seulement 0,23% par an. Au cours des 10 dernières années, même avec le meilleur effort de l'industrie photovoltaïque, l'efficacité des cellules polycristallines a augmenté seulement de 4%.

Une exigence essentielle pour l'efficacité PV est que les cellules dans un module se comportent uniformément. L'industrie photovoltaïque passe par de grandes longueurs pour assurer ceci:

1. Premièrement, les cellules solaires sont triées pour collecter ceux générant la même sortie de courant dans des conditions normales d'essai;
2. en outre, après que les cellules sont connectées en série pour un module, elles sont testées pour l'uniformité utilisant une machine d'électro-luminescence en forçant le courant nominal par le circuit. Toutes les cellules dépareillées, qui peuvent être dues à des fissures ou à une mauvaise soudure, sont fixées avant que les cellules solaires soient stratifiées au verre trempé;
3. Enfin, un autre test d'électro-luminescence est effectué après laminage.

Une telle validation stricte est exigée pour assurer le fonctionnement approprié de champ puisque les cellules solaires défectueuses générant le courant le plus bas peuvent surchauffer et délaminer en absorbant le courant généré par d'autres cellules dans un module ou dans un champs de modules connectés en série. Ces types de défaillance dans un système installé sont très coûteux à remplacer ou à réparer.

La température est un autre facteur impactant l'efficacité du PV. Il est bien connu que la puissance de sortie des modules PV diminue de façon spectaculaire à mesure que sa température augmente.

Les modules solaires évalués à 25°C fonctionnent à des températures beaucoup plus élevées dans les conditions réelles du terrain; par conséquent, il y a une baisse substantielle de la puissance de sortie @-0,46%/K (fiche technique du module SolarTech)

De nombreux établissements d'enseignement et industries ont conçu des configurations de circuits de refroidissement de l'eau pour les modules photovoltaïques pour augmenter l'efficacité par unité de surface du module. Cependant, ces conceptions entrainent des variations de température à travers un module PV induisant ainsi des performances inégales pour les cellules. Plus précisément, dans les systèmes BIPV-T réels, comme l'eau traverse le module solaire dans les configurations existantes de tuyaux d'eau froide, il capte la chaleur. Les cellules ne sont pas refroidies uniformément.

Par conséquent, les cellules solaires près de l'entrée sont les plus froides, tandis que celles près de la sortie ont une température plus élevée. Les cellules plus chaudes perdent de la tension de façon significative et génèrent ont une très faible augmentation de leur courant. Comme les cellules sont connectées en série dans un module, la tension d'un module est limitée par le nombre de cellules à la température la plus élevée, réduisant ainsi l'efficacité globale du module et la puissance dans la plage de 8 -20% en fonction de la valeur de la température ambiante. Ceci indique qu'il est très important de refroidir le module PV efficacement pour garder ses performances. Pour surmonter ce problème, cette étudie suggère un nouveau circuit de refroidissement de l'eau pour les modules BIPV-T pour assurer un refroidissement individuel uniforme de toutes les cellules solaires dans un module.

Les objectifs de cette étude sont les suivants:

- Développer un nouveau module BIPV-T dans lequel chaque cellule d'un module PV est refroidie uniformément;
- Effectuer des études de simulation sur l'efficacité thermique et électrique d'un tel module BIPV-T;
- Concevoir et fabriquer un prototype du module BIPV-T qui respecte les normes de l'industrie photovoltaïque;
- Tester et valider les performances électriques et thermiques.

Ce travail de recherche développe le concept et la fabrication d'un prototype d'un nouveau module solaire photovoltaïque-thermique (BIPV-T) intégré au bâtiment (collecteur). Le concept propose le refroidissement uniforme individuel de chaque cellule solaire dans un module avec de l'eau pour améliorer les performances des modules photovoltaïques (PV). Une étude de simulation a été réalisée à l'aide du logiciel TRNSYS qui montre une amélioration jusqu'à 11% par rapport au module sans refroidissement et une amélioration de plus de 4% des performances si des cellules individuelles pouvaient être refroidies uniformément par rapport à un refroidissement non uniforme. Sur la base de l'analyse de nos résultats de simulation, un nouveau concept de fabrication de tuyauterie de refroidissement (échangeur de chaleur) est proposé. Ceci améliorera la performance par rapport au refroidissement en série des modules BIPV-T utilisé conventionnellement. Cela contribuera à ouvrir une nouvelle conception de la technologie photovoltaïque basée sur le module BIPV-T proposé.

Un module photovoltaïque-thermique pour l'intégration du bâtiment BIPV-T a été conçu avec un nouveau circuit de refroidissement pour un refroidissement uniforme des cellules solaires. L'analyse TRNSYS révèle un gain de 4,35% d'amélioration de l'efficacité par rapport au module sans refroidissement et jusqu'à 10,58% d'amélioration de l'efficacité électrique du module PV si refroidi uniformément. Le nouveau module BIPV-T a fourni une efficacité thermique supplémentaire de 48,3% en collectant de la chaleur de l'eau de refroidissement.

Dans cette étude, la conception, la fabrication et le test du modèle réel d'un module photovoltaïque de 140 W, 36 cellules avec un nouveau circuit de refroidissement de tuyau sont discutés. L'évaluation des performances du module a l'intérieur et a l'extérieur est presentée. Les essais à l'intérieur ont montré une uniformité de température de 2,1°C tandis que les performances à l'extérieure ont, montré une uniformité de 6 à 8°C due au refroidissement des cellules solaires individuelles. Une amélioration de plus de 4% dans les performances électriques du module PV a été observée. Un second prototype amélioré a obtenu une uniformité de 1.3°C même dans les essais extérieurs.

Une étude complémentaire de ce travail indique une amélioration de la conception de la nouvelle configuration des tuyaux de refroidissement pour le module BIPV-T. L'idée est de réduire sa hauteur et d'améliorer le transfert de chaleur entre les cellules solaires et le tuyau d'eau de refroidissement. Le nouveau design de refroidissement de l'eau est basé sur le refroidissement

indépendant des cellules solaires individuelles dans un module PV. Un modèle BIPV-T utilisant quatre cellules solaires à haut rendement a été fabriqué et testé à l'extérieur en plein soleil naturel. Même l'efficacité des cellules solaires commerciales les plus efficaces utilisées pour ce modèle diminue à des conditions de fonctionnement élevées. Le résultat montre une amélioration de 8.8% de la puissance de sortie par rapport à la puissance observée dans l'état de stagnation et l'efficacité électrique a augmenté de 0,92% lorsqu'il est refroidi par circulation d'eau. L'efficacité thermique supplémentaire de 57,4% a été obtenue en gain de chaleur par l'eau de refroidissement. L'amélioration de la conception de la nouvelle configuration de tuyauterie de refroidissement réduit le coût par un facteur de six, ce qui le rend attrayant pour la production commerciale.

ABSTRACT

This research work develops the concept and a prototype of a novel Building-Integrated Photovoltaic-Thermal (BIPV-T) solar module (collector). The concept proposes water cooling individual solar cells in a module uniformly to improve performance of photovoltaic (PV) modules. A simulation study was conducted using TRNSYS software that shows upto 11% improvement over module without cooling and 4.3% improvement in performance if individual cells could be cooled uniformly. Based on the analysis of our simulation results, a novel concept of a cooling pipe layout (heat exchanger) is proposed. This will improve the performance over conventionally used series cooling of solar cells in BIPV-T modules. This will help to open a new design of photovoltaic technology based on the proposed BIPV-T module.

A photovoltaic-thermal module for building integration BIPV-T was design with a novel cooling pipe circuit for uniform cooling of solar cells. The TRNSYS analysis reveals upto 4.35% efficiency improvement over module without cooling and upto 10.58% improvement in PV module electrical efficiency if cooled uniformly. The new BIPV-T module delivered additional 48.3% thermal efficiency by collecting heat in cooling water.

In this study design, fabrication and testing of actual field model of a 140W, 36 cell photovoltaic module with novel cooling pipe circuit is discussed and performance evaluated in indoor and outdoor condition has been presented. The indoor testing showed 2.1°C temperature uniformity while outdoor performance shows 6 to 8°C uniformity in cooling of individual solar cells. An improvement upto 5.7% in electrical performance of PV module was observed. Further improved second prototype achieved 1.3°C uniformity even in outdoor testing.

A subsequent study discusses an improvement in design of novel cooling pipe configuration for BIPV-T module. The idea is to reduce its height and improve heat transfer between the solar cells and the cooling water pipe. The novel water-cooling design is based on independent cooling of individual solar cells in a PV module. A BIPV-T model using four high efficiency solar cells was fabricated and tested outdoor in natural sunlight. Even the efficiency of the most efficient commercial solar cells used for this model drops at elevated operating conditions. The result shows 8.8% improvement in power output over power observed in stagnation condition and electrical efficiency increased by 0.92% when cooled by water circulation. Additional thermal efficiency

upto 57.4% was through heat gain in cooling water. The improvement in design of novel cooling pipe configuration reduces the cost by a factor of six, making it attractive for commercial production.

TABLE OF CONTENTS

LIST OF TABLES

LIST OF FIGURES

LIST OF SYMBOLS AND ABBREVIATIONS

β - [degrees] The slope of the collector surface.

η - [0..1] Efficiency.

θ - [degrees] The angle of incidence.

ρ - [0..1] The ground reflectance.

$\tau\alpha$ - [0..1] The transmittance-absorptance product for the solar collector.

ε - [0..1] The emissivity of the top surface of the collector (PV surface).

σ - [constant] The Stefan-Boltzmann constant.

λ- [m] The thickness of the absorber plate.

Area - [m^2] The area (top) of the solar collector; this can be either gross area or net area but should be consistent with the provided loss coefficients and PV power conversion coefficients.

b_0 - [-] The incidence angle modifier multiplier.

Cp - [kJ/kg.K] The specific heat of the fluid flowing through the PV-T collector.

C_B - [kJ/hr.K] The conductance between the absorber plate and the bonded tube.

D_{tube} - [m] The diameter of the tubes.

F_R - [-] The collector heat removal factor.

G - [kJ/hr.m^2] The total horizontal solar radiation.

G_b - [kJ/hr.m^2] The beam solar radiation.

G_d - [kJ/hr.m^2] The ground reflected solar radiation.

Gref – The solar radiation at reference condition (1000W/m^2 for PV cells and modules).

G_t - [kJ/hr.m^2] The total solar radiation (beam + diffuse) incident upon the collector surface.

h_{fluid} - [-] The internal fluid heat transfer coefficient.

h_{inner} - [kJ/hr.m^2.K] The heat transfer coefficient from the back of the collector to the air.

h_{outer} - [kJ/hr.m^2.K] The heat transfer coefficient from the top of the collector (PV surface) to the ambient air.

h_{rad} - [kJ/hr.m^2.K] The radiative heat transfer coefficient from the top of the collector (PV surface) to the sky.

IAM - [-] The incidence angle modifier.

K - [kJ/hr.m.K] The thermal conductivity of the plate material.

$K_{\tau\alpha}$ – Incidence angle modifier coefficient.

L - [m] The length of the collector along the flow direction.

m - [kg/hr] The flow rate of fluid through the solar collector.

N_{tubes} - [-] The number of identical tubes carrying fluid through the collector.

Power - [kJ/hr] The rate at which electrical energy is produced by the PV cells.

$Q_{loss,top,conv}$ - [kJ/hr] The rate at which energy is lost to the ambient through convection off the top of the collector.

$Q_{loss,top,rad}$ - [kJ/hr] The rate at which energy is lost to the sky through radiation off the top of the collector.

$Q_{loss,back}$ - [kJ/hr] The rate at which energy is lost to the ambient through the back of the collector.

Q_{fluid} - [kJ/hr] The rate at which energy is added to the flow stream by the collector, this term includes the energy that is also lost from the fluid stream through the back of the collector.

$Q_{absorbed}$ - [kJ/hr] The net rate at which energy is absorbed by the collector plate (does not include PV power production).

Q_u - [kJ/hr] The rate at which energy is added to the flow stream by the collector.

q'_{fin} - [kJ/hr.m] The heat transfer to the fin base per unit length of collector.

q'_{fluid} - [kJ/hr.m] The heat transfer to the fluid stream per unit length of collector.

q'_u - [kJ/hr.m] The heat transfer to the fluid stream per unit length of collector.

R_t - [h.m^2.K/kJ] The resistance to heat transfer from the PV cells to the absorber plate.

R_b - [h.m^2.K/kJ] The resistance to heat transfer from the absorber through the back of the collector.

R_1 - [h.m^2.K/kJ] The resistance to heat transfer provided by the material between the PV cells and the absorber.

R_2 - [h.m^2.K/kJ] The resistance to heat transfer provided by the material between the absorber plate and the back surface of the collector.

S - [kJ/hr] The net absorbed solar radiation (total absorbed PV power production).

T_{abs} - [°C] The absorber plate temperature.

T_{amb} - [°C] The ambient temperature for convective losses from the top surface.

T_{back} - [°C] The environment temperature for convective losses from the bottom surface.

T_{fluid} - [°C] The bulk temperature of the fluid flowing through the solar collector.

$T_{fluid,in}$ - [°C] The temperature of the fluid flowing into the solar collector.

$T_{fluid,out}$ - [°C] The temperature of the fluid flowing out of the solar collector.

T_{fluid} - [°C] The local fluid temperature.

T_{PV} - [°C] The PV cell temperature.

T_{sky} - [°C] The sky temperature for long-wave radiation calculations.

$\overline{T}$ - [°C] The mean temperature.

W - [m] The width (x-direction) between adjacent fluid tubes in the collector.

Width - [m] The width of the collector.

$X_{Cell\ Temp}$ - [1/°C] The multiplier for the PV cell efficiency as a function of the cell temperature.

X_{NS} - [-] The multiplier to account for collectors connected in series (thermally).

$X_{Radiation}$ - [h.m^2/kJ] The multiplier for the PV cell efficiency as a function of the incident radiation.

Y - [-] A variable indicating the direction of flow through the collector (y=L is the collector outlet).

Subscripts:

B - beam radiation

D - diffuse radiation

G - ground diffuse

G - radiation

H - total horizontal

N - normal incidence

nominal - refers to the reference conditions

PV - photovoltaic

S - sky diffuse

T_{total} - (beam + diffuse)

Abbreviations:

ASHRAE American Society of Heating, Refrigerating and Air-Conditioning Engineers

BIPV Building-integrated photovoltaics

BIPV-T Building-integrated photovoltaics with thermal energy recovery

IEC International Electrotechnical Commission

I-V Current-Voltage

NIST National Institute of Standards and Technology

NOCT Normal Operating Cell Temperature

INOCT Installed Normal Operating Cell Temperature

pc-Si Polycrystalline silicon

I-V Current-Voltage

PV Photovoltaic

PV-T Photovoltaic with thermal energy recovery

SNL Sandia National Laboratories

STC Standard Testing Condition

TESS Thermal Energy System Specialists

TRNSYS Transient System Simulation Program

LIST OF APPENDICES

CHAPTER 1 INTRODUCTION

Solar energy can be converted through two technologies. The thermal conversion which allows solar heat to thermal energy. The photovoltaic (PV) technology which permits the direct conversion of solar light to electricity. The thermal conversion consists of solar collector, solar water heater and thermal heat exchangers. The thermal efficiency

$$\eta_{\mathrm{TH}} = \frac{\dot{m} C_p (T_{\mathrm{o}} - T_{\mathrm{i}})}{G_T A_c} \quad (1)$$

Where, G_T is the global irradiance on a collector aperture kW/m^2 or kJ/(h·m^2), $\dot{m}$ is mass flow rate of fluid in lit/hr, C_p is specific heat of water 1calories/gram/°C or 4.1813 kJ/(kg.K), T_{o} is the outlet temperature of fluid in °C or K, T_i is the inlet temperature of fluid in °C or K and A_c is solar collector area in m^2.

The PV conversion is the utilisation of semiconductor based on p-n junction. The efficiency of PV module is given as

$$\eta_{\mathrm{PV}} = \frac{IV}{G_T A_c} \quad (2)$$

Where, I is the output current, V the output voltage and A_c is the aperture area of the solar module.

The PV system is very sensitive to the temperature. Its performance decreases when temperature increases. This decrease of the performance is related to the production of heat. Accordingly, the PV module production can be significantly affected by the ambient temperature where it is installed.

With the significant progress in the utilization of PV modules worldwide, the installation capacity will rise from 3 GWp in 2010 to 22 GWp in 2020. It is, therefore, important to develop

1. Cooling system to decrease panel operating temperature.
2. To recover heat from PV module for some uses for example domestic hot water supply.

PV modules are rated under Standard Test Conditions (STC) with an ambient 25°C solar cell temperature. In operating conditions however, the Normal Operating Cell Temperature (NOCT) is usually greater than 20°C above this ambient temperature so that the module delivers a lower power

than its rating – usually ~0.4% per °C above STC. In hot climates, solar cell temperatures are even higher, thereby decreasing the output electrical energy of PV modules further.

When a PV module is flush with the roof or wall of a building, its natural cooling from back of PV module is impeded, raising the temperature further: when the ambient temperature is 25°C, the solar cell temperature will increase to 45°C (NOCT) + 18°C = 63°C. In warmer climates, the cell temperature will be even higher, reducing the power output substantially.

In the past, researchers have tried many different matrixes for cooling PV modules**.** Unfortunately, each of these configurations causes non-uniform cell temperatures across the module thereby achieving less benefit. As the water traverses the cooling pipe, it picks up heat; consequently, the temperature of cells near the inlet is lower than that of cells near the exit of the pipe. The precise heat distribution depends on the cooling pipe configuration. Higher temperatures at a cell lead both to a decrease in voltage at the cell and a much smaller increase in the current generated at that cell; since all cells are connected in series the cell at the lowest temperature determines the final output current for the module. This consequently reduces the power efficiency of the entire solar module.

The concept of Building-Integrated Photovoltaics-Thermal (BIPV-T) and Photovoltaic-Thermal (PV-T) is not new [1], but in recent years its practical applications are becoming popular. Crystalline modules remain to be the dominant PV technology, accounting for over 90% of the worldwide production and usage. Despite a massive increase in production capacity, prices of photovoltaic modules for consumers remain high. Moreover, in the last 40 years, the commercial efficiency of most widely produced crystalline PV cells has increased at a slow pace from 13% in 1979 to 22% in 2018, a mere 0.23% per year.

A critical requirement for PV efficiency is that cells in a module behave uniformly. The PV industry goes through great lengths to ensure this:

1. Firstly, solar cells are sorted to collect those generating the same current output under standard test conditions.
2. Furthermore, after the cells are connected in series for a module, they are tested for uniformity using an electro-luminescence machine by forcing rated current through the circuit. Any mismatched cells, which may be due to cracks or poor soldering, are fixed before the solar cells are laminated to the tempered glass.

3. Finally, another electro-luminescence test is performed after lamination.

Such stringent validation is required to ensure proper field operation since faulty solar cells generating the lowest current can overheat and delaminate by absorbing the current generated by other cells in a module or in an array of series-connected modules. Such kinds of failure in an installed system are very expensive to replace or repair.

Temperature is another factor impacting PV efficiency. It is well known that the power output of PV modules decreases dramatically as its temperature rises. Solar modules rated at 25°C operate at much higher temperatures in actual field conditions; consequently, there is a substantial drop in power output @-0.46%/K (SolarTech Module datasheet).

Numerous educational institutions and industries have designed configurations of water-cooling circuits for PV modules to increase efficiency per unit area of module. However, these designs result in temperature variations across a PV module thereby inducing uneven cell performance. Specifically, in the actual BIPV-T systems, as the water traverses the solar module in existing cool-water-pipe configurations, it picks up heat. The cells are not cooled uniformly. Consequently, solar cells near the inlet are the coolest, while those near the outlet have a higher temperature. Warmer cells lose voltage dramatically and generate little high current; but since cells are connected in series in a module, its voltage is limited by the number of cells at the highest temperature, thereby reducing the overall module efficiency and power in the range of 8-20% depending of the value of the ambient temperature. This indicates it is very important to cool the PV module efficiently to keep its performances. To overcome this problem, this study investigates a new water-cooling circuit for BIPV-T modules to ensure uniform cooling of all solar cells in a module.

The objectives of this study are to:

- Develop a new BIPV-T module in which each cell of a PV module is cooled uniformly;
- Conduct simulation studies on the thermal and electrical efficiency of a such BIPV-T module;
- Design and fabricate a prototype of the BIPV-T module which respects the PV industry norms;
- Test and validate the electrical and thermal performance.

CHAPTER 2 REVIEW OF LITERATURE

The review of literature covers the following aspects of this project:

1. Water based cooling system design for PV-T and BIPV-T photovoltaic modules.
2. Short comings in cooling configurations in photovoltaic modules.

2.1 Water based cooling system design for PV-T and BIPV-T photovoltaic modules

In this section various water-based cooling systems for PV-T and BIPV-T modules studied and analysed have been discussed since 1987. Some of the findings in these studies became the starting point of our BIPV-T project. In Section 2 of review shortcomings in various designs studied have been discussed.

Stultz [1] of Jet Propulsion Laboratory California Institute of Technology, Pasadena, California performed a study on photovoltaic modules on behalf of the Department of Energy, USA. The study included a temperature profile of photovoltaic modules in natural sunlight. It reported an operating temperature of 61.6°C for insulated roof-integrated photovoltaic modules. When cooled with water circulation, the photovoltaic module exhibited an increase in module efficiency.

The Table 2-1 shows temperature rise ΔNOCT over normal operating cell temperature (NOCT) for roof installation of PV module in different mounting options. The insulated roof installation is similar to performance for BIPV mounting. This is a compelling situation for need to design a Building Integrated PV-Thermal (BIPV-T) module with cooling system to reduce the temperature.

The photovoltaic-thermal (PV-T) module using Spectrolab module was tested on a hot summer day having 35℃ ambient. The module efficiency increased by approximately 0.83% an increase of 16% from uncooled module by circulating cool water at 23℃.

Table 2-1 Nominal operating cell temperature (NOCT) for a residential roof installation [1]

Case No.	Configuration	NOCT (°C)	ΔNOCT* (°C)
Lincoln Laboratory Mounting			
1	Module at center of roof (No flow beneath module)	55.5	9.5
2	Module at east/west edge of roof (Permits east-west air flow)	49.9	3.9
Modified Configuration			
3	Sides closed, top/bottom edges open (Permits flow bottom to top)	50.8	4.8
4	All edges open (Permits flow in all directions)	49.4	3.4
Shingle Type Mounting (Hard mounted to roof)			
5	Roof uninsulated	58.0	12.0
6	Roof insulated	61.5	15.5
*NOCT of this module is 46°C for the normal field installation.			

This study was conducted to improve performance of PV module only and no thermal gain in heated water was measured. Therefore, this study lacks study on overall efficiency improvement by collecting warm water. However, it gives very important data showing increase in NOCT if PV modules are installed on roof top particularly an insulated roof.

Martin K. Fuentes [2] of Sandia National Laboratories, USA, published a report for roof-integrated photovoltaic modules. He reported astonishing findings, that Installed Nominal Operating Cell Temperature (INOCT) for a roof-integrated module (direct mounting without any gap) to be 17 to 20°C above Nominal Operating Cell Temperature (NOCT) measured at 800W/m^2 solar intensity, 20°C ambient temperature and wind speed of 1m/second. The Table 2-2 shows installed operating temperature with zero gap between roof and back of PV panel as 66 to 68°C, whereas NOCT was measured between 48 to 49°C. This means power output of a Building-Integrated PV (BIPV) module rated at 25°C will drop substantially depending on its temperature derating factor.

Table 2-2 Variation of INOCT with standoff height. The standoff height is measured from the roof to the module frame [2]

Standoff height, inches (mm)	INOCT (°C)	INOCT – NOCT (°C)
0.0"* (0.00 mm)	68.1	20.0
0.0" (0.00 mm)	65.8	17.0
1.0" (25.40 mm)	59.8	11.0
3.0" (76.20 mm)	51.2	2.0
6.0" (152.40 mm)	48.1	-1.0
9.0" (228.60 mm)	46.1	-3.0

*Insulation was placed under the modules to simulate a worst-case situation.

This study too supports the need to use a cooling system for BIPV modules when flushed with the roof. This is the first time the effect of gap between roof and back of PV module on operating temperature was presented. It's a very useful tool in designing a roof integrated PV system. This information is very useful in understanding the installed normal operating cell temperature (INOCT) which is applicable for BIPV modules.

M. Bakker, *el al.*, published an internal study [3] on dual flow photovoltaic/thermal combi panel. They used a unique design of a hybrid photovoltaic thermal collector. As shown in Figure 2-1, they created a glass-topped enclosure for a photovoltaic laminate (an unframed solar panel) with a 2 mm gap around the laminate, creating a shell which acts as a heat exchanger into a cooling liquid. The panel is divided into three segments; for each segment a system of heat balance equation is solved.

The study concluded that despite its excellent thermal performance, the dual flow concept remained very heavy and fragile due to the large amounts of glass required, reducing its viability for large-scale applications. A modified concept with only one channel below the PV laminate, possibly in the form of a channel sheet, would greatly simplify the construction, yet retain a very high thermal efficiency.

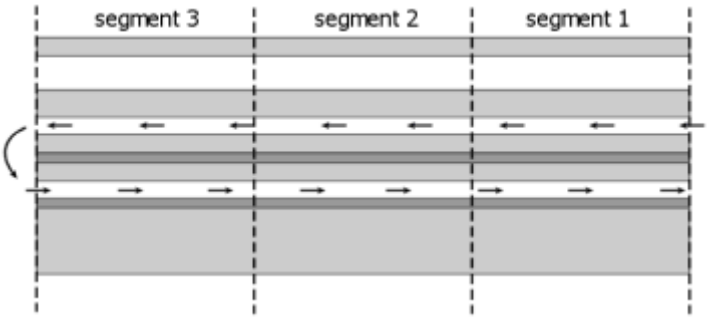

Figure 2-1 Schematic representation of the thermal model [3]

Though PV-T modules with additional glass (glazing) proposed here will increase thermal performance by reducing losses, it is not recommended. If the cooling system stops on a hot sunny day, the temperature will rise above 130℃ which will melt the encapsulation material such as ethylene vinyl acetate (EVA).

Zondag H. A., *et al.*, [4] built a 3D dynamic model and steady-state 1D, 2D and 3D models. A prototype combi module (PV-T) was also built Figure 2-2. The performance of the prototype was found close to the data generated by the model. The 1D model was found to be several times faster to obtain the results than 2D and 3D models; however, 2D and 3D models would be useful in more complicated combi panel designs. The cross-section of cooling pipe attached to module and heat flow is shown in Figure 2-2 (a) and (b). The Figure 2-3 shows heat flow from cooling water tube to solar cells.

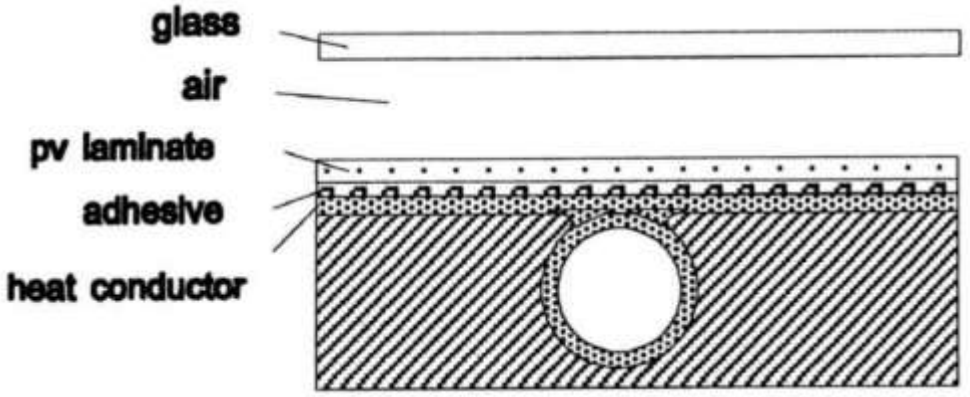

(a)

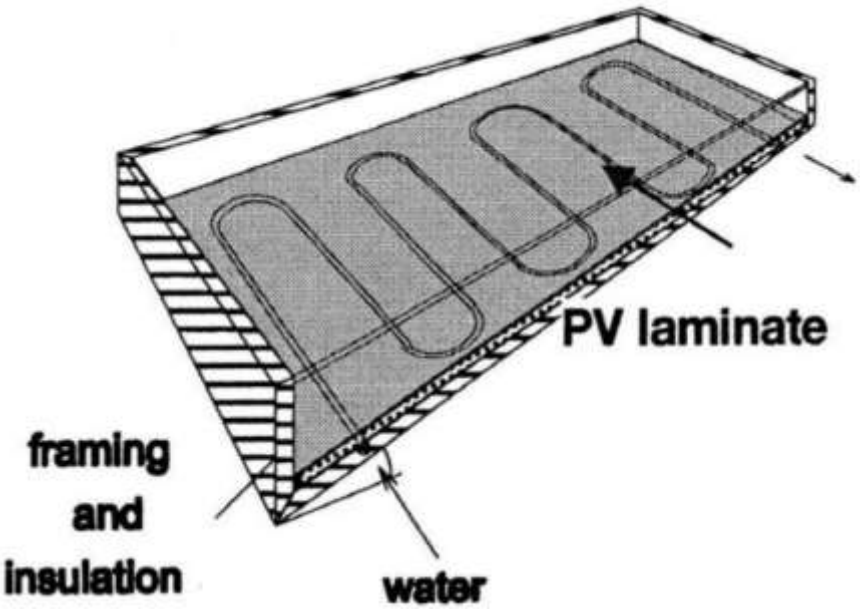

(b)

Figure 2-2 The Combi-panel (a) Cross Section (b) Cooling Pipe Layout [4]

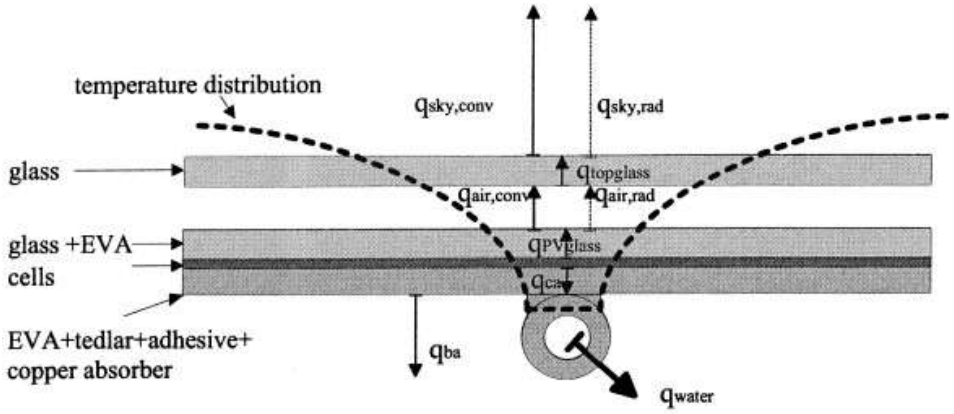

Figure 2-3 Cross section of the Combi panel. The material layers in the Combi-panel are indicated, as well as the temperatures and the various heat fluxes. The dashed line shows the temperature distribution over the surface of the panel [4]

The study claims 5% accuracy between experimental and modeling results. While thermal efficiency of 33% was obtained, the electrical efficiency of 6.7% was reported. However, this study has been conducted only for spiral flow cooling pipe configuration. This configuration will cause

every solar cell within a module to operate at different temperature causing mismatching. I do not recommend using this cooling circuit configuration.

Miroslav Bosanac, et al., [5] concluded that with the current technologies, the PV-T combination has a lower efficiency than two separate systems.

The survey conducted with various architects and several shortcomings were listed as follows:

- In colder climate building requires heating in winter when solar gain is lowest.
- The module temperature must be higher than indoor air temperature leading to module temperature to operate at higher temperatures.
- Heat exchanger is necessary for antifreeze fluid that requires even higher module temperature for space heating.
- The PV-T module can get very hot due to back insulation that can cause damage if cooling fluid circulation fails.
- The fabrication of PV-T module is more complex than making PV and thermal collectors separately.

However, PV-T offers many advantages for which more R & D work is needed.

- The area occupied by PV-T modules is smaller for combined heat and electricity generation.
- The economics of combined energy gain for PV-T module and systems will be better than using two separate units for electricity and heat production.
- Installed look of PV-T integrated in the building will have better looks than using PV and thermal systems separately.
- The PV-T modules will have saving in installation costs as compared to separate PV and thermal collectors. This may be important point in commercialization.
- Direct use of low temperature produced by PV-T modules for swimming pools and for other uses in combination with heat pumps will have more acceptability.

This study is very well done, listing advantages and disadvantages of PV-T modules. One of the major missing advantage is using BIPV-T modules as building material for roof and façade. This application will offset cost of replacing roofing and façade material such as shingle and glass. The

other advantage of his design is that both air and water is heated while cooling the solar cells. The disadvantage of this design is that air will have much poor heat transfer to cool the PV-T module. In addition, flow path of both water and air is from one end to other that will cause cells to operate at different temperatures as the water and air pick up heat from cells along the cooling path.

Charalambous, P.G., *et al.*, [6] covered-flat-plate and concentrating water-based PV-T collectors. They discuss results on analytical and numerical models, and on simulation and experimental work and qualitative evaluation of thermal and electrical output of the flat-plate-based PV-T collector (Figure 2-4). Various parameters such whether the PV-T collector is covered or uncovered, mass flow rate, tube spacing, tube diameter, fin thickness and configuration designs are evaluated. The study suggests that uncovered PV-T produces the largest combined thermal and electrical energy. The paper concludes that PV-T efficiency and cost-effectiveness must be improved for their utilization.

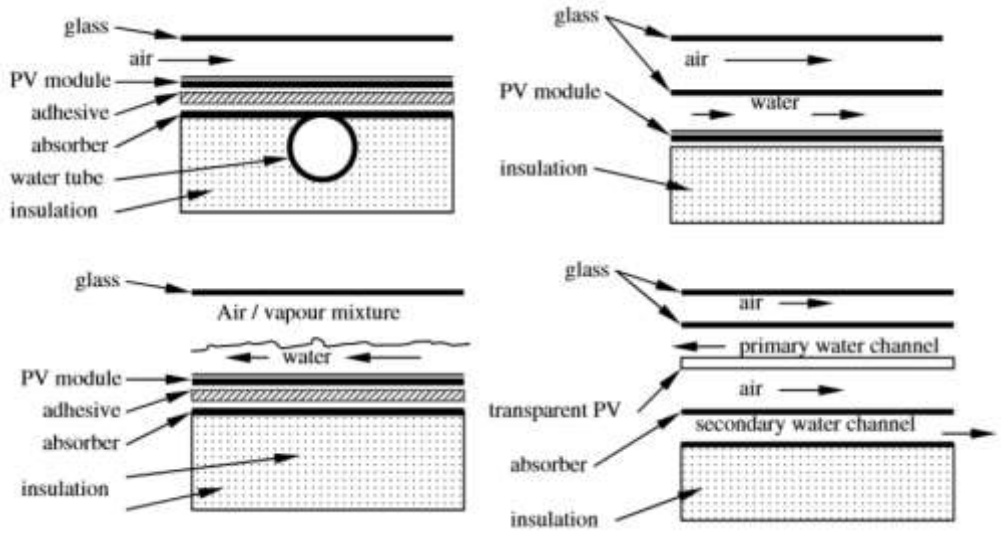

Figure 2-4 Types of water PV-T collectors [6]

I agree that unglazed PV-T modules will have best combination of electrical and thermal energy. By placing a glass on top of PV-T module will increase the output temperature of cooling fluid but will cause the PV efficiency to fall. Accordingly, PV-T modules should not be used as solar thermal collectors. It can damage PV module due to overheating with time.

Fanney, *et al.*, [7] describe the apparatus used to collect the experimental data, test procedure utilized and resulting parameters of three different solar modules. The measurements were done in two different laboratories with different climatic conditions, (Table 2-3 and Table 2-4). The

magnitude of current and voltage temperature coefficients between the two laboratories varied as much as 17% though impact of these on predicted performance through simulation was minimal, less than 2%. The study is based on an annual performance of solar modules instead of peak power at standard test condition (STC) of 1000W/m^2, 25°C cell temperature and 1.5 air mass.

Table 2-3 Comparison of current temperature coefficients for three different modules measured at NIST and SNL [7]

	Mono Crystalline	Mono Crystalline	Silicon Film	Silicon Film	Triple Junction	Triple Junction
	Short Circuit, A	Peak Current, A	Short Circuit, A	Peak Current, A	Short Circuit, A	Peak Current, A
NIST*	0.001753	-0.001543	0.004680	0.001600	0.005610	0.007350
SNL**	0.001496	-0.001722	0.004781	0.002000	0.006584	0.007498

*National Institute of Standards and Technology, **Sandia National Laboratories

Table 2-4 Comparison of voltage temperature coefficients for three different modules measured at NIST and SNL [7]

	Mono Crystalline	Mono Crystalline	Silicon Film	Silicon Film	Triple Junction	Triple Junction
	Open Circuit, V	Peak Voltage, V	Open Circuit, V	Peak Voltage, V	Open Circuit, V	Peak Voltage, V
NIST*	-0.152386	-0.153578	-0.12995	-0.13039	-0.0931	-0.04773
SNL**	-0.1735	-0.1756	-0.1412	-0.1401	-0.1037	-0.05074

In recent years many software have been developed to predict the annual performance based of module performance at STC. While this study is good to compare annual energy production of solar modules, it cannot replace the need of the determination of modules performance at STC. Effectively, sun simulator used for testing of module at STC during production is fast and solar industry measured 100% of solar modules for quality control and grading of modules.

Ivan Katic [8] tested a PV-T module called PV-Twin (brand name) for performance evaluation. In this study a 230W photovoltaic panel with serpentine tube on copper was used as cooling from the rear. The PV-Twin module was insulated from the back and was cooled with water circulation. The testing was done in accordance with EN12975 standard. At 40°C mean temperature of cooling water the thermal efficiency of 54% was achieved whereas for 80°C mean temperature, the thermal efficiency dropped down to only 19% as shown in Table 2-5. The PV module delivered 146.3W at a 77°C module temperature as shown in Table 2-6. The calculated efficiency was only 8.99%, which was attributed to a partial defect in one of the quadrants. Nevertheless, the combined PV and thermal efficiency exceeds well beyond the efficiency of PV module if used alone.

Table 2-5 Thermal Efficiency of PV-Twin [8]

$T_m \approx$	Data 1		Data 2		Data 3		Data 4	
°C	T_{red}	η	T_{red}	η	T_{red}	η	T_{red}	η
40	0.0105	0.54	0.0097	0.53	0.0088	0.54	0.0091	0.54
60	0.0333	0.36	0.0285	0.37	0.0338	0.34	0.0379	0.34
80	0.0564	0.19	0.0472	0.25	-	-	-	-

Note: $T_{red} = (T_m - T_a)/G$ is the difference between mean water temperature and the ambient temperature divided by solar radiation and T_m is the mean temperature of inlet and outlet temperature of cooling water.

Table 2-6 Electrical Performance of PV-Twin [8]

Data corrected to STC					Measured values									
Im0 A	Um0 V	Ppk W	Isc0 A	Uoc0 V	Ipmax A	Upmax V	Pmax W	Isc A	Uoc V	Rp kOhm	Rs Ohm	FF	T °C	E W/m^2
7.00	32.8	229.6	8.17	44.6	5.85	25.0	146.3	6.83	34	>0.21	1.6	0.63	77.0	835

Where, Imo is current, Umo is voltage, Ppk is peak wattage Isc0 is short circuit current, Uoc0 is open circuit voltage at STC. Ipmax is current, Upmax is voltage, Pmax is power, Isc is short circuit current, Uoc is open circuit voltage, Rp is shunt resistance, Rs is series resistance, FF is fill factor, T is module temperature at E=835W/m^2 radiation.

PV-Twin is a brand name of PV-T module. It uses a serpentine attached to copper plate to cool the PV module from back. This is an example of PV module being misused primarily to extract heat by sacrificing electrical efficiency. The initial electrical efficiency based on testing STC was

14.11% (for 1.627m^2 area for 230W PV module) which dropped down in PV-T mode to 8.99% a loss of electrical 5.12%. The thermal efficiency at mean temperature of 60°C obtained is 36% hence PV-Twin is assumed as satisfactory. The lower performance of electrical efficiency is attributed to defect in PV module rather than non-uniform cooling. In is anticipated that the long run solar cells in this PV-Twin will fail.

Y. Tripanagnostopoulos proposed three different methods for placing a water heat exchanger inside air channel (Figure 2-5). The purpose of Mode A, Mode B and Mode C was to study a design of PV-T module where thermal heat could be collected in the form of warm air as well as warm water. He concluded that placing the exchanger at the rear surface of module as shown in Mode A, performed the best for the combined water and air heat extraction from the PV module. According to the author, the design is cost effective for operation in low temperatures.

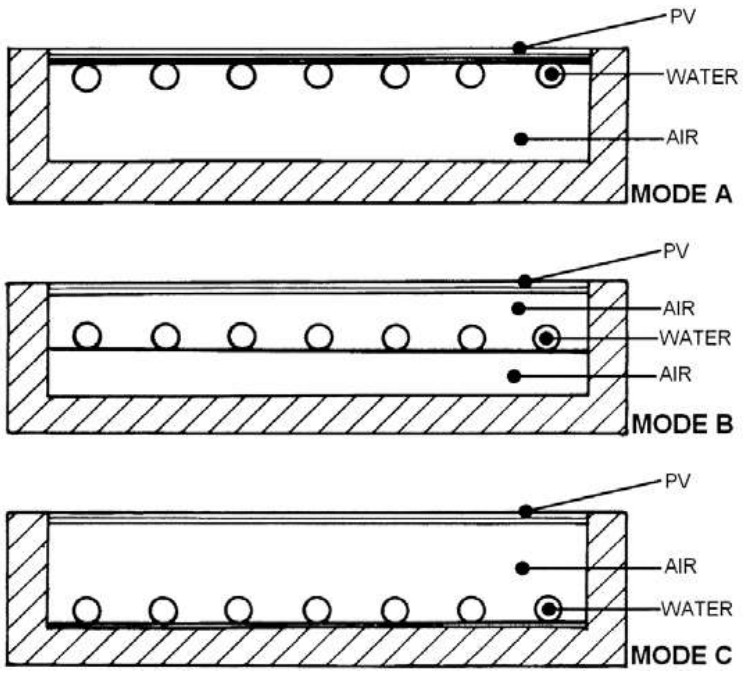

Figure 2-5 Alternative PV-T/dual design modes, used to determine the optimum arrangement of the water and the air heat exchanger [9]

All three Mode A, Mode B and Mode C are sharing the heat collection through air and water flow for cooling the module. It is obvious all three PV-T design cooling fluid flows from one end to the other of PV-T module which will cause temperature of cells at inlet to be lower than at outlet. The mismatching of cell output will still occur.

Anderson T., *et al.*, [10], in their paper conducted a theoretical analysis of a novel Building-Integrated Photovoltaic/Thermal (BIPV-T) collector through the use of modified Hottel-Whillier model. They discussed how key design parameters influence the performance of BIPV-T collector. They concluded that thermal efficiency of BIPV-T made very little difference for the material used for constructing the BIPV-T collector as seen in Figure 2-6. The $(T_{in}-T_a)/G''$ is called inlet parameter where T_{in} is inlet temperature in °C of cooling water, T_a is ambient temperature in °C and G″ is solar radiation intensity in W/m^2. This implies that cheaper material like steel could be used for reducing the costs. They further concluded that good thermal contact between photovoltaic cells and the absorber plate is important and suggested use of thermally conductive adhesive to improve thermal contact. The Figure 2-6 shows performance of the BIPV-T for absorber based on stainless steel(304), steel(5% Cr), aluminum, copper which thermal conductivity is 24, 40, 240 and 400W/m.K. The Figure 2-7 shows the thermal efficiencies for varying absorber sheet conductivities of 45, 90, 135 and 180W/m.K used at the back of PV module for heat transfer.

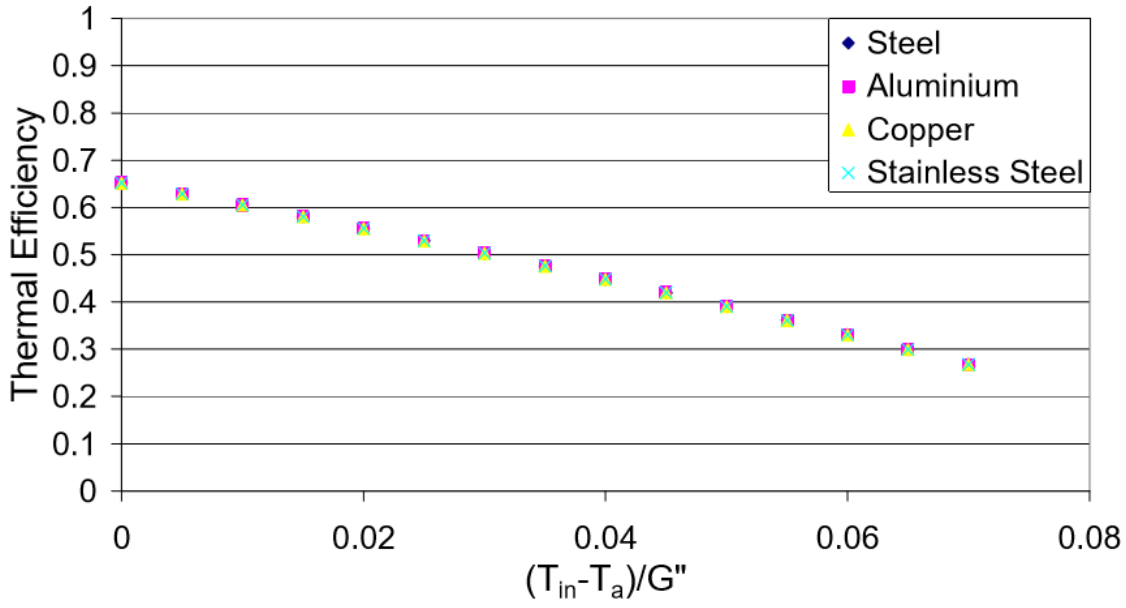

Figure 2-6 BIPV-T thermal efficiency for varying collector material [10]

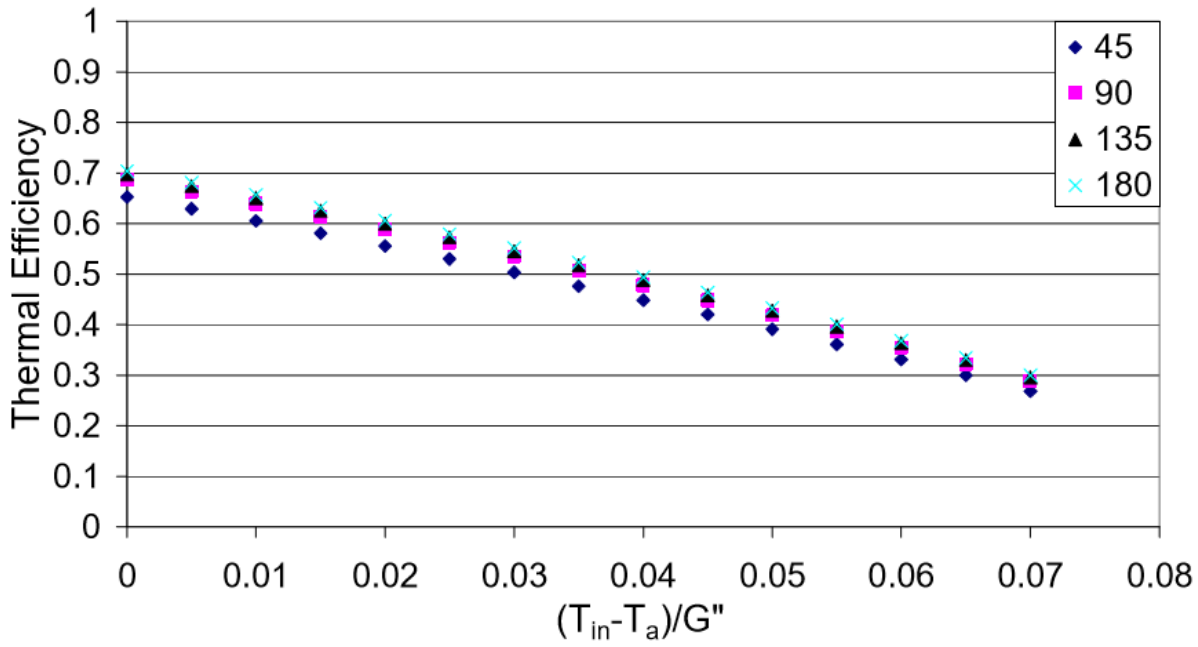

Figure 2-7 BIPV-T thermal efficiency for varying PV absorber conductivities [10]

This study needs to be verified by making an actual prototype with different material and testing. The thermally conductive adhesive with conductivity ranging from 45 to 180W/mK to glue absorber at the back of PV module is not readily available. However, this study is based on serpentine water cooling tube attached to absorber plate and is focused on improving thermal performance. The serpentine cooling pipe the cooling water goes over all solar cells in a module that will cause non uniform cooling of solar cells and loss in electrical efficiency. The actual testing of product is required to prove the technical and economic viability of proposed design.

Touafek, *et al.*, [11] fabricated a water-cooled PV-T collector using a galvanized channel at the back of PV module for water circulation as shown in Figure 2-8. For this design, they reported thermal efficiencies ranging between 50% and 80% depending on the time of the day. They achieved a 3°C temperature rise for inlet water temperature of 34°C and outlet water temperature of 37°C in ambient temperature of 33°C. They did not report the efficiency of the PV cell or module.

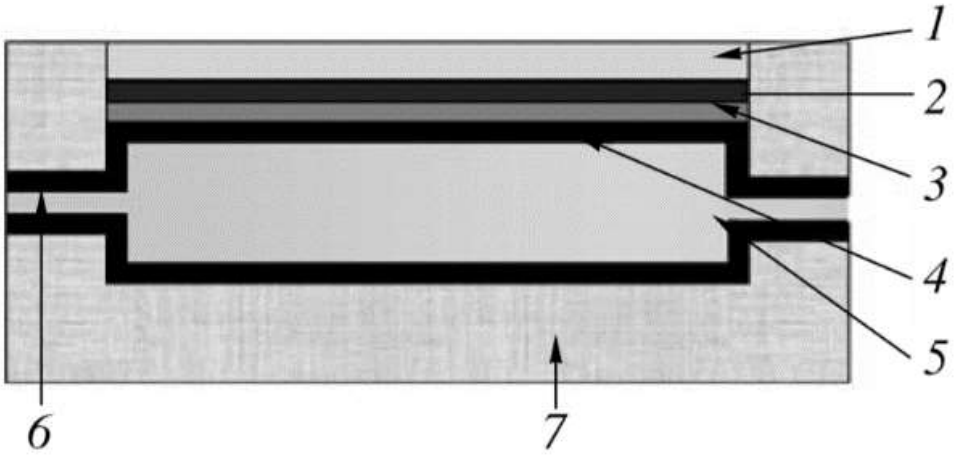

Figure 2-8 Simplified diagram of new PV-T collector with: 1-Tempered glass; 2- Photovoltaic cells; 3-Tedlar; 4-The absorber; 5-Exit of the coolant; 6-Entry of the coolant; 7-Insulation. [11]

This article does not mention electrical output or efficiency of PV-T collector tested. The cooling flow is one end to other where solar cell temperature from one end to other will vary causing mismatching. The cooling water chamber below the module is impractical as weight of PV module will increase substantially on roof top. Moreover, the chamber has to be made really strong to hold weight of water.

T.T. Chow [12] reviewed the trend of development of photovoltaic-thermal technology. He covered the work done in recent years. The main feature of any PV-T design is shown in Figure 2-9. He concluded that different designs whose cross-sections are shown in Figure 2-10 suit different geographical locations needs. In colder climates PV-T systems are useful for electricity and year-round space heating, whereas locations with generous sunshine areas can use electricity and preheated water year around. He mentioned further that very few PV-T systems were commercially available at the time. The reliability and cost of commercial-available PV-T systems need to be addressed in cooperation between institutions and manufacturers to make significant contributions in the market.

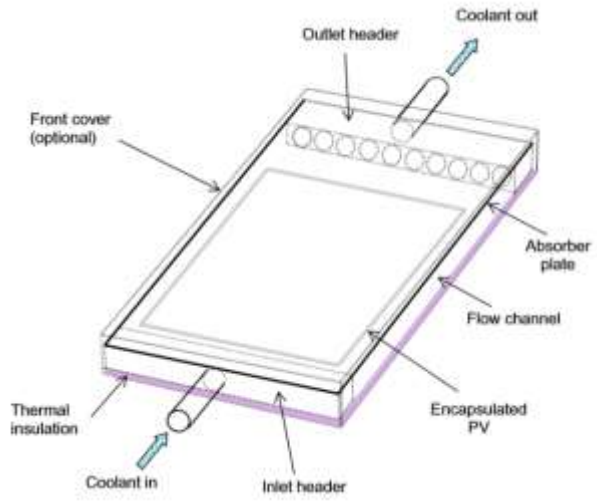

Figure 2-9 Main features of a flat-plate PV-T Collector [12]

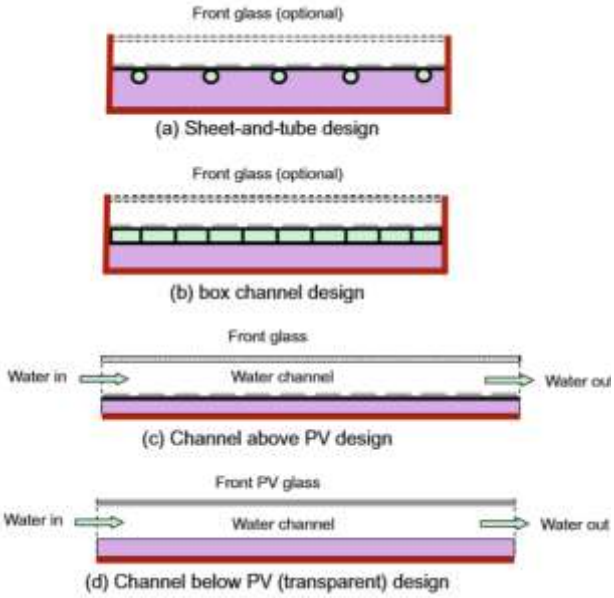

Figure 2-10 Cross-section of some common PV-T water collector designs [12]

The review of various flat plate PV-T collector designs and flow path show movement of cooling water from one end to other end of PV-T collectors. Similar to other designs the solar cells near the entry will remain cooler than at exit where water is warmer. All these designs will cause non-uniform cooling of solar cells resulting in mismatch.

Hofmann, *et al.*, [13] proposed standardization of measurements of a PV-T collector and different measurement procedures. The paper illustrates indoor testing methods for PV-T collectors as seen in Figure 2-11(a) and (b). The author proposed performance of both Electrical and Thermal efficiency with respect to thermal loss coefficient $(T_m-T_{amb})/G$. The mean temperature of inlet and outlet temperatures is denoted as T_m in K and ambient temperature is denoted as T_{amb} in K and solar radiation denoted as G in m^2K/W.

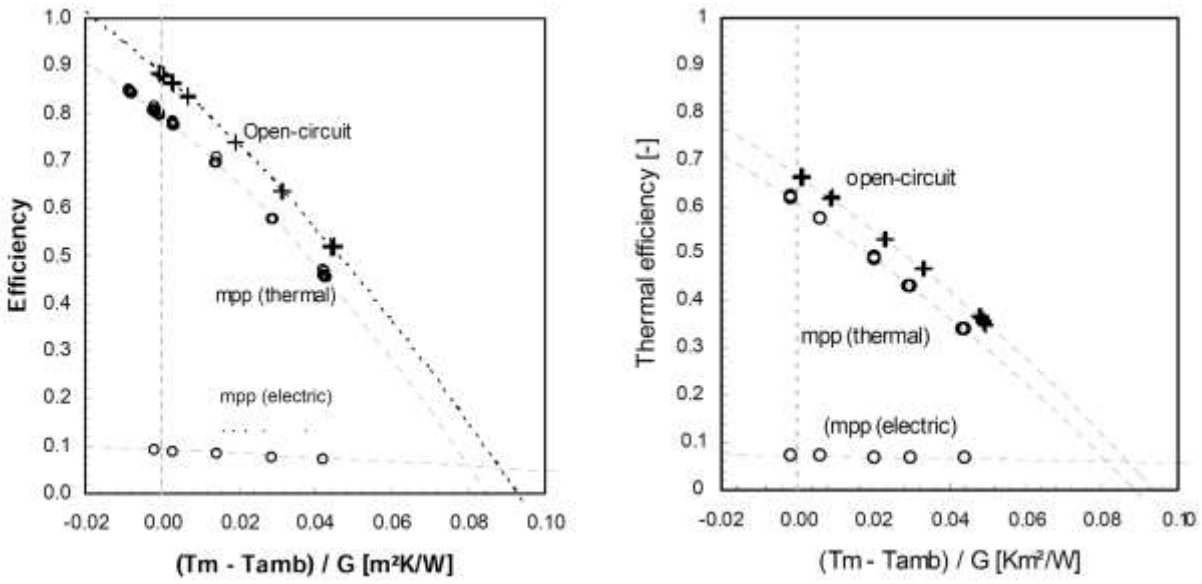

(a) (b)

Figure 2-11 Thermal and electrical performance measurements of a typical glazed PV-T collector with c-Si as cell technology (a) and CdTe technology (b) [13]

Since PV-T and BIPV-T modules did not have an exclusive standard for testing, the proposed testing method is a good step forward [13]. However, the method described is for indoor testing using a sun simulator where atmospheric conditions and various parameters can be controlled and maintained through out the test. This method is good if performance of PV-T and BIPV-T modules are to be compared. It is impossible to achieve exact solar spectrum with sun simulator. This method required steady state sun simulator which is extremely expensive.

Sopian, *et al.*, [14] conducted theoretical analysis of three PV-T water cooling circuit layout. They concluded that a Split flow PV-T collector design shown in Figure 2-14 has better performance compared to Direct flow and Parallel flow shown in Figure 2-12 and Figure 2-13. They reported a thermal efficiency of up to 51.8% but did not report the electrical efficiency of PV cells.

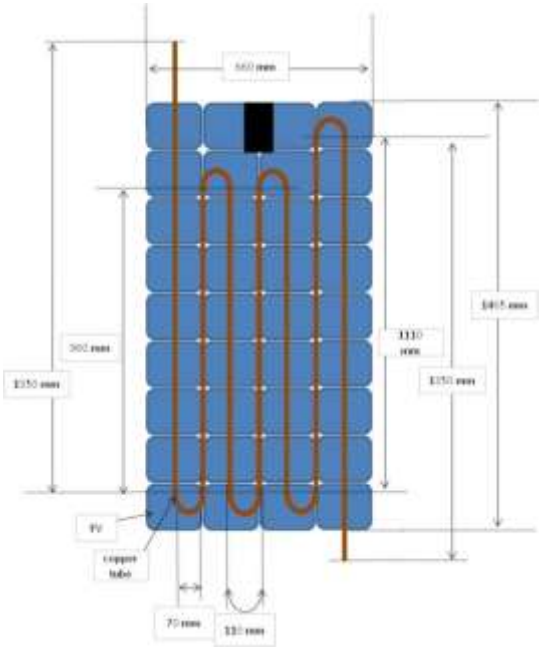

Figure 2-12 Schematic direct flow PV-T diagram [14]

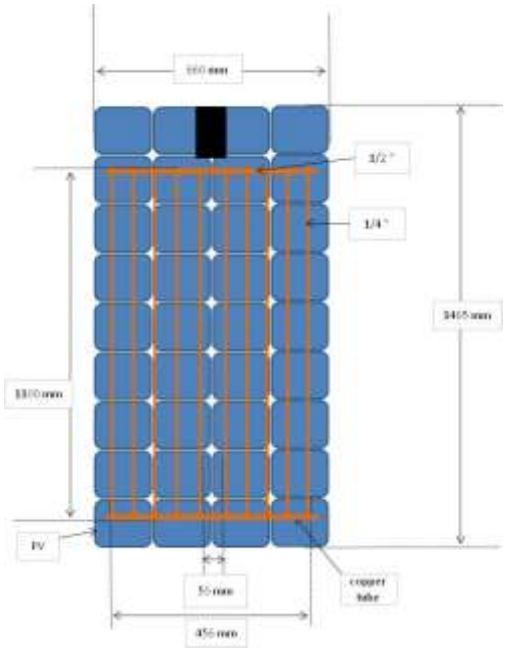

Figure 2-13 Schematic parallel flow PV-T diagram [14]

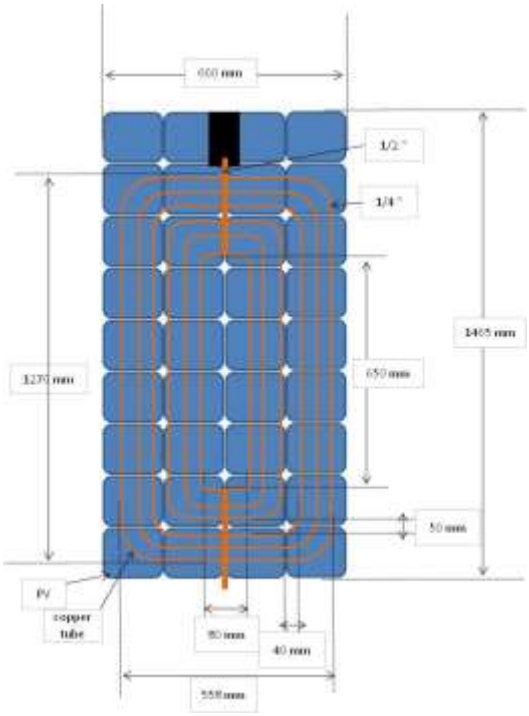

Figure 2-14 Schematic split flow PV-T diagram [14]

The three designs analysed were based on thermal performance of PV-T modules. In all three cases the cooling water enters at first cell and exits after flowing over many cells to collect heat. It clearly shows, all solar cells along the flow path will have non-uniform temperature that will cause electrical mismatching. Moreover, solar cells on either side of junction box shown in black at the top are not even cooled and will operate at higher temperature. These designs will have maximum electrical mismatch between the first cell which receives the coldest water for cooling to last cell where the warm water exists. All cooling pipe configurations are commonly used in solar thermal collectors. The primary aim is to recover heat and increase overall efficiency of PV-T module. They have not address the important issue of mismatching which is important for PV modules.

López, *et al.*, [15] developed an innovative low-cost prototype of a PV-T module using pipes of a floor heating system filled with a special brine to cool the PV cells. The comparative performance of PV-T versus identical uncooled PV module of 130W is shown in Figure 2-15. The daylong testing from 8:30PM to 7PM on a clear sunny day showed 200 litres cold water temperature increased from 20°C to 24°C. A 6% increase in the electrical output in watt-hour was achieved though it is not as high as expected.

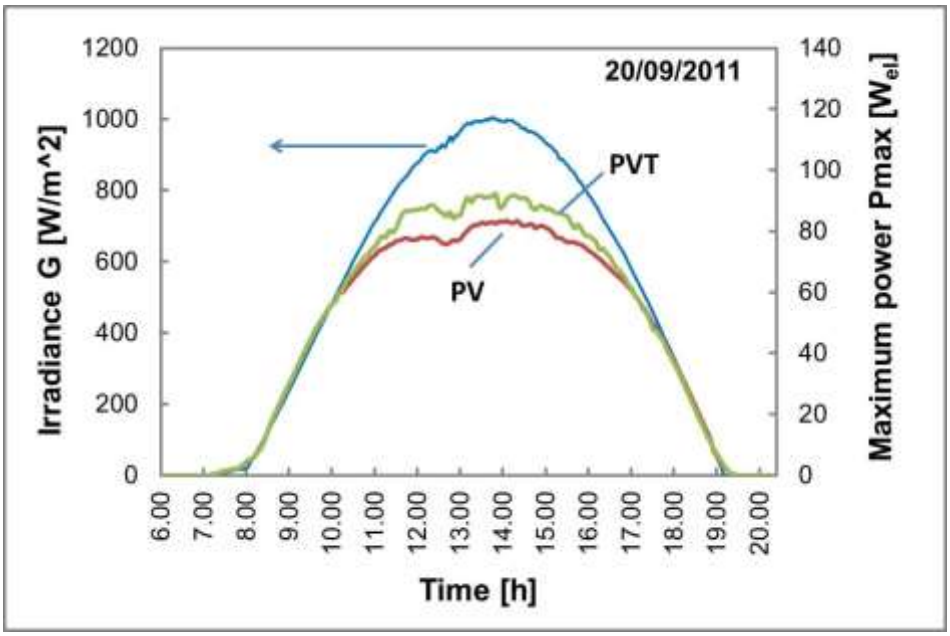

Figure 2-15 Electrical power production by the cost-effective PV-T module prototype and the same PV module under real environmental conditions [15]

The PV-T design uses serpentine type of cooling pipe configuration. There is no mention of solar cells temperature without which effectiveness of cooling cannot be accessed. The Figure 2-15 shows daylong performance PV-T module on a sunny day. The cooling water temperature of 20°C and water output temperature of 24°C over 8.5 hours duration achieved is low. With power coefficient of -0.43%/°C, a 130W module operating temperature is approximately 38.4°C near noon time the module power should have been higher for PV-T module. The effectiveness of cooling therefore is poor. This could be due to non-uniform cooling as well as poor contact between cooling plate and back of PV module.

Dupeyrat, *et al.*, [16] evaluated PV-T collector concepts as in Figure 2-16 using a two-dimensional model under steady state conditions. They reported that direct lamination of single crystal silicon solar cells on an optimized metal heat exchanger as shown in Figure 2-17 (a) and (b) leads to the best results. An experimental PV-T collector was built using a lamination method. The thermal efficiency at zero reduced temperature was measured at 79% under PV operation with electrical efficiency of 8.8%. This sums up to nearly 88% overall efficiency; however, the electrical efficiency of the PV-T collector is lower than a similar standard photovoltaic module.

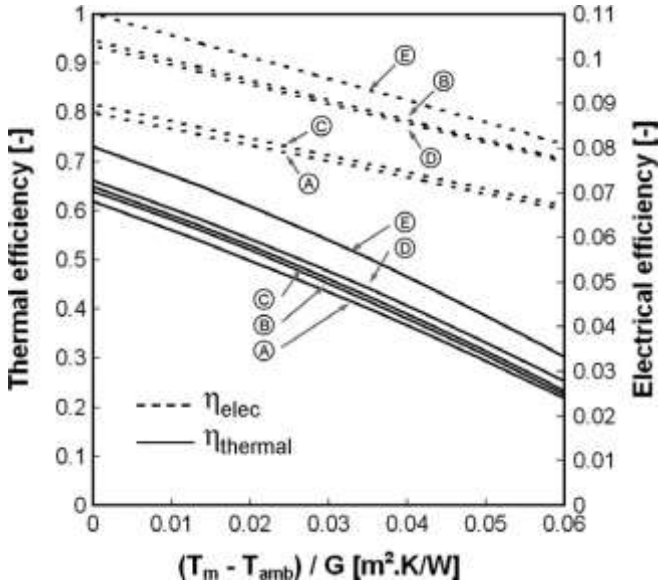

Figure 2-16 Thermal and electrical efficiency curves of a typical PV–T collector for two different bonding methods [16]

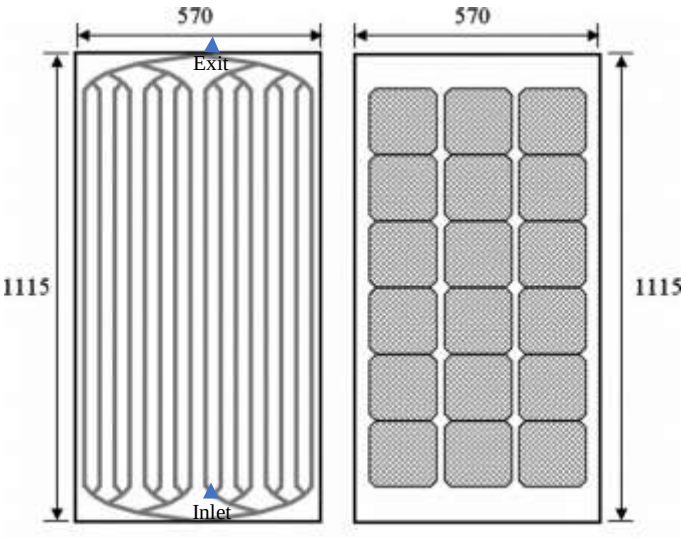

(a) Rear side (b) Front side

Figure 2-17 Representation of the front and rear side of the developed PV-T absorber [16]

The protype studied was built with single glazing that caused the stagnation temperature to build between 142.5°C in open circuit mode and 136.3°C in operating mode. Such high temperatures are detrimental to PV-T module lamination using ethylene vinyl acetate encapsulant which melts around this temperature. The cooling water flows from one end to the other end of PV module. That means all solar cells are not being cooled uniformly. This could be reason for achieving only 8.8% electrical efficiency that drops down below 7% as cooling water temperature increases. However, the study shows laminated heat exchanger to the back of module performs better than glued heat exchanger as shown in Figure 2-16.

Hosseini, *et al.*, [17] conducted an experimental study on a PV system cooled by a thin film of water flowing on top of the solar panel. They found that applying a film of water for cooling photovoltaic panel decreased the temperature and reflection loss and increased the efficiency of the combined photovoltaic and thermal system. The heat removed by the water from the panel was used in a heat exchanger to extract heat before recirculating in the drip cooling system. The performance module temperature and efficiency is presented in Figure 2-18 and Figure 2-19 respectively.

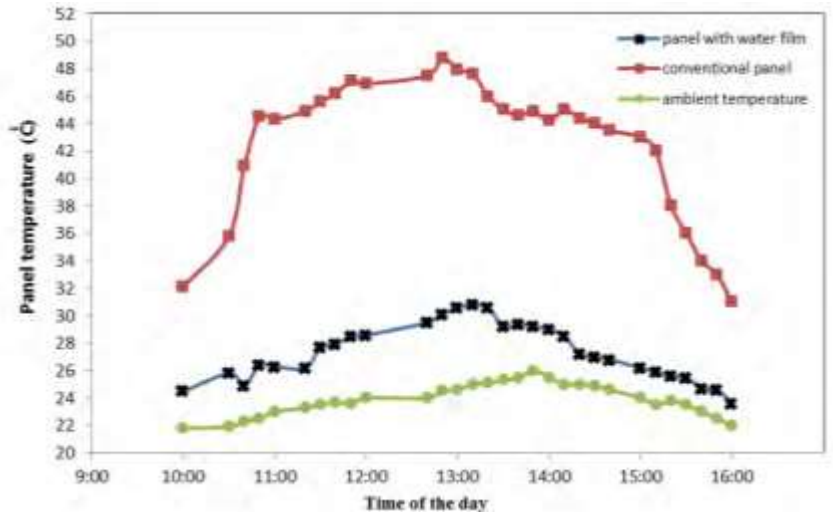

Figure 2-18 Comparison of conventional photovoltaic panel temperature with the temperature of the panel in the combined system [17]

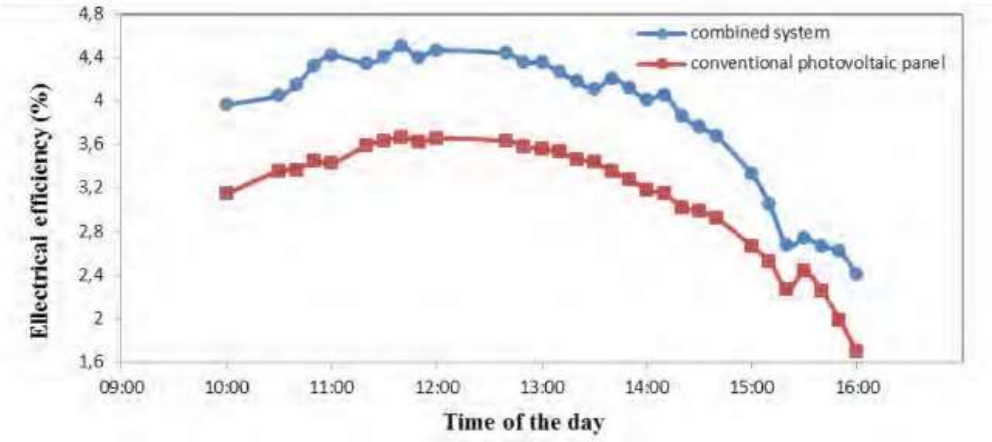

Figure 2-19 Comparison of conventional photovoltaic panel electrical efficiency with the electrical efficiency of the combined system. [17]

This study is based on flowing a thin film of water from top of solar panels. The film of water is not uniformly flowing over the PV-T modules. The idea is very impractical as wind and dust both will effect the performance of module. The water will be contaminated in open atmosphere, the heat loss will be high as compared to contained water flow in pipes with insulation. The non-uniform cooling cannot be prevented that will cause mismatching of cell electrical outputs. The efficiency at 1PM increased by 0.5% as shown in Figure 2-19 where as temperature of PV-T reduced by 18°C in Figure 2-18. Based on power temperature coefficient of -0.44%/°C, the efficiency should not have increased more than 0.277%. There is some mistake in result.

Eurofins Test Center, Italy, [18] type-tested an glazed Hybrid photovoltaic thermal module in natural sunlight. The instantaneous thermal efficiency performance is shown in Figure 2-20. The glazed 170W hybrid module with 90mm thick insulation at the back reached a whopping 124°C stagnation temperature at 946W/m^2 solar radiation at 24.6°C ambient temperature. The thermal efficiency ranging between 30% and 50% depending on the cooling water flow rate, inlet water temperature, ambient temperature and solar radiation intensity. This hybrid module is certified to EN 12975-2:2006, EN61215:2006 & EN61730:2007 norms and sold commercially.

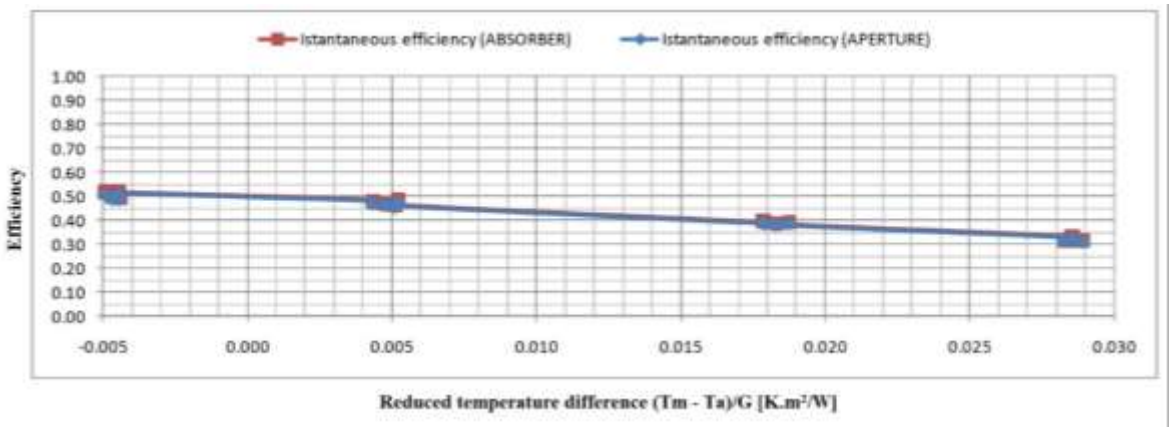

Figure 2-20 Instantaneous efficiency curve for PowerTherm hybrid collector [18]

The thermal performance enhancement using a glazing on top of a PV-T collector is cause of concern as the stagnation temperature is shooting to 124°C. This is the melting point of EVA encapsulant used to laminate solar cells to solar grade glass and backsheet. The UL 1703, IEC 61215 and IEC61730 certified PV modules are tested and certified only upto 85°C. It is not recommended to use a PV module like a solar thermal collector with a glazing to increase temperature. Moreover, the purpose of designing a PV-T module is to improve cooling and extract heat. When a PV-T module is used primary as water heater, the purposed of PV-T design is defeated.

Solimpiks Solar Energy Systems, Turkey, [19] commercialized two models of Photovoltaic-Thermal Collectors. The PowerVolt model is unglazed for higher electrical output and PowerTherm model is glazed for higher thermal output. See Figure 2-21(a) and (b). In both models the overall efficiency increases substantially due heat extraction in cooling water as compared to using just the conventional solar module by itself. Due to the use of high insulation, the stagnation temperatures increase to 111°C for PowerVolt and 124°C for PowerTherm as compared to the

45°C Normal Operating Cell Temperature of photovoltaic module. The PowerVolt is rated at 190W and PowerTherm at 170W electrical power. Both these products have been certified by the Eurofins Testing Facility in Italy. PowerVolt performance has already been discusses in Figure 2-20.

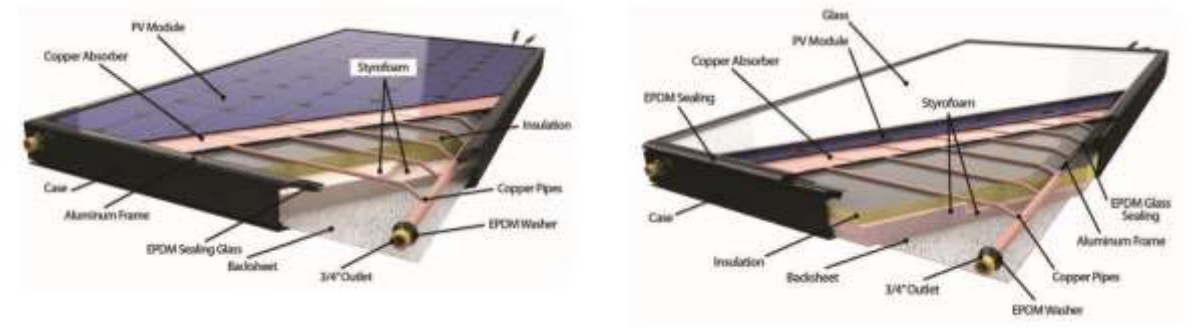

(a) PowerVolt (b) PowerTherm

Figure 2-21 (a) PowerVolt and (b) PowerTherm PV-T collectors from Solimpiks [19]

Both models use parallel flow cooling pipe attached to cooling plate. Though header pipes are placed on long side of the PV-T module, the cooling water still has to travel over six solar cells. Each cell therefore will have different temperature thus causing mismatching. Infact, all home installation use more than one PV-T module to meet electricity demand which may have series and parallel connection of more than one PV-T modules. If cooling water too has to flow in series connected module, a greater number of cells will suffer mismatching.

Eurofins Test Center, Italy, [20] tested a Hybrid Photovoltaic-Thermal Module (PV-T) manufactured by SKORUT, Poland. The hybrid module rated at 230W electrical power was insulated with 50mm thick mineral wool insulation at the back. Three 230W hybrid modules connected together and cooled by water circulation. As shown in Figure 2-22 combined electrical and thermal power output of 198W, 427W and 770W at 400W/m^2, 700W/m^2 and 1000 W/m^2 solar intensity respectively at (Tm – Ta) = 10°C was achieved. Tm is mean temperature between cooling water inlet and outlet temperatures where a Ta is the ambient temperature. This hybrid module was approved as per certification norms UNI EN 12975-2:2006, EN61215 & EN61730 covering both thermal solar systems and photovoltaic modules.

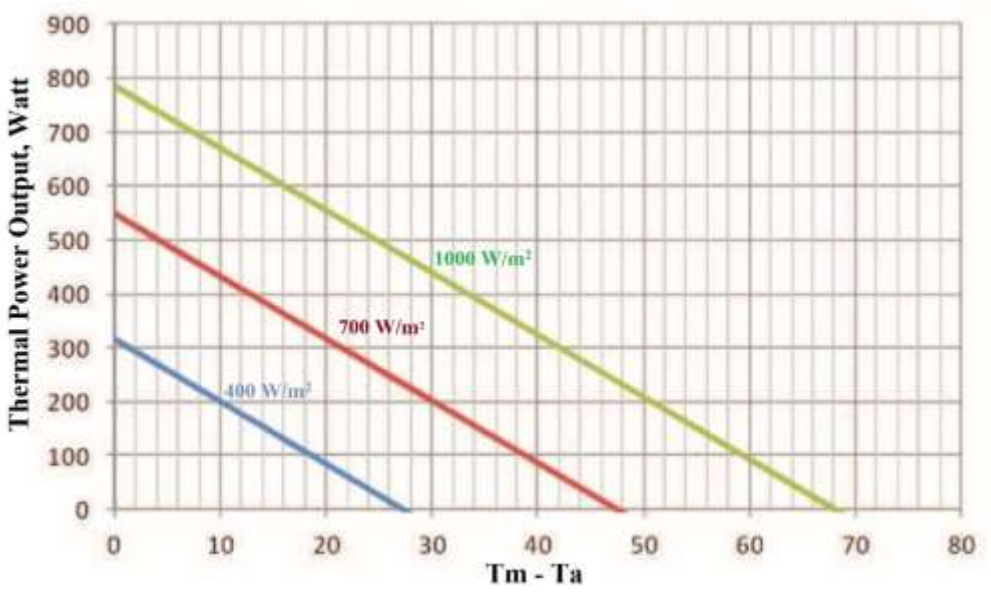

Figure 2-22 Performance of PV-T module [20]

This design uses 60 cell PV module for fabricating a PV-T module . The thermal heat extraction plate is attached to a sinusoidal cooling pipe configuration where water passes over all 60 cells before exiting the PV-T module. This design will have much more temperature difference between solar cell at the inlet of cooling water than the solar cells at the outlet of cooling water. This will result in large mismatching. Since combine electrical and thermal output and efficiency has been reported as 50% it is impossible to know the contribution of PV module. Moreover, there is no data for individual cell temperatures. Hence extent of mismatching loss cannot be estimated.

Tomas Mastuska [21] outlined drawbacks of Building-Integrated Photovoltaics (BIPV-T) in roof and façade. He concluded that BIPV-T collectors produce 5% lower electrical output as compared to a separate installation. Extreme temperatures of photovoltaic cells could cause a degradation problem even in moderate climates where operating temperatures may rise to above 85°C as shown Figure 2-24. According to his simulation study, a high-tech BIPV-T collector configuration shows a negligible temperature difference between the PV and liquid at nominal conditions (efficiency factor F´= 0.99); and a low-tech BIPV-T configuration results in large temperature difference around 25K due to worse heat removal from the PV cell (F´ = 0.69). The heat production is from several times to 10 times higher than electricity production as shown in Figure 2-26. Low-tech BIPV-T collectors could contribute with a reduced performance level but still with considerable improvement when compared to BIPV modules without cooling. He outlined effect of spacing

between riser tube and bond conductance C_{bond} between tube and sheet on the performance of BIPV-T modules as shown in Figure 2-23 and Figure 2-25.

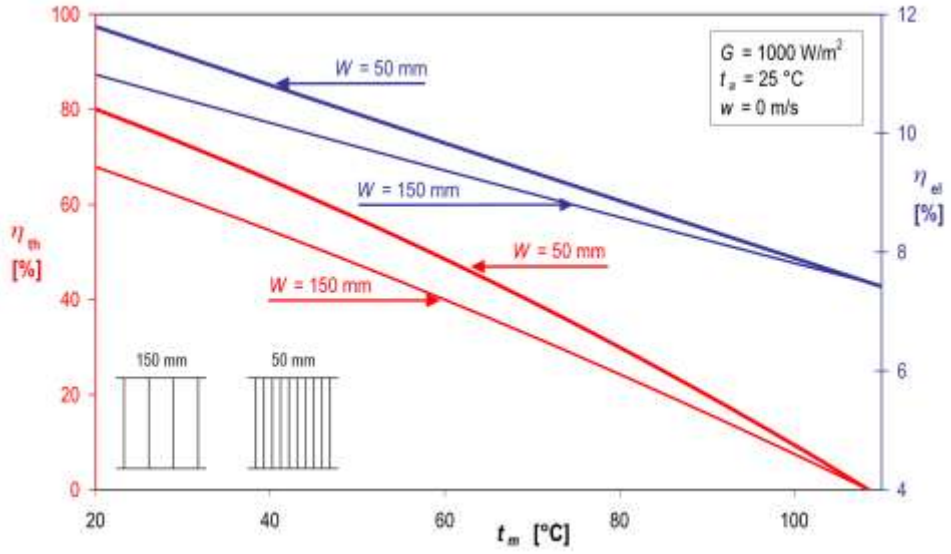

Figure 2-23 Spacing of risers of BIPV-T, at R=6 m^2K/W [21]

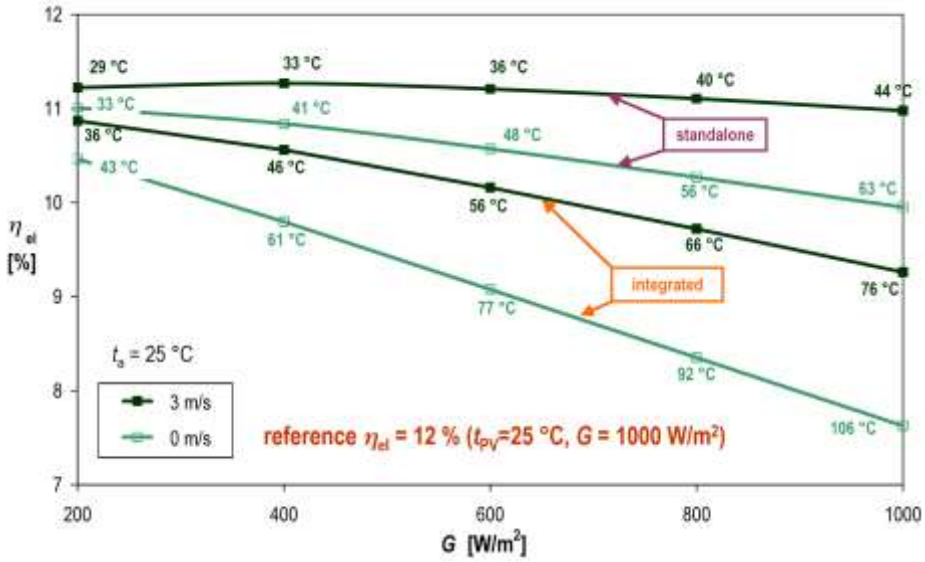

Figure 2-24 PV cells temperature & efficiency without cooling [21]

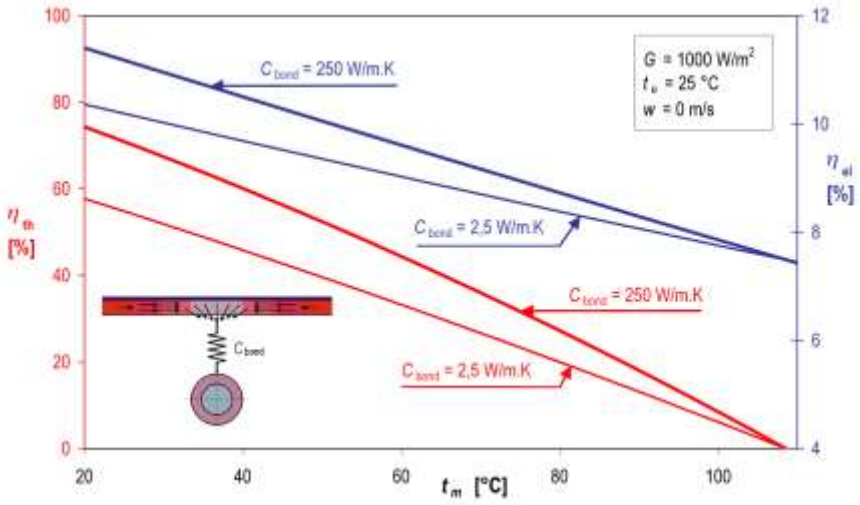

Figure 2-25 BIPV-T Absorber pipe bond at R= 6 m^2K/W [21]

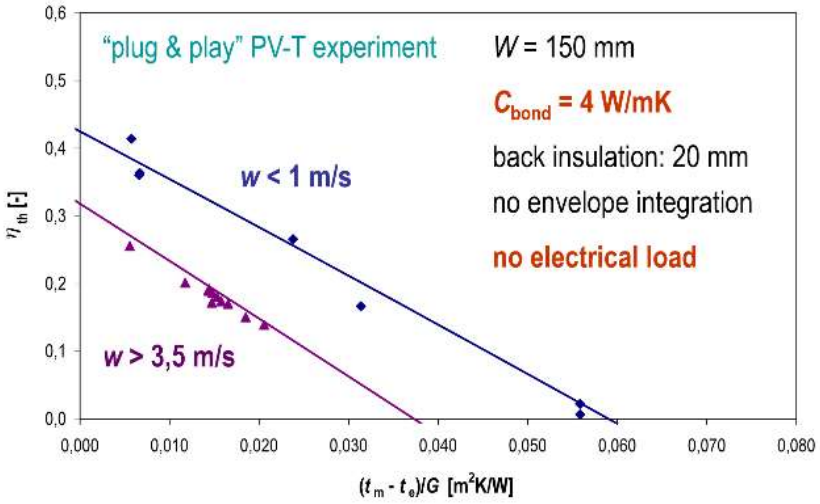

Figure 2-26 Field Test Thermal Performance [21]

Author has covered important parameters affecting the performance of BIPV-T modules. The effect of PV cell temperature and efficiency without cooling is shown in Figure 2-24. His study complements the study published in References [1] and [2], emphasising the importance of cooling BIPV module. The solar cell temperatures in uncooled BIPV-T module may exceeds 85°C which is maximum temperature for PV module certification as per UL1703, IEC61215 and IEC61730 standards.

John A. Duffie, *et al.*, [22] covers flat plate solar collector theory, photovoltaic generator characteristics and models, testing and design methods for solar thermal and photovoltaic systems. The most important is the Thermal Process Simulation Program (TRNSYS) which also covers the analysis of Photovoltaic-Thermal (PV-T) modules. The TRNSYS simulation was used as the base for developing the idea of novel cooling circuit for BIPV-T module described in this thesis. As shown in Figure 2-27, the thermal efficiency of solar collector is plotted against inlet parameter *(Ti-Ta)/*G_T, m^2C/W where *Ti* is the inlet temperature of water, *Ta* is ambient temperature and G_T is solar radiation falling on solar collector. The solid line is based on aperture area of the solar collector whereas dashed curve is for gross area of the collector. The data with sun screen is used to obtain points over range of values. $F_R(\tau\alpha)_n$ is called no loss coefficient as shown in Figure 2-27 and slope is denoted as $F_R U_L$ where F_R is heat removal factor, $(\tau\alpha)_n$ is transmission absorptance product. The useful heat Q_u collected in heating water is given as:

$$Q_u = A_c F_R[G_T(\tau\alpha)_n - U_L(T_i - T_a)] \quad (1)$$

Where, A_c is area of solar collector.

The instantaneous efficiency is given as,

$$\eta_i = \frac{Q_u}{A_c G_T} = F_R(\tau\alpha) - \frac{F_R U_L(T_i - T_\alpha)}{G_T}$$

T_i can be replaced by T_m which is the mean temperature water at inlet and outlet.

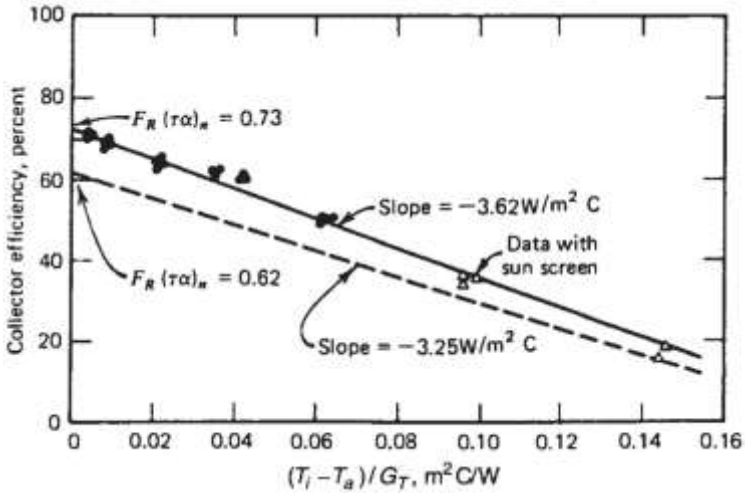

Figure 2-27 Test points for a liquid heater based on collector aperture area. [22]

This is the most standard way of evaluating the thermal performance of solar thermal collectors and is valid for establishing the thermal performance of BIPV-T. The scattering of points is due to variations in relative proportions of beam, diffuse, and ground reflected components, wind effects and angle of incidence. The graph shown in Figure 2-27 is used for designing solar thermal systems. This graph is shows efficiency with respect to inlet parameter $(Ti-Ta)/G_T$, the European method uses mean temperature *Tm* instead of inlet temperature *Ti*. In our work we used European standard which is more established and used by majority of countries.

The ELIOSYS Testing Laboratory in Belgium [23] tested and certified 250W monocrystalline PV-T module in accordance with IEC61215 and IEC61730. The unglazed, uninsulated PV-T module delivered 243.2W at STC and 166.3W at NOCT. The NOCT temperature recorded 49.5°C at 800W/m^2 solar radiation. The results are shown in Table 2-7(a), (b) and (c).

Table 2-7 Test results of DualSun PV-T module [23]

a) Temperature coefficient measurement [23]

Sample	T (°C)	P_{max} (W)	V_{oc} (V)	I_{sh} (A)	Temp. Coefficient	
PV: 130000562 TH: 24558/25	18	238.2	37.63	8.36	α (%/°C) Current Coefficient	0.048
	23	233.3	37.04	8.37		
	28	228.7	36.51	8.39	β (%/°C) Voltage Coefficient	-0.32
	33	223.3	36.05	8.41		
	38	217.8	36.34	8.43	Δ (%/°C) Power Coefficient	-0.44
	43	212.6	34.64	8.45		
	48	206.7	34	8.48		

Note: Temperature coefficients were calculated at 1000 W/m^2 solar radiation, T is cell temperature, P_{max} is maximum power, V_{oc} is short circuit voltage and I_{sh} is short circuit current.

b) Measurement of Normal Operating Cell Temperature (NOCT) [23]				
Sample	NOCT 1(°C)	NOCT 2 (°C)	NOCT 3(°C)	Final NOCT (°C)
PV: 130000562 TH: 24558/25	52.9	47.2	48.5	49.5
Note: Measurements are carried out at 800 W/m^2 solar radiation				

c) Performance at STC and NOCT [23]						
Sample		P_{max} (W)	V_{oc} (V)	I_{sh} (A)	V_{mp} (V)	I_{mp} (A)
PV: 130000562 TH: 24558/25	STC	243.2	37.73	8.47	29.89	8.14
	NOCT	166.3	33.77	6.67	26.33	6.32
Note: Both tests were carried out under a solar simulator STC: Standard test condition,1000W/m^2 solar radiation, 25°C cell temperature, Air Mass 1.5 V_{mp} is voltage and I_{mp} is current respectively at maximum power						

One of the drawbacks of DuelSun PV-T module is that cooling plate does not cover all solar cells. They used junction box at the top where cooling of top rows of cells cannot take place. The cooling plate does not even reach to the bottom row of solar cells. The cooling water flows from bottom end and exits at top end of the PV-T collector. This will result in top row and bottom row of solar cells getting much hotter than the solar cells in the middle of the PV-T module. A thermal imaging of cooling should have been performed to know how much non-uniformity is resulting in cooled and uncooled solar cells. Normal operating cell temperature (NOCT) upto 52.9°C is recorded for uncooled module. With metal heat exchanger pasted at the back NOCT should have been lower.

Goh Li Jin, *et al.*, [24] fabricated a split flow PV-T design using copper tubes placed below a PV panel working as a heat absorber as shown in Figure 2-28 and Figure 2-29. The collector was tested indoor under various solar irradiances and different fluid flow rates. The electrical and thermal efficiency of the PV-T collector was presented for various solar intensities and flow rates under indoor test conditions as shown in Table 2-8. The electrical efficiency varied from 4 to 6%, whereas the thermal efficiency reached a maximum of 57%.

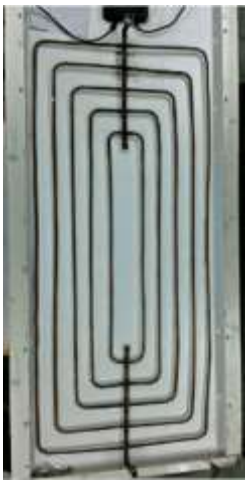

Figure 2-28 Actual split flow absorber design [24]

Figure 2-29 Thin aluminum foil is placed on all copper tubes [24]

Table 2-8: Electrical and Thermal performance [24]

Solar irradiance	Fluid flow rate	PV cell temperature	Temperature difference	Electrical efficiency	Thermal efficiency
W/m^2	LPM	°C	*(To – Ti)*, °C	%	%
300	0.5	48.45117	5.226835	4.73656	55.37142
300	2.0	43.8185	0.18773	5.215432	7.955025
300	4.0	46.23478	1.549316	5.100551	131.3303
600	0.5	57.76924	4.90951	5.174498	26.00489
600	2.0	57.19538	2.238415	5.659525	47.42611
600	4.0	56.93749	1.004594	5.96784	42.57801
800	0.5	66.82916	5.577729	-	22.15825
800	2.0	65.9006	2.885635	-	45.85424
800	4.0	61.74425	1.797308	-	57.1319

Note: Where *Ti* is inlet temperature and *To* is outlet temperature of cooling water

The temperatures and efficiencies in Table 2-8 are shown in six decimal places which is unnecessary for evaluating performance of a PV-T modules. The spit flow water cooling design used here is awkwardly place at the back of solar module. The cooling pipe does not reach upto the top row of solar cells because of junction box. Both inlet and outlet header pipes are vertical and distributes water to concentric pipes to cool the back of solar panel. The cooling water flow path for outer most pipes takes longer cooling path than the one in the inner most pipes. The cooling water at the exit of the outer most riser pipes will pick up more temperature than other pipes which traverse to shorter distance. This is a very bad design for cooling PV-T module causing non-uniform cooling of solar cells. Individual cell temperatures or temperature distribution of cells from top has not been measured to know the extent of mismatching. Since there is no cooling sheet attached to pipes the cooling of solar cells will be along the length of pipe and not the complete area of solar cells. The PV module used is rated at 110W having area of 0.97 m^2 with 11.35% efficiency at STC. This module should have delivered 9.17% efficiency at 600W/m^2 and cell temperature of 56.94°C instead it is delivering only 5.97% efficiency. The thermal efficiency is at 600W/m^2 is 45.58% which gives overall efficiency of 51.55% even though PV-T electrical efficiency is 3.2% lower than expected. The article does not explain how thermal efficiency of 131.33% is achieved at 300W/m^2 solar radiation.

2.2 Shortcomings in cooling configurations in photovoltaic modules

The past 10 years saw significant research advances in PV-T and BIPV-T solar modules. Our novel water-cooling pipe configuration for BIPV-T was conceived after noting shortcomings in various designs presented in this section.

Popescu, *et al.*, [25] analyzed photovoltaic thermal collectors and proposed an enhancement of heat transfer from the photovoltaic panel to a cooling fluid as shown in Figure 2-30. The inlet and outlet are shown in blue and red arrows respectively.

The water cooling circuit follows oscillatory design where water flows up and down the PV-T module. The overall energy conversion increases from about 12 – 15% (electrical only) combined electrical and thermal 86% which is highest reported ever.

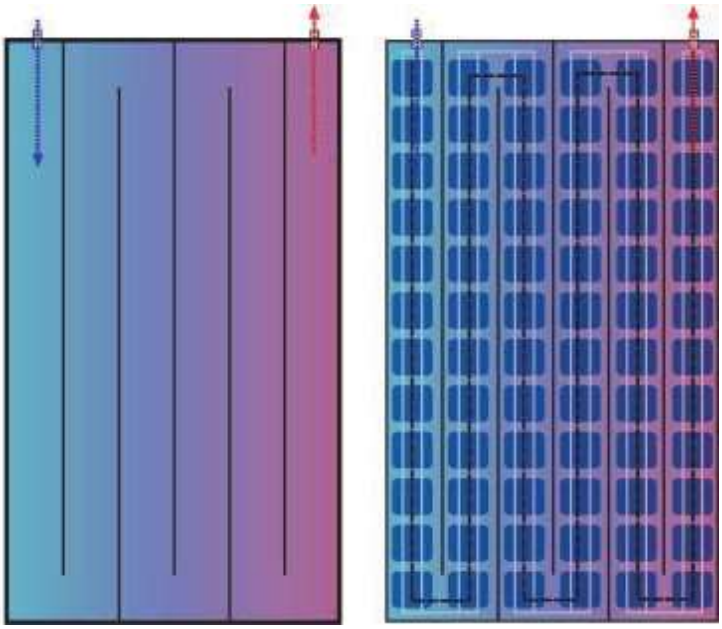

Note: Inlet and outlet are shown in blue and red arrows respectively

Figure 2-30 PV cell matrix arrangement and water circulation in PV-T module on the right and insulated back on the left [25]

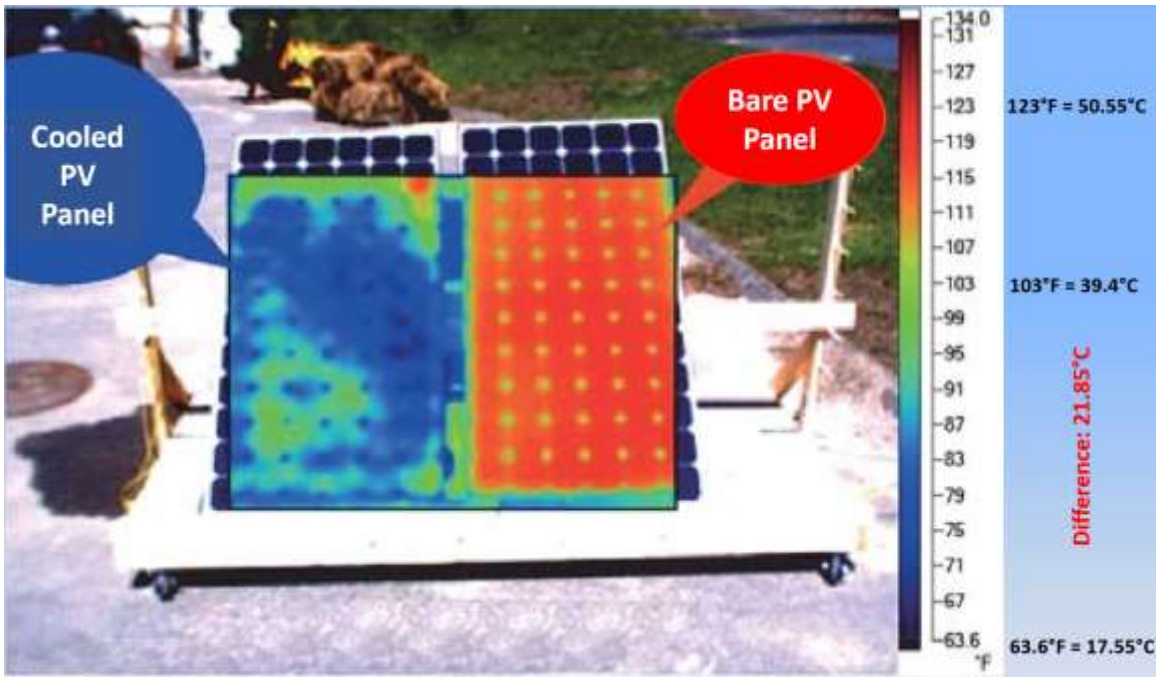

Figure 2-31 SunDrum solar PV-T system thermal data [25]

Adopting a conventional solar water heating pipe layout for PV-T modules is not a good approach. The Figure 2-31 shows very poor cooling uniformity that will damage the PV cells in the long run due to mismatching causing hot spots. The thermal imagery of cooled PV-T module shows many hot spots due to non-uniform cooling. The temperature difference is about 22°C and the cell at the exit point of cooling water shows even higher temperature over 50°C. Even one cell mismatch can cause serious damage to any PV module.

Sebastian Dittmann [26] studied unglazed PV-T collector performance in indoor and outdoor conditions. He used 60 cell module with 240W output at STC. The indoor study was done by circulating hot water at 55°C. The infra red image Figure 2-32 shows 20.2°C from hottest to coldest spot in the PV-T module. In outdoor conditions difference in hot to cold spots of PV-T module increases to 23.02. The picture shows sinusoidal type cooling pipe.

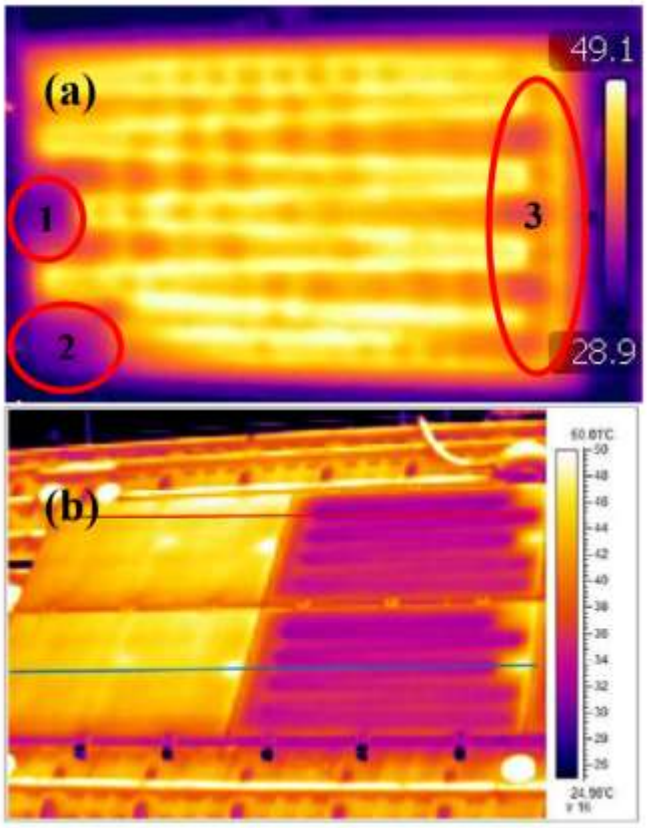

Figure 2-32 (a) Infrared image of the PV-T collector with a fluid temperature of 55°C and an ambient temperature of 25°C (no solar irradiance). (b) PV-T collectors in real operation conditions and equivalent PV modules without heat exchanger, i.e. without cooling [26]

The temperature inhomogeneity is clearly visible in Figure 2-32(a) at 55°C fluid temperature in indoor testing. The temperature difference between low to high is 20.2°C. The temperature variation in outdoor PV-T testing in sunlight is shown in Figure 2-32(b). The inhomogeneity increased to 25.1°C. This is major problem in using water cooling pipe configuration meant for solar water heater where temperature uniformity is tolerable. The PV cells in module need cells temperature uniformity within close tolerance to prevent hot spot formation which can damage the solar cells.

TUV Reinland Energie Laboratory in Germany [27] tested and certified a commercial model of Photovoltaic-Thermal collector from DualSun, France. In this design, the cooling plate was made from two stainless steel sheets spot-welded together and pasted at the back of photovoltaic module for better heat transfer contact. The testing was done in an indoor steady-state condition where inlet water temperature, ambient temperature and wind speed could be controlled. The thermal efficiency reach upto 56% at 818W/m^2 solar radiation, wind speed 0.9 m/s and ambient 23.77 °C and electrical efficiency of 10.15% at cell temperature of 65.6°C (dropped from 14.66% at STC) The stagnation temperature of the PV module reached 72°C without any insulation. The PV-T module achieved overall efficiency of 66.15%.

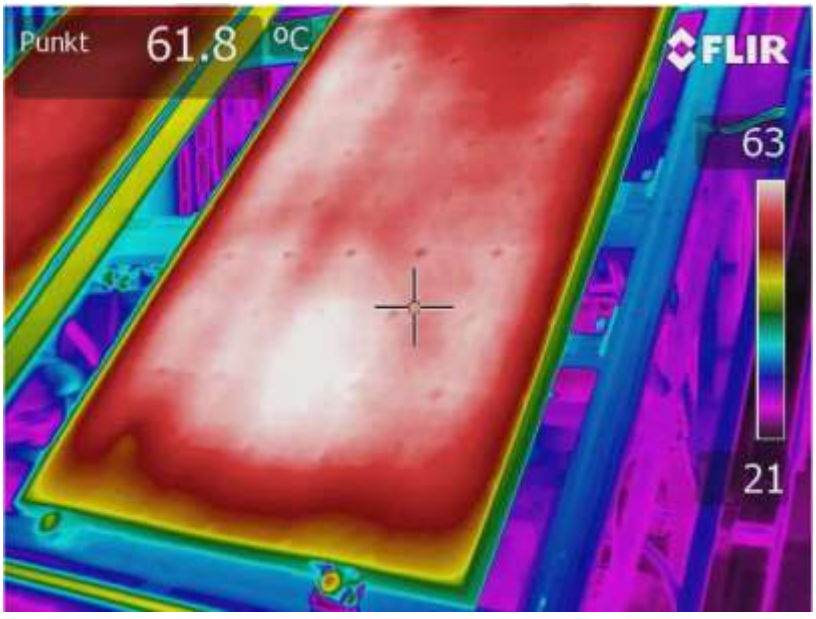

Figure 2-33 Thermography stagnation front side of DuelSun PV-T module [27]

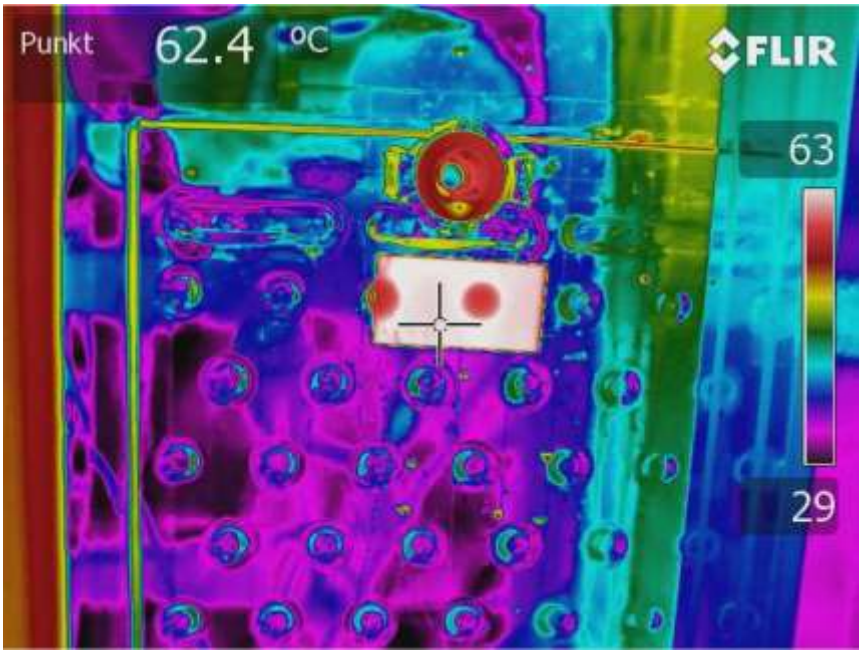

Figure 2-34 Thermography stagnation back side of DuelSun PV-T module [27]

Comments [27]**:**

Referring to Figure 2-33 and Figure 2-34, the certifying agency TUV observed high stagnation temperature variation 42°C from top and 34°C on the cooling plate attached at the back of the PV-T module. This is another example of non-uniform heating of cell in sunlight if cooling sheet is not transferring the heat uniformly from the back of the PV-T module. The actual outdoor testing conducted by DualSun company is described in reference [28] in next review.

Laetitia Brottier et al [28] published simulated study and actual test results of temperature distribution of unglazed BIPV-T module with 60 cells using stainless steel plate type cooling system. The infra-red measurement shows 32°C difference in cold to hot spot in the module Figure 2-35(a) and (b). The high temperature differential all around is due to cooling plate being smaller than full size of the PV-T module. The water enters from the bottom and exits from top of module.

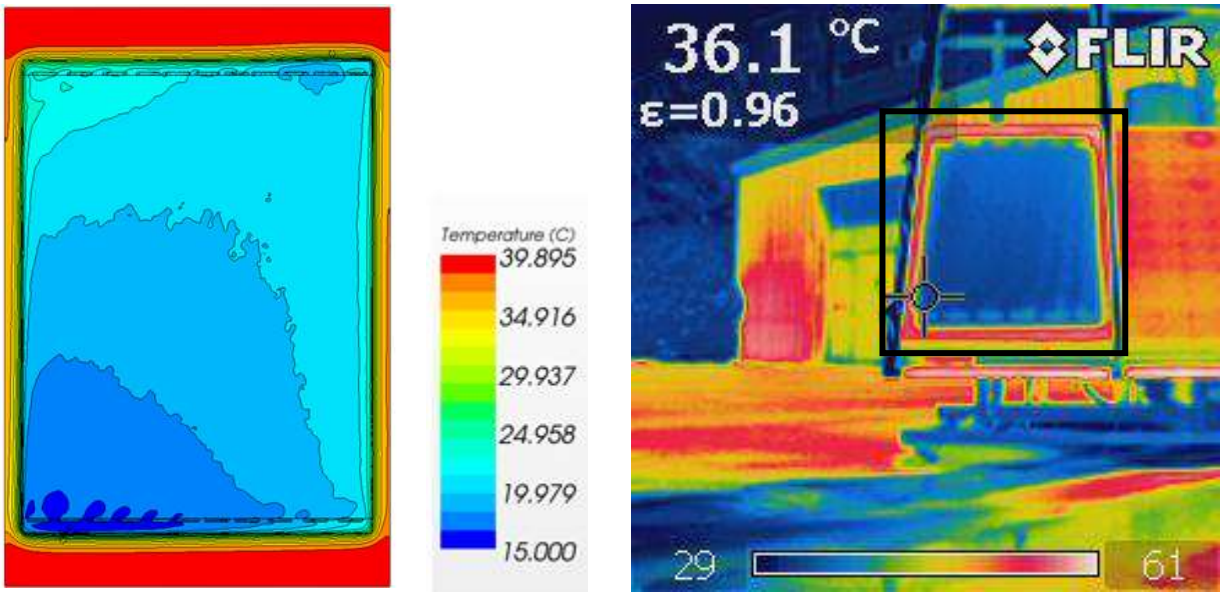

(a) (b)

Figure 2-35 Temperature field: (a) Computational fluid dynamics (b) Infra-red measure [28]

The Figure 2-35(a) is the simulated thermal image while Figure 2-35(b) is the actual testing using a sun simulator. The PV-T module is shown inside black line in Figure 2-35(b). The temperature of the module is lowest at the bottom where cooling water enters and the temperature is highest on the edges where cooling plate is not extended due to presence of PV-T junction box at the top. There are three defects in this cooling plate. The first defect is that cooling plate is not covering the complete length and width of the module and second defect is that the water moves from bottom to top. Therefore, top row are solar cells in PV-T modules are much hotter than at the bottom. There is third defect as seen in Figure 2-35(a) where flow path of cooling water is not moving uniformly instead it is moving toward path of least resistance. This third defect can be sorted out if cooling water flows at adequate pressure depending on collector size and construction. This kind of non-uniform cooling is damaging to solar cells in PV-T module. Mismatch of temperature will give rise to hot spots which can cause premature failure of the module.

Yihua Hu [29] studied the effect of mismatching in series connect PV modules. His investigation is based on conventional PV module which discusses mismatching fault and uses thermography based temperature distribution analysis. He studied three different cases viz minor mismatch, medium mismatch and heavy mismatch using thermography. Minor mismatch is shown in Figure

2-36. He reported that the minor mismatch cell temperature rises to 87.2°C while normal cells operate at 44.3°C, a difference of 42.9°C. Minor mismatch is most detrimental as there is no protection built into the module. For medium and heavy mismatch built-in diodes in junction box protect the modules. In our study it is the minor mismatch that occurs due to non-uniform cooling.

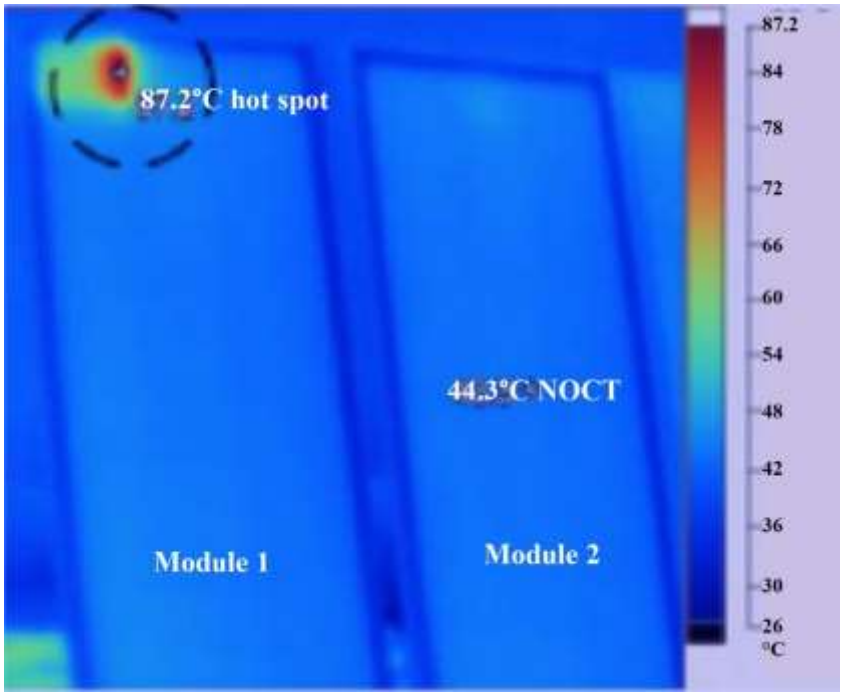

Figure 2-36 Test at a minor-fault condition-Output characteristics and thermography [29]

The type of mismatch shown in Figure 2-36 can occur in BIPV-T module due to non-uniform temperature in series connected solar cells. It will ruin the solar cells subjected to hotspot. The hot spot temperature is exceeding the test condition of 85°C for certified PV modules. Therefore, uniform cooling method as proposed in our multiple sub-header design will prevent such defect to arise.

Ibrahim, *et al.*, [30] conducted a simulation study on various types of water cooling pipe design for PV-T collectors. As in the previous study, the best performance was achieved for the Spiral Flow design of PV-T collectors with a thermal efficiency of 51.4 % and PV cell efficiency of 11.98%. These multiple cooling pipe configuration shown in Figure 2-37 to Figure 2-38 are intended to cool PV cells to increase electrical output.

In direct flow design shown in Figure 2-37 the cooling water enters on one end at the bottom, flows through several parallel pipes and comes out on the other end at the top. On the top end large space

has been left open probably for junction box. There are two problems that will cause non-uniform cooling of solar cells. One the water flow goes over many cells before exiting which will result in different temperature of all cells through which it moves. Secondly, the solar cells under the large uncooled opening will operate at much higher temperature causing mismatching losses.

In spiral flow design shown in Figure 2-38 the cooling water enters on one end at the bottom and moves in spiral fashion to the center of the PV-T module, then it moves backwards returning with heated water before coming out at the top end. This design has two problems, one that cooling water picks up heat from entry to center from one part of solar cells it cools, then it returns over the same cells before exiting. Firstly, it has long path going into the center of the module picking up heat causing each cell to operate at different temperature. Secondly, when it returns through another portion of same solar cells the water temperature will be higher thus non-uniformity of temperature will occur for each cell. This will cause more losses in each cell.

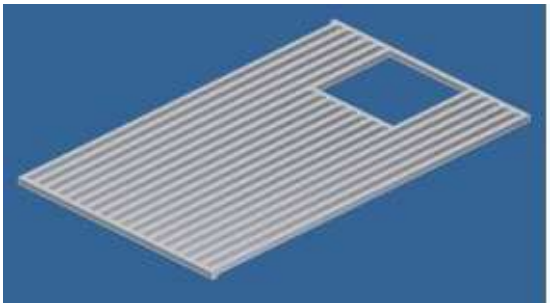

Figure 2-37 Direct flow design [30]

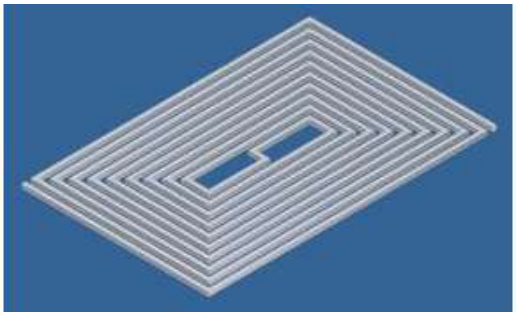

Figure 2-38 Spiral flow design [30]

Oscillatory flow design as shown in Figure 2-39 and Serpentine flow design shown in Figure 2-40 lets the water flow over number of cells in a PV-T module before coming out. Each cell through which the water flows will dissipate heat which will be transferred to next cell and so on. These two designs are non-uniform cooling scheme.

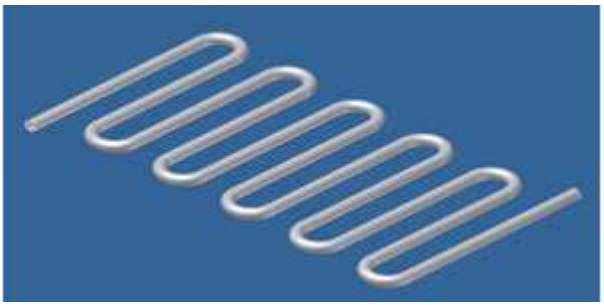

Figure 2-39 Oscillatory flow design [30]

Figure 2-40 Serpentine flow design [30]

The parallel-serpentine flow shown in Figure 2-41 have same disadvantage as in direct flow and serpentine flow explain for Figure 2-37 and Figure 2-40. All cells will operate at different temperatures as the cooling water picks up heat.

The web flow design as in Figure 2-42 has no specific pattern. The water enters from one end of the pipe, moves to center then to the other end of the web and returns back to same end as inlet to exit. This design will have cooling water in different part of the module causing non-uniformity.

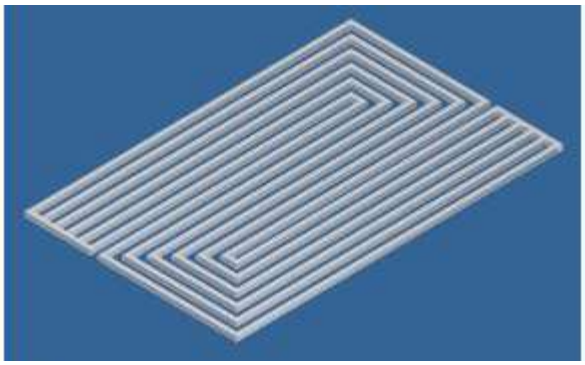

Figure 2-41 Parallel-serpentine flow design [30]

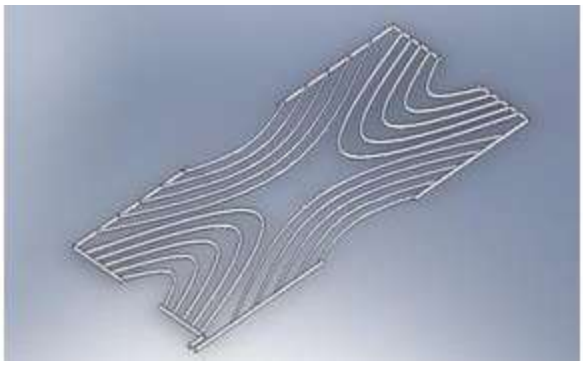

Figure 2-42 Web flow design [30]

Modified serpentine-parallel flow design as shown in Figure 2-43 has six parallel flow path cooling water that enters from one end to the end. Then it returns back to inlet end moving over the center of the PV-T module then again goes back to opposite end to exit. It has similar non-uniform cooling pattern as discussed in parallel-serpentine design shown in Figure 2-41.

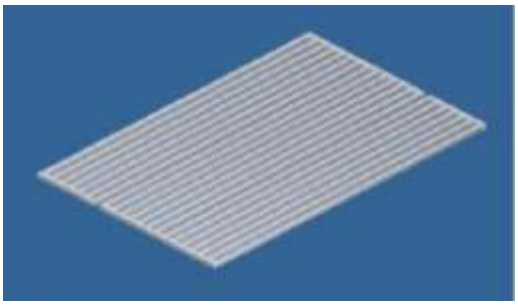

Figure 2-43 Modified serpentine-parallel flow design [30]

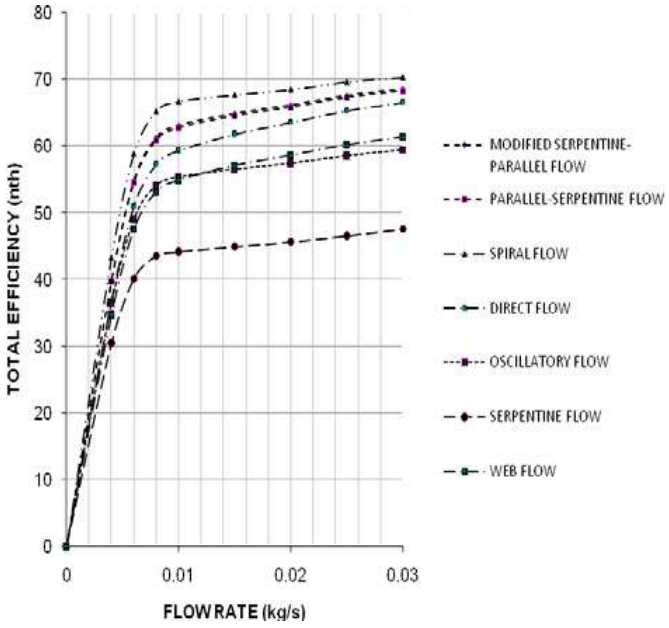

Figure 2-44 Flow rates configuration of various absorber collectors [30]

None of these configurations will cool all cells uniformly causing current output to vary for each cell. The mismatching of current output will result in reduced performance and in the long term will cause damage to the module.

Alboteanu, *et al.*, [31] proposed a cooling system for photovoltaic modules as shown in Figure 2-45. The infrared images show a PV module maximum temperature of 51°C in front and 42°C at the back when the cooling water was not circulated. The module temperature dropped to 39°C at the highest point at the back of the module when cooling water was circulated. Though simulation result showed module temperature variation less than 1°C, the actual testing showed temperature variation on the surface of module exceeded 10°C.

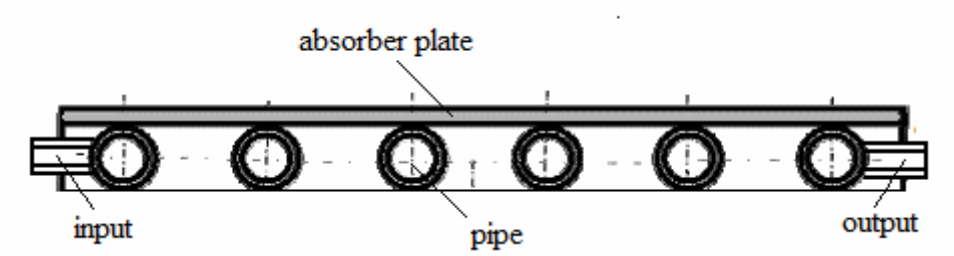

Figure 2-45 Section of cooling system [31]

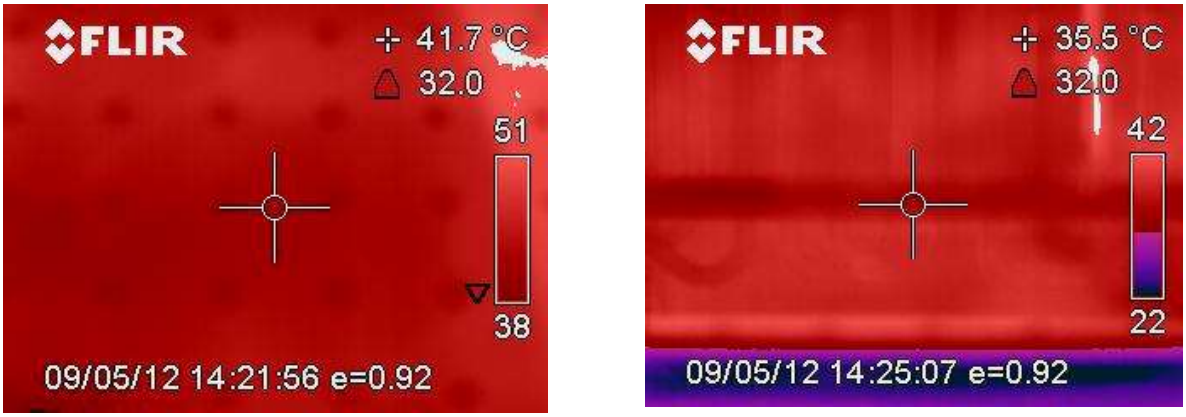

(a) (b)

Figure 2-46 (a) Captured image on the front surface of PV module, (b) Captured image on the back surface of PV module with disconnected water pump. [31]

Figure 2-47 Captured image on the back surface of PV module with connected water pump. [31]

This is a parallel flow design of cooling tube where water enters at the bottom of PV-T module and exits at the top end. The cells will have cooling from one end to the other where water will pick up heat from one cell and goes over next cell till it reaches the exit. The cells temperature will vary from one end to the other. A 150W, 72 cell PV-T module was tested outdoors. The water temperature between inlet and outlet was about 2°C but cell temperature as per thermal imaging show more than 10°C temperature across solar cells. A water pump was used to circulate water but there is no mention of flow rate. Like any conventional parallel flow design this too will cause mismatching of solar cells output due to non-uniform cooling.

Ahmed Fudholi, *et al.*, [32] investigated the performance of three types of PV-T water collectors direct flow, spiral flow and web flow designs consisting of a combined PV module and an absorber collector. The results indicated that the Spiral Flow absorber produced the best result at 800W/m^2 and 0.041kg/s water flow rate, achieving a PV efficiency of 13% and thermal efficiency of 54.6%. The test shows that the efficiency increases as the mass flow rate increases; however, the temperature decreases after a mass flow rate of 0.024kg/s. This similar to the problem discusses in [30] before except that actual product was fabricated and tested.

Table 2-9 PV-T Solar Collector Characteristics [32]

Description	**Symbol**	**Value**	**Unit**
Ambient temperature	T_a	20	°C
Collector area	A_c	0.65	M2
Number of glass cover	N	1	-
Emittance of glass	ε_g	0.88	-
Emittance of plate	ε_p	0.95	-
Collector tilt	ɵ	14	-
Fluid thermal conductivity	k_f	0.613	W/m°C
Specific heat of working fluid	C_p	4180	J/kg°C
Back insulation conductivity	k_b	0.045	W/m°C
Back insulation thickness	l_b	0.05	m
Insulation conductivity	k_e	0.045	W/m°C
Edge insulation thickness	l_e	0.025	m
Absorber conductivity	k_{abs}	51	W/m°C
Absorber thickness	l_{abs}	0.002	m
Fin conductivity	k_f	84	W/m°C
Fin thickness	δ	0.0005	m
Heat transfer coefficient from cell to absorber	h_{ca}	45	W/m°C
Heat transfer inside tube	h_{fi}	333	W/m°C
Transmittance	τ	0.88	-
Absorptance	α	0.95	-

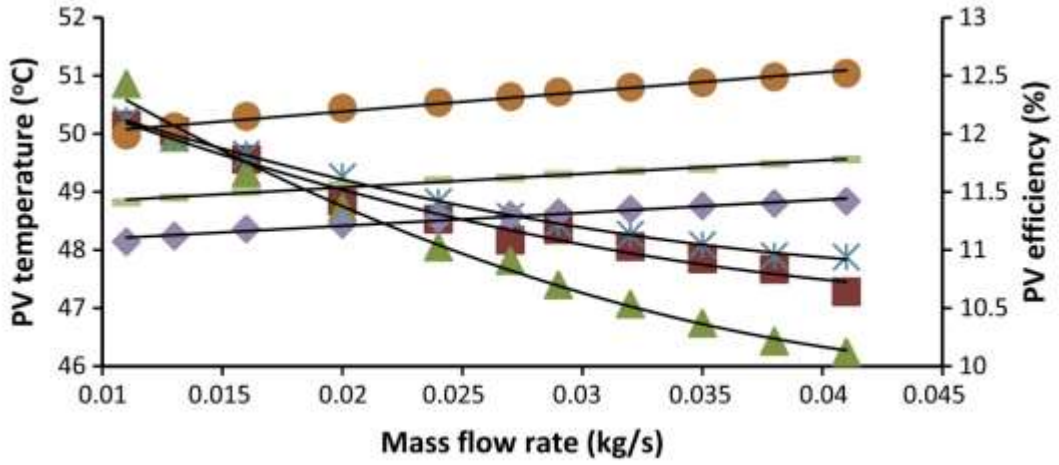

Figure 2-48 Changes in PV efficiency with the mean PV temperature of the PV-T absorber collector under 800 W/m^2 of solar radiation. [32]

The three designs studied here have already been analysed in simulation study [30] and our opinion is that none of these three designs will have uniform cell temperature. Since the specification of PV module is not mentioned it is difficult to ascertain the performance increase shown in Figure 2-48.

Allan, *et al.*, [33] studied serpentine and header-and-rise types of water cooling pipe layout for PV-T collectors. They concluded that for the same mass flow rate, the serpentine layout has superior performance due to a reduced heat loss coefficient. Also, the use of a cover reduces the overall heat loss coefficient of the serpentine collector by 50%. They stated that in PV-T collector, the thermal efficiency is the biggest contributor to overall output. The Figure 2-49 and Figure 2-50 shows the electrical, thermal and combined power of PV-T module with serpentine and header-riser water cooling pipe performance respectively. The header-rise is same as parallel flow shown in Figure 2-13. The serpentine flow showed better thermal output than header and riser flow. However, the temperature distribution of the PV-T collector is shown in Figure 2-51 show both serpentine and parallel flow design will have non uniform cooling of solar cells. All tests were done using indoor sun simulator.

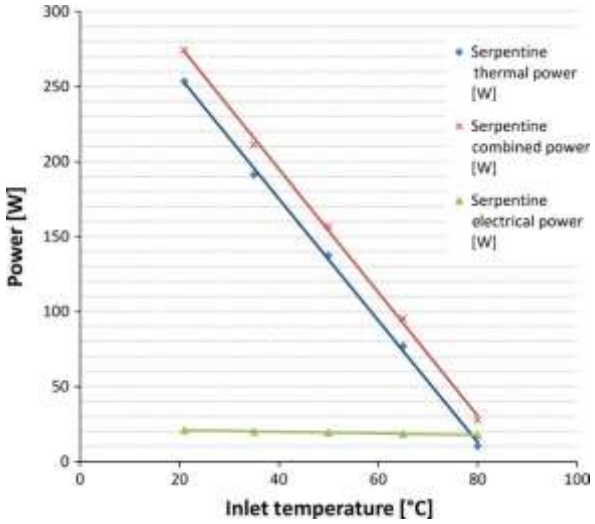

Figure 2-49 Combined power output of an uncovered serpentine PV-T collector [33]

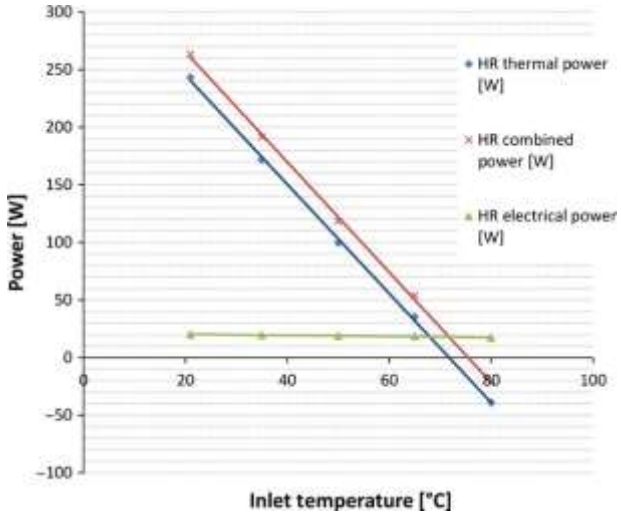

Figure 2-50 Combined power output of a header riser PV-T collector [33]

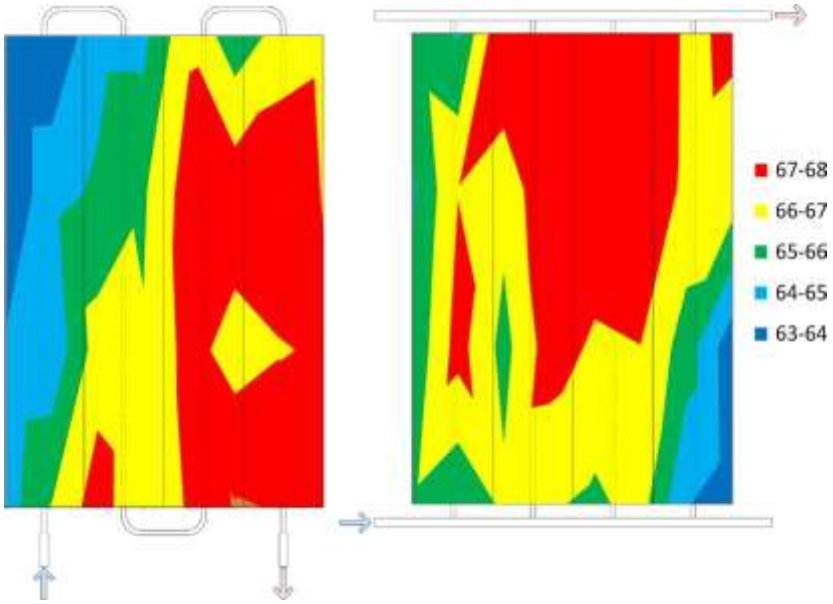

Figure 2-51 Temperature comparison of temperature distribution for serpentine (left) and header riser (Right) uncovered absorbers at inlet temperature [33]

In this study two unframed PV module of size 785mm x 129mm with 6 monocrystalline cells were used in both cases. The PV-T area of 785mm x 568mm was used. The combined efficiency of serpentine cooling configuration reached 61% overall efficiency and 8% electrical efficiency with 21°C water inlet temperature. A non-uniform cooling along the flow path of both types of cooling

configuration is visible in Figure 2-51. The hotter portion of cells are most toward exit of cooling water flow. The length of module is small so the temperature distribution show only 3°C difference from inlet to outlet of PV-T module. Longer PV-T will have much more temperature differential in serpentine configuration than header-tube configuration. Indoor study in controlled environment does not give the field performance which will show the actual picture.

Buonomano, *et al.*, [34] conducted numerical and experimental analyses for evaluating the technical and economic feasibility of PV-T collectors. The experimental setup was modelled and partly simulated in the TRNSYS environment. In this experiment, the performance comparison was made with identical conventional PV modules. The simulated results show that the overall PV-T efficiency is about 26%. The experimental results obtained shows the average thermal efficiency of PV-T collectors is around 13% and the electrical efficiencies of both technologies are almost coincident and equal to 15%.

The electrical energy produced by the PV panels (1778 kWh/year) is higher than the PV-T one (1156 kWh/year) from a 6.5m^2 total collector area. PV-T collectors additionally produce a significant amount of thermal energy (1433 kWh/year).

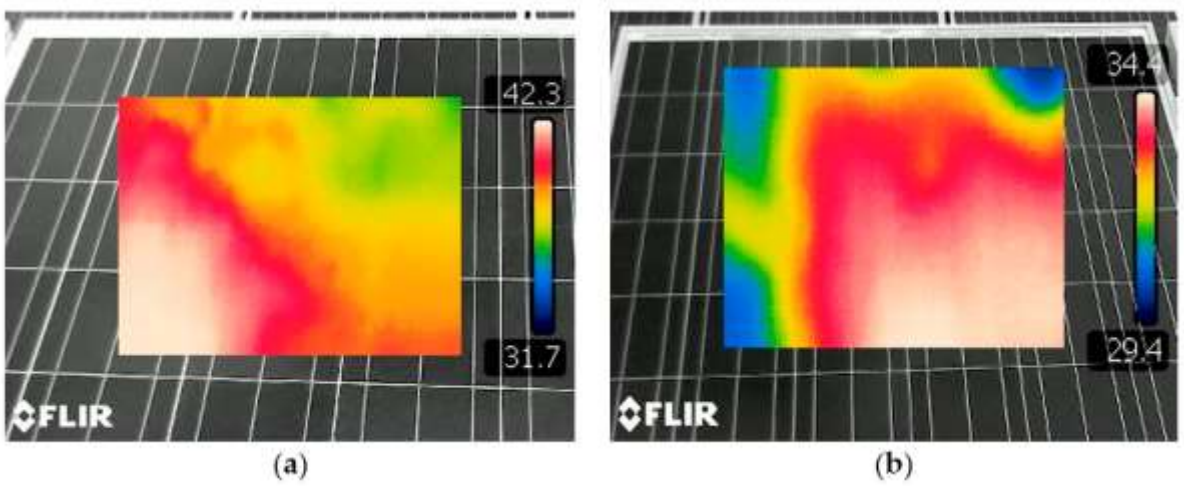

Figure 2-52 (a) PV panel and (b) PV-T collector. Temperature by thermal imaging camera [34]

A flat polycrystalline silicon unglazed PV-T solar collectors (called Janus), for the production of electricity and thermal energy. Basically, a Janus collector is made by an aluminium plate integrated with a conventional PV panel by a thin butyl layer. The aluminum plate with cooling water channel does not extend upto top and bottom row of solar cell. Figure 2-52(a) and (b) looks

like not showing temperature distribution of full module. The PV-T shows only 5°C difference in temperature distribution which is not possible if cooling water is not flowing over top and bottom row of cell. Even for middle portion. The thermal image of the PV-T collector shows non uniformity in cooling the solar cells.

Longsheng Lu, *et al.*, [35] worked on a concept of a water-based PV-T collector in which solar cells were directly placed on the bottom of its glass cover as seen in Figure 2-53(b). The PV-T collector was tested in thermosiphon mode for evaluation. The new PV-T collector exceeded the electric performance of a traditional PV-T by nearly 10% but exhibited a 30% lower thermal efficiency.

As the covering factor increased, the electric efficiencies of both the new and the traditional PV-T collectors went up gently, and the thermal efficiency of the new PV-T collector dropped more than that of the traditional one. As the covering factor was changed from 0.05 to 1, the thermal efficiency of the new PV-T dropped nearly 70%.

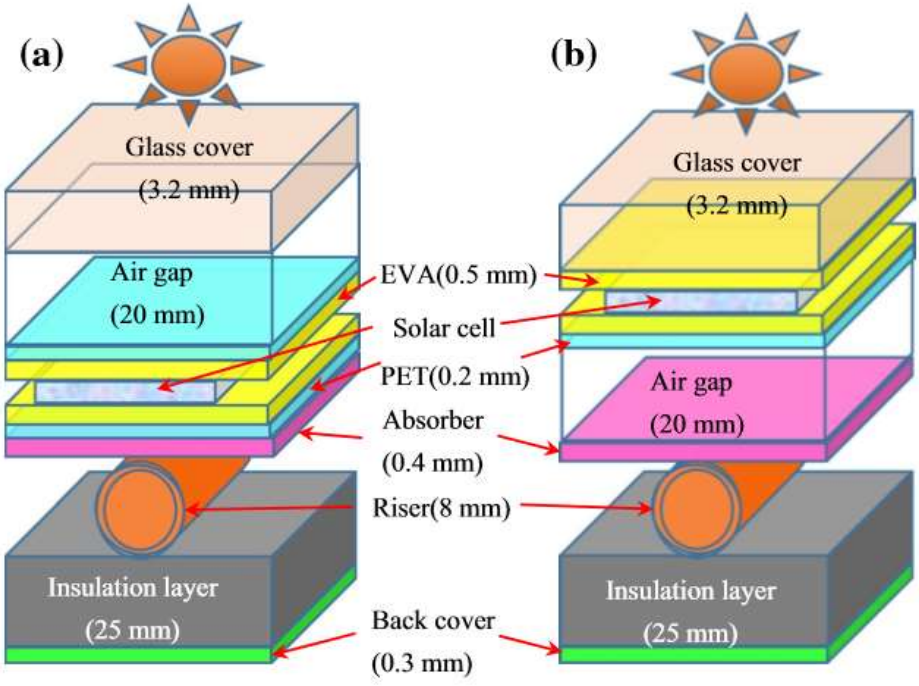

Figure 2-53 Cross section of the PV-T solar Collector: (a) Traditional PV-T; (b) New PV-T. PET polyethylene terephthalate, EVA ethylene-vinyl acetate copolymer [35]

As the water mass in tank increased, the thermal efficiencies of both the new and the traditional PV-T collectors grew moderately, but their electric efficiencies remained almost constant. When

the water mass increased from 100 to 300kg, the final water temperature in the tank of the traditional PV-T collector declined more than 17°C, whereas that of the new one declined less than 6°C.

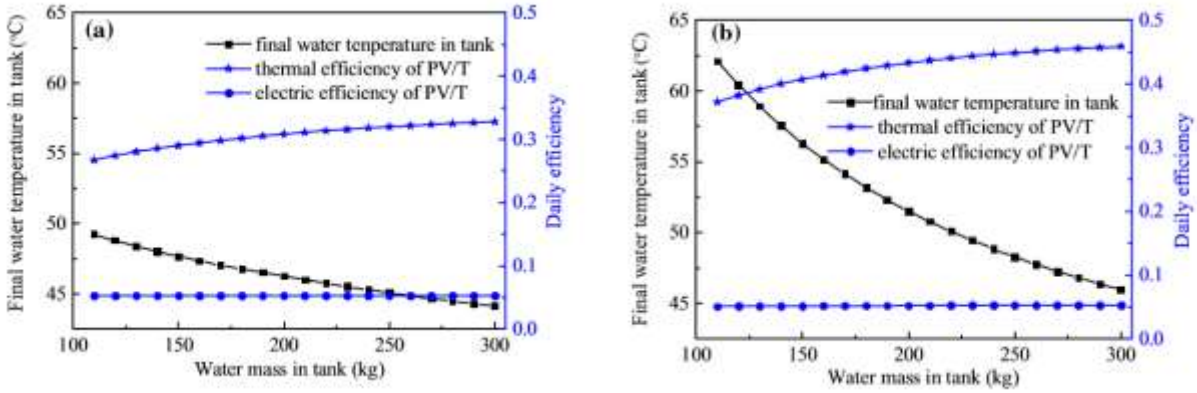

Figure 2-54 Effect of water mass in tank on the performance of PV-T collectors in simulation: (a) New PV-T; (b) Traditional PV-T [35]

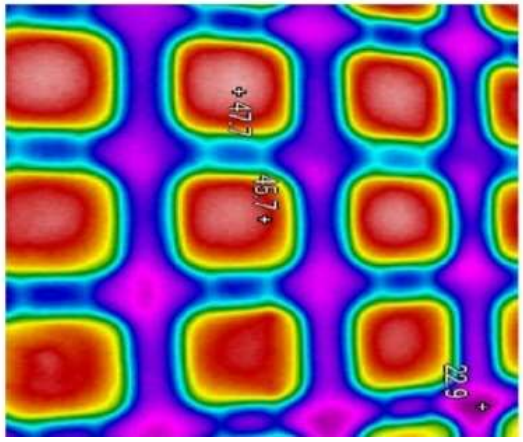

Figure 2-55 Infrared thermographic image of the glass cover of the new PV-T (°C) [35]

The thermal imaging of PV-T collector show non uniformity in cell temperature which is clearly visible in Figure 2-55. This is one reason why the new design of PV-T collector did not perform well. Also providing the 20mm air gap between the back of PV module and absorber plate as shown in Figure 2-53(b)is not a good idea. The air will act like an insulator and prevent good transfer of heat from PV module to cooling absorber.

The solar cell best efficiency status report published by National Renewable Energy Laboratory (NREL), USA, [36] shows that monocrystalline cells laboratory efficiency reached 25.3% and polycrystalline cell efficiency reached 22.1%. See Figure 2-56 for year wise progress in silicon

based solar cells efficiency. In 1977, the monocrystalline cell best efficiency recorded was 13.5% implying an increase of 11.8% in 40 years, which works out to only 0.295% per year. Similarly, for polycrystalline, the best cell efficiency increased at the rate of 0.245% per year. The reason we selected to show Figure 2-56 with only silicon solar cells because silicon cells have 95% of world market.

Since achieving higher solar cell efficiency over the year is so low [36], it is very important to find ways to operate the solar modules at highest operating efficiency. The BIPV-T modules operate at higher temperatures, reducing the efficiency of solar cells. Therefore, cooling BIPV modules by water circulation will help in increasing the efficiency. Further to minimize mismatch losses the cells must be cooled uniformly. Also, BIPV-T modules provide extra thermal energy which boosts the overall energy output.

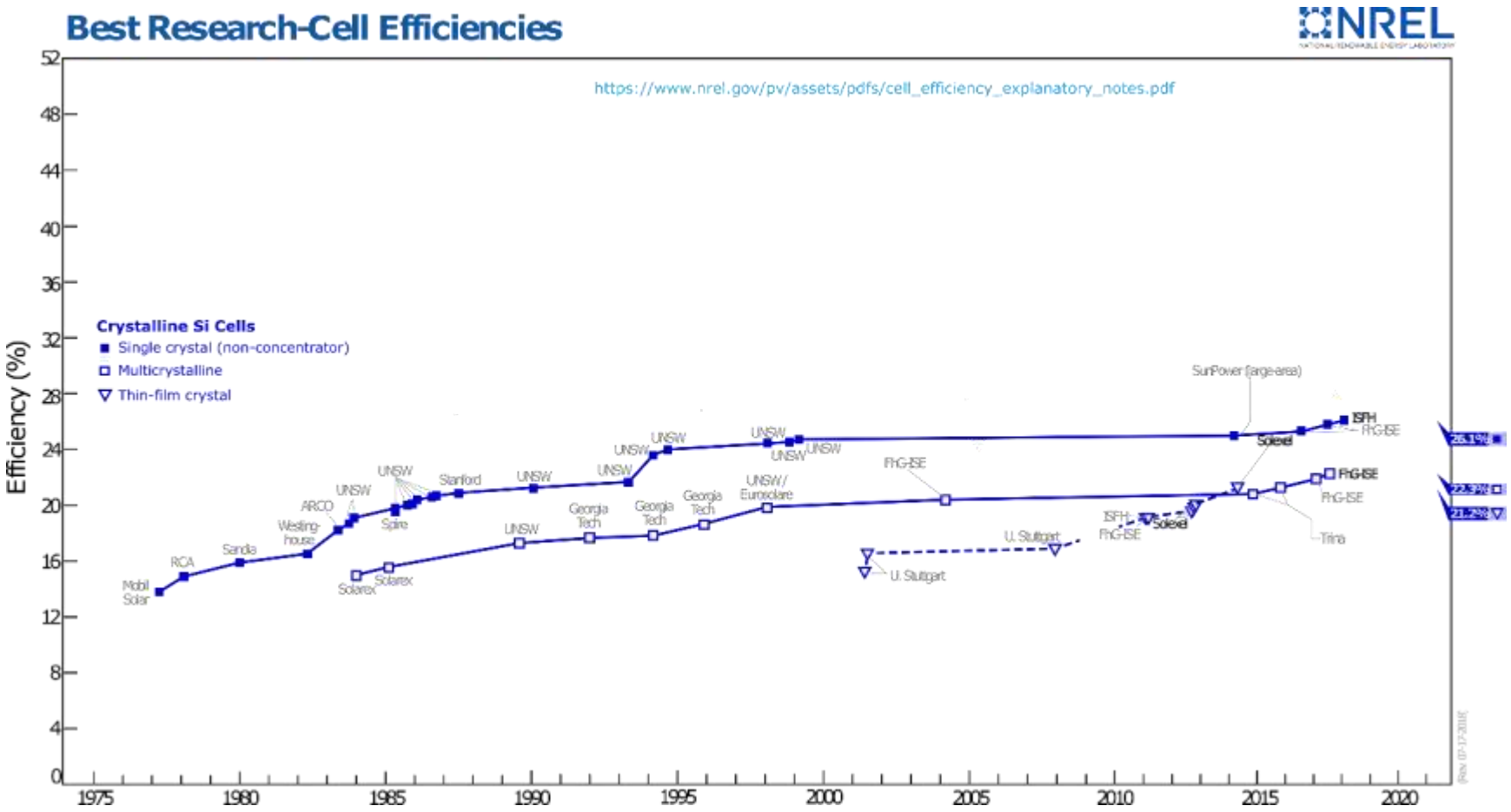

Figure 2-56 Mono, Poly and Thin film crystalline Solar Cell efficiencies since 1977 [36]

Table 2-10 Summary of review of BIPV-T and PV-T modules and cooling pipe matrix

Type of Review	Results	Reference
Mounting Flushed with roof	Operating temperature of PV module reaches 18°C above Normal Operating Cell Temperature (NOCT).	Stultz [1]
	Installed operating temperature (INOCT) reaches 17-20°C above NOCT.	Martin K. Fuentes [2]
	Integrated (BIPV) modules can reach 36°C as compared to standalone in no wind conditions.	Tomas Mastuska [21]
Mismatch of solar cells in a PV module	Minor mismatch of one solar cells in a PV module can reach >87°C as by-pass diode protection works only in medium or major mismatch.	Yihua Hu [29]
Water Cooled PV-T and BIPV-T modules	5% deviation between modeling and experimental performance of spiral flow cooling pipe configuration was achieved. Thermal efficiency of 33% and PV efficiency of 6.7% was obtained.	Zondag H. A., *et al.* [4]
Advantages and Disadvantages of PV-T and BIPV-T modules	The PV-T module can get very hot if heavily insulated that can cause damage if cooling fluid circulation fails. Saves space and installation cost as compared to separate PV and solar thermal collector installations.	Miroslav Bosanac, et al., [5]
Effect of operating temperature on PV-T modules	Insulated PV-Twin operates at 77°C at 835W/m^2 solar radiation and power drops by 36% as compared under standard test condition (STC). Thermal efficiency gained 34-54%.	Ivan Katic [8]
Water cooling circuit layout for PV-T modules	Theoretical analysis reveals that performance of split flow water cooling is better than direct flow and parallel flow design.	Sopian, *et al.* [14]

	The simulation study on 7 different water cooling pipe matrix conducted shows spiral flow performs the best amongst seven designs.	Ibrahim, *et al.* [30]
Non uniform cooling of solar cells in a module causing mismatching	For 72 cell module with spiral flow water cooling layout, the lowest to highest cell temperature varied by 22°C.	Popescu, *et al.* [25]
	For 60 cell module using stainless steel absorber, the lowest and highest cell temperature varied by 32°C.	Laetitia Brottier et al [28]
Best research efficiency of crystalline solar cells	From 1977 to 2018 the laboratory cell efficiency of monocrystalline reached 25.3% from 13.5%. whereas for polycrystalline 22.1%.	NREL, USA, [36]

2.3 Conclusion

The review of past work attributed to developments, studies, proposed designs and configurations, testing and certifications for water-based cooling of PV-T and BIPV-T technologies reveals that:

1. Individual solar cell cooling within a solar module has not been considered;
2. The importance of uniformity in cooling of individual cells has also not been proposed or studied. This counteracts the effort by the PV industry to use matched solar cells in a module;
3. The stagnation temperature of some of the certified PV-T design reaches close to the melting temperature of EVA encapsulant used in manufacturing of PV modules;
4. Some of the PV-T/BIPV-T configurations proposed are impractical for commercialization.

CHAPTER 3 OBJECTIVES AND THESIS ORGANIZATION

To address the aforementioned problems associated with Building-Integrated Photovoltaic Thermal (BIPV-T) modules, this study explores an approach within the parameters laid down by PV module test standards and the industry norms to achieve a reliable and durable product. Adherence to this standard is required to support the 25-year warranties offered by PV module manufacturers based on accelerated life testing conducted by certifying authorities. This study documents the design, fabrication, and testing of a suitable BIPV-T module and attempts to rectify any observed short comings.

3.1 Thesis Objectives

The main objective of the thesis is to design fabricate and test for the first time a new BIPV-T module which allow individual cooling of the solar cells of the module.

There are five specific objectives for this research work:

1. Develop a new BIPV-T module in which each cell of a PV module is cooled uniformly;
2. Conduct simulation studies on the electrical and thermal efficiency of a such BIPV-T module.

In particular, the software TRNSYS will be used to analyse the effect of various operating parameters on the performance of BIPV-T fabrication with individual cooling of the solar cells and compare them to those of conventional configuration where the cells are not cooled;

3. Design and fabricate a prototype of the BIPV-T module which respects the PV industry norms:
    a. Select a standard PV module already certified in accordance with IEC and UL norms;
    b. Design and fabricate a novel water-cooling copper tube configuration for this solar module and find means to attach it to a copper sheet to efficiently conduct the heat;
    c. Attach the sheet to the back of PV module using suitable means to conduct heat from each solar cells to the cooling water;
    d. Suitably insulate the back of the module to impede PV module cooling to simulate building integration.

4. Test and validate the electrical and thermal performance of this module. Accordingly, we will develop a suitable test rig to test the BIPV-T in accordance with European or ASHRAE norms. Accordingly, the following aspects will be considered and used:
    a. Mounting structure with adjustment for inclination;
    b. Water circulation at varying flow rate and pressure;
    c. Instruments to measure solar radiation intensity electrical output of the module. These will also help to measure the voltage, the current, the power, the ambient temperatures, the temperatures of the water inlet and outlet, the flow rate, the wind speed.
5. To test and validate the performance of new BIPV-T module.

The following achievements are expected with the results which will be obtained from the above objectives:

a. Better cooling of a BIPV-T module as compared to what has been achieved until now;
b. A new BIPV-T with individual cell cooling which leads to a uniform temperature.

3.2 Methodology

Approaches consist of using TRNSYS software to design a new BIPV-T where individual cells are cooled and to fabricate a prototype and test it. This will be done through the following steps:

1. Use TRNSYS software to simulate the temperature profile of each cell during cooling and determine the efficiency of the new BIPV-T. In particular, we will input parameters of individual items to be entered such as thermal conductivity of copper tube and sheet, sheet size and thickness, conductive silicone bind width and thickness, number of copper tube per cell, specific heat of water, size of solar cells, power of solar cells at reference solar radiation and cell temperature, temperature correction factor for power, resistance of solar module substrate and back material and reflectance and emissivity of glass cover, etc.
2. Fabricate a prototype of a BIPV-T based on the parameters used for the simulation. The main following steps for the fabrication of the prototype are used:
    a. Removal of PV module junction box to access the complete area at the back;

b. Gluing of copper sheet at the back of PV module using conductive adhesive and carefully pulling out electrical output through a slit form in copper sheet;

c. Preparation of a novel cooling pipe matrix for the uniform cooling of each solar cells;

d. Gluing of the novel cooling pipe matrix (layout) to copper sheet pasted at the back of the PV module;

e. Taking our electrical connection from top frame of the PV module using cable glands;

f. Packing insulation at the back of PV module and holding it in place with a sheet;

The PV module is now converted into a new BIPV-T module to extract heat from the PV module by cooling the solar cells uniformly.

3. Study the effect of the water cooling flow rate on the efficiency of the new design by achieving the following steps:

    a. Fabrication of the mounting structure for outdoor testing of BIPV-T module;

    b. Connection of a cold water tank to the bottom of BIPV-T module through a circulation pump and a battery operated water pump with an electronic controller to regulate the water flow rate;

    c. Taking the cooling water from the output for BIPV-T module out from the top and installation of the pressure gage and a shut off valve at the exit to increase the cooling water pressure for proper distribution of water in the cooling pipe;

    d. Installation of a water tank at the exit of the cooling water to collect the water after single pass through the BIPV-T module and a 2 litre graduated glass cylinder and stopwatch for measuring the water flow rate.

4. Measurement of the cell temperature and the BIPV-T module efficiency with the variation of the water flow rate. This will be achieved through the following step:

    a. Installation of the solar radiation intensity measuring sensor in the same plane as the BIPV-T module being tested;

b. Connection of an automated electrical output measuring device to the electrical wires of the BIPV-T module and utilisation of the power output and solar input for calculating the efficiency of BIPV-T module;

c. Utilisation of a digital infra-red temperature meter for measuring the temperature of each cell before cooling and during the cooling;

3.3 Thesis Organization

This thesis is divided in seven chapters and follows the prescribed format of an article-based thesis.

Chapter 1 introduces this thesis covering background of project, its relevance and scientific contribution of the study. In Chapter 2, the thesis describes literature review where the following aspects of the project are covered:

1. Water based cooling system design for PV-T and BIPV-T photovoltaic modules
2. Short comings in cooling configurations in photovoltaic modules

Chapter 3 outlines the three main objectives of this thesis, research questions, how to address the research question and the originality of work.

Chapter 4 covers the first article entitled “Concept and simulation study of a novel building integrated photovoltaic-thermal (BIPV-T) module” submitted for publication in Applied Energy.

This article discusses the concept of a novel method to water cool uniformly individual solar cells to improve performance of photovoltaic (PV) modules. A simulation study was conducted using TRNSYS software that shows much improvement in performance of PV module if individual cells could be cooled separately. Accordingly, a layout of new uniform water cooling circuit for individual solar cells in a BIPV-T module is proposed and compared with conventional water cooling circuit

Chapter 5 covers the second article entitled “Development of a new building integrated PV-thermal solar module” submitted for publication in Applied Energy.

This article deals with design photovoltaic thermal module for building integration with novel individual solar cells cooling pipe circuit. This new design has never been developed before. In the

first step, the design, fabrication and testing of a field model of a 140W, 36 cells photovoltaic module with the novel cooling pipe circuit is discussed and their performances evaluation in indoor and outdoor condition have been presented. The outdoor performance shows uniformity in cooling of individual solar cells and improvement in the electrical performance of the PV module.

In the second step, the design developed in the first step was used to fabricate a new commercial prototype with improved performances by using a better conductive bond between the tube and sheet by bracing/soldering than using conductive silicone glue used in the first step prototype. The result shows marked improvement in module efficiency when cooled by water circulation. The cost reduction in novel cooling circuit by a factor of 6 per square meter of PV module was obtained over first design.

A general discussion which linked the various parts of the thesis and the interpretations of the important results are shown in chapter 6. A conclusion and key recommendations of further work to be done are indicated at the end in chapter 7.

CHAPTER 4 ARTICLE 1: CONCEPT AND SIMULATION STUDY OF A NOVEL BUILDING INTEGRATED PHOTOVOLTAIC THERMAL (BIPV-T) SOLAR MODULE

A. Samson Myles* and O. Savadogo* and Kentaro Oishi

Laboratory of New Materials for Energy

Département de Génie Chimique

École Polytechnique de Montréal

***Correspondence to:**

austin-samson.myles@polymtl.ca

and

osavadogo@polymtl.ca

Submitted to Applied Energy on July 23, 2019

4.1 Abstract

This paper discusses concept of a novel Building Integrated Photovoltaic-Thermal (BIPV-T) solar module (collector). The concept proposes uniform water cooling of individual solar cells in a module to improve performance of photovoltaic (PV) modules. A simulation study was conducted using TRNSYS software that shows much improvement in performance of PV module if individual cells could be cooled separately. Based on our analysis, a novel concept of a cooling pipe layout (heat exchanger) is proposed that will improve the performance of overall energy efficiency of the PV module over conventionally used series cooling of solar cells in BIPV-T modules. This will help to open a new design of BIPV-T technology based on our proposed BIPV-T module.

4.2 Introduction

When a PV module is flush with the roof or wall of a building, its natural cooling from back of PV module is impeded (Sandia) [1]. That means when ambient temperature is 25°C, solar cell temperature will increase to 45°C (NOCT) + 18°C = 63°C. In warmer climates than 25°C, the cell temperature will be higher than 63°C, thereby reducing the power output substantially.

In the past, researchers have tried many different matrixes for cooling PV modules [2-14]. Unfortunately, each configuration which has been tried so far causes non-uniform cooling of individual solar cells in a module. Various cooling pipe layout proposed in the past [15] suffer from major disadvantage that solar cells used within a solar module will operate at different temperatures thereby achieving less benefit [15]. They do not integrate circulation of cooling water at individual cell level and this impacts negatively the electrical performance of the BIPV-T system.

As the temperature of the cooling water picks up heat starting at first solar cells at inlet, its temperature continues to rise. As the cooling water flows, solar cells next in order for cooling receives higher temperature than first solar cells Figure 4-1 depending on cooling pipe configuration. Hence the drop in voltage of the solar cells in module will increase as its temperature rises and efficiency will be lower. Though current output increases slightly at higher temperatures, it does not contribute in increasing power output. However, with the temperature increase, voltage decreases more significantly than the increase in current in same conditions.

This is because current generated by solar cells at lowest temperature will be the final output current for the module. This progressive increase in the cell temperature appears when the water flows from the first cell at the inlet to the last cell at the outlet. For example, the current coefficient is in the order of the +0.04% and those of voltage is -0.4%. The solar module voltage drops significantly when its temperature increases. To solve this problem, we suggest in this work to develop a novel cooling system based on individual cell cooling to extract maximum heat from the BIPV-T module to maximize electrical output.

Accordingly, first, we will use TRNSYS to design a new configuration of a BIPV-T water cooling path. Secondly, we simulate the thermal behaviour of the module using different water flow rates through individual cell. The simulated results will be compared to those of classic parallel tube flow cooling design. Thirdly, we will analyse the thermal behaviour of the BIPV-T obtained in this work to those of the parallel tube type cooling system.

4.3 BIPV-T Module Energy Balance Using Simulation Model and Experimental Input Parameters

Based on the TRNSYS simulation model, the following equation is shown for the energy balance on the photovoltaic panel neglecting conduction along the surface [8]:

$$\mathbf{0} = \boldsymbol{S} - \boldsymbol{h_{outer}}(\boldsymbol{T_{PV}} - \boldsymbol{T_{amb}}) - \boldsymbol{h_{rad}}\left(\boldsymbol{T_{PV}} - \boldsymbol{T_{sky}}\right) - \frac{\boldsymbol{T_{PV}} - \boldsymbol{T_{abs}}}{\boldsymbol{R_T}} \qquad \textbf{(1)}$$

where,

$\boldsymbol{S}$ [kJ/hr] – The net absorbed solar radiation (total absorbed – PV power production)

$\boldsymbol{h_{outer}}$ [kJ/hr·m^2·K] – The heat transfer coefficient from top of the PV module surface to ambient air;

$\boldsymbol{T_{PV}}$ [°C] – The PV cell temperature

$\boldsymbol{T_{amb}}$ [°C] – The ambient temperature for convective losses from top surface

$\boldsymbol{h_{rad}}$ [kJ/hr·m^2·K] – The radiative heat transfer coefficient from the top of PV surface to the sky

$\boldsymbol{T_{abs}}$ [°C] – The PV surface temperature (absorber temperature)

$\boldsymbol{R_T}$ [h·m^2·K/kJ] – The resistance to heat transfer from PV cells to the absorber plate at the back

The PV power output can be calculated as [8]:

$$\boldsymbol{PV_{power}\left[\frac{kJ}{hr}\right] = (\tau\alpha)_n \cdot IAM \cdot G_T \cdot A_{PV} \cdot \eta_{PV}} \quad \textbf{(2)}$$

where,

$\boldsymbol{(\tau\alpha)_n}$ – The transmission-absorptance product for the PV module at normal incidence

$\boldsymbol{IAM}$ – Incidence angle modifier

$\boldsymbol{G_T}$ [kJ/hr·m^2] – The total solar radiation incident upon the surface of BIPV-T module

From the relation (2), $\boldsymbol{\eta_{PV}}$ the module efficiency is very sensitive to the temperature variations. Efficiency $\boldsymbol{\eta_{PV}}$ can be expressed by

$$\boldsymbol{\eta_{PV} = \textbf{Efficiency of PV module} = \eta_{nominal} \cdot X_{CellTemp} \cdot X_{Radiation}} \quad \textbf{(3)}$$

where,

$\boldsymbol{\eta_{nominal}}$ is the module efficiency at standard test condition (STC)

$$\boldsymbol{X_{CellTemp}[1/°C] = 1 + \textbf{Eff}_T(T_{PV} - T_{ref})} \quad \textbf{(4)}$$

$\boldsymbol{X_{CellTemp}}$ is the multiplier for PV cells efficiency is a function of the temperature

$$\boldsymbol{X_{Radiation}\ [h.m^2/kJ] = 1 + \textbf{Eff}_G(G_T - G_{ref})} \quad \textbf{(5)}$$

$\boldsymbol{X_{Radiation}}$ is the multiplier of radiation;

where, $\boldsymbol{G_{ref}}$ is 1000W/m^2 (3600 kJ/hr·m^2)

$\boldsymbol{\textbf{Eff}_T}$ is the module temperature coefficient. This coefficient is always negative, and its value depends on the module technology

In this work: $\boldsymbol{\textbf{Eff}_T}$ = -0.0048 [1/C] and $\boldsymbol{\textbf{Eff}_G}$ = is 2.5x10^{-5} [h.m^2/kJ]

The thermal output of the BIPV-T module can be calculated as [8, 9]

$$\boldsymbol{Q_u = m \cdot C_p\,(T_{fluid,out} - T_{fluid,in})} \quad \textbf{(6)}$$

where,

$\boldsymbol{Cp}$ [kJ/kg.K] – The specific heat of the fluid flowing through the BIPV-T collector

$\boldsymbol{Q_u}$ [kJ/hr] – The rate at which energy is added to the flow stream by the BIPV-T module

$\boldsymbol{m}$ [kg/hr] – The flow rate of fluid through the collector of the BIPV-T module

$\boldsymbol{T_{fluid,out}}$ [°C] – The temperature of fluid flowing out of the BIPV-T module

The thermal efficiency of BIPV-T module can be calculated as follows [8, 9]:

$$\boldsymbol{\eta_{thermal} = \frac{Q_u}{G_T \cdot A_{PV}}} \qquad \textbf{(7)}$$

Based on these above concepts, the input parameters used to achieve TRNSYS Simulation are indicated in Table 4.1. We use a solar module of 1.483m length and 0.665m width. In the designed prototype the collector length is 1.466m and width 0.66m. The absorber plate is made of copper sheet to paste at the back of the module. Its thickness is 0.0005m and the thermal conductivity is given by the supplier is 1386kJ/hr.m.K (385W/m.K). For each solar cells we used 2 tubes in contact with copper sheet to circulate water to collect heat. The diameter of each tube is 0.03m. The contact (bond) width between plate and to be is taken as 0.01m whereas bond thickness is taken as **0.01925m.** The bond thickness (th) is calculated from the simple relation,

$$\boldsymbol{th = \frac{c_b}{(k_b b)}} \qquad \textbf{(8)}$$

Where, $\boldsymbol{c_b}$ is the copper sheet and tube interface conductance, $\boldsymbol{k_b}$ is the bond thermal conductivity and $\boldsymbol{b}$ is the bond width. In our case $\boldsymbol{c_b}$ = 200W/mk, $\boldsymbol{k_b}$=1386 kJ/hmk and $\boldsymbol{b}$ = 0.01m

The thermal resistance of the substrate is calculated as

$$\frac{Total\ thickness\ of\ PV\ laminate\ material}{Mean\ thermal\ conductivity\ of\ PV\ laminate\ material}$$

The total thickness of PV laminate is 0.00818m and mean thermal conductivity of PV laminate material [4] is taken as 136.7W/mK. Therefore, the thermal resistance works out to $6x10^{-5}$ m^2K/W ($1.7x10^{-5}m^2K/kJ$).

The resistance of the back insulation is taken as 1 x 10^{-4} hm^2K/kJ from manufacturers data, the reflectance is calculated as (1-(glass transmittance x cell absorptance)) where transmittance of the glass is taken as 0.9 and the absorptance of the cell is taken as 0.9. Therefore, the reflectance works out to (1-0.9x0.9) = 0.19.

IAM is the incidence angle modifier and is calculated from following equation

$$\boldsymbol{K_{\tau\alpha} = 1 - b_0\left(\left(\frac{1}{\cos\theta} - 1\right)^n\right)} \qquad \textbf{(9)}$$

where $\boldsymbol{b_0}$ is the incidence modifier coefficient and $\boldsymbol{n}$ is a constant specific to type of coating on the absorber. In our study for a flat cover $\boldsymbol{n}$ is taken as 1.

The PV reference temperature is taken as 25°C which is the reference temperature define for the PV performance under standard test condition (STC). The PV cell reference radiation of 3600 kJ/hr.m^2(or 1000W/m^2) is the same as solar radiation used for testing PV module under standard test condition (STC). The PV efficiency at reference condition is once again efficiency of PV module at STC. In our case it is taken as 0.142 or (14.2%). The efficiency modifier for the temperature is the temperature coefficient for power output of the PV module. This is given by the PV module manufacturer obtained from module certifying authority like TUV or UL. We have used the manufacturers data as -0.0048 (or 0.48%/°C). The efficiency modifier for the radiation depends on air mass. It has been neglected as the modules are tested at near noon time when the air mass is close to 1.

Table 4.1 Input parameters for simulation using TRNSYS software

S.N.	DESCRIPTION	VALUE	UNIT
1	Collector length	1.483	m
2	Collector width	0.665	m
3	Absorber plate thickness	0.0005	m (24 gage)
4	Thermal conductivity of the absorber	1386	kJ/hr·m·K
5	Number of tubes	8	-
6	Tube diameter	0.03	m
7	Bond width	0.01	m
8	Bond thickness	0.01925	m
9	Bond thermal conductivity	1386	kJ/hr·m·K

10	Resistance of substrate material	0.000017	$h \cdot m^2 \cdot K/kJ$
11	Resistance of back material	R6.7	$h \cdot m^2 \cdot K/kJ$
12	Fluid specific heat	4.18	kJ/kg·K
13	Reflectance	0.19	Fraction
14	Emissivity	0.9	Fraction
15	1st order IAM (b_0)	0.136	-
16	PV cell reference temperature	25	°C
17	PV cell reference radiation	3600	$kJ/hr \cdot m^2$
18	PV efficiency at reference condition	0.175	Fraction
19	Efficiency modifier - temperature	-0.0048	1/°C
20	Efficiency modifier - radiation	0	$h \cdot m^2/kJ$

NOTE: To determine the flow rate for simulation reference EUROFINS, Italy [5] and TUV Reinland [6] which is conducted outdoors and indoors respectively.

4.4 TRNSYS Analysis

4.4.1 Conventional BIPV-T Cooling Circuit Analysis

Figure 4-1 shows the how conventional cooling circuits for BIPV-T or PV-T modules are used [1, 3, 5, 8]. Infact, various cooling circuit (cooling pipe layout) proposed such as parallel flow [3, 5, 8], split flow [2], direct flow [2], spiral flow, parallel serpentine [2], web flow, duel pass, drip flow, oscillatory flow etc. All these concepts could be explained through Figure 4-1. All these flow models are characterized by one inlet fluid flow through the panel to one output fluid flow. In this case the same fluid goes in one line from a cell to another cell of the panel. In other words, we take

one string of cells which is shown in Figure 4-1, we see that the same cooling fluid is going from cell1 to cell 9. In such configuration the temperature of cell 9 will higher then temperature of cell1. The Figure 4-1 outlet temperature of cooling fluid from cell1 is denoted as t1 and outlet temperature of fluid at the exit of cell 9 is denoted as t9 where t9 > t1. Therefore, in this cooling pipe configuration the temperature of the cells in a module cannot be uniform.

Using the experimental parameters tabulated in Table 4.1 for running TRNSYS simulation, Figure 4-2 shows the variation of each cell temperature with the number of the cell; from n^{o}1, the number of the first cell which receives the inlet of the flow rate to n^{o}9 the number of the last cell from which we have the outlet of the flow rate result for 9 series connected solar cells in a 4 x 9 (36 cell) solar modules. The temperature increases from cell n^{o}1 to cell n^{o}9 for a given flow rate. For a fixed number of cells, the temperature of the cell decreases when the fluid rate through the panel increases.

These results are in agreement with those published elsewhere by Zondag H. A., *et al.*, [16] where it was found a progressive increase of the cell temperature from the first cell at the inlet of the fluid flow to the last cell of the outlet of the fluid flow. The thermal efficiency obtained in his work was 33% for combi panel as compared to 54% for conventional thermal panels. Electrical efficiency of Combi panel was found to be 6.7% as compared to 7.2% for conventional PV panels measured in the same condition.

Figure 4-2 shows how the current output of solar cell increases with temperature. However, it will have negligible effect in output power as cell with lowest cell current output will be the net current output for series connected solar cells.

For the purpose of explanation and clarity, Figure 4-1 depicts conventionally made water cooling pipe configuration. A nine cells series connected solar cells are shown. separately for analysis as cooling water will get divided in four parallel paths. Therefore, the performance of each 9 series connected solar cells will be identical but non-uniform.

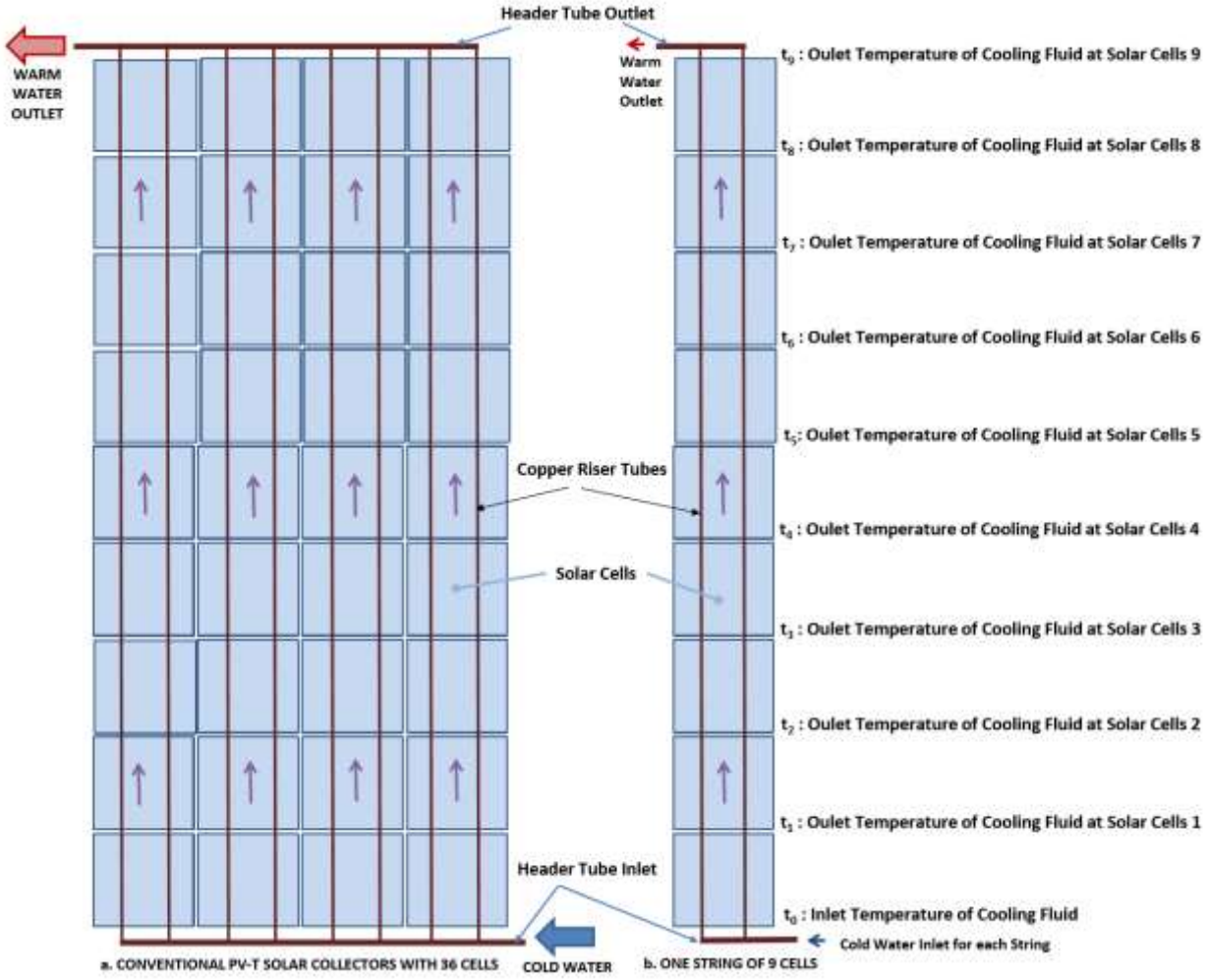

Figure 4-1 Conventional BIPV-T and PV-T cooling pipe layout

Figure 4-3 shows the variation of the wattage power with the number of the cell. When the cell number increases the cell wattage power decreases. From the cell n^o 1 to cell n^o 9, the drop in the power increases when the flow rate decreases for each cell. This results in power drop of solar cell indicates that power output of each cell will be different. The net effect of this cooling scheme is a limited increase in output power of solar modules. But the performance in power of the module is significantly worst without cooling. As shown in Figure 4-3, the power of each of the 9 cells will vary as the cooling water moves from one solar cell to next. The graph also shows that first cells will have higher power where cooling water enters the cooling circuit. When compared to the power of the non cooled system which temperature will rise to 53.83°C, the power drops to 2.806 W whereas the cooled first cell has a voltage of 3.102 W at a flow rate of 1.67/litres per hour. With

this wattage at 53.83°C used for comparison, the gap of the wattage in the first cell is around 0.300 Volt whereas it is 0.008 Volt for the last cell if the water cooling flow rate is 1.67 litres/hour. In Figure 4-3, we see that when the water flow rate increases, difference of wattage increases from the situation without cooling (2.806 Watts) to the value of 3.110 Watt for the first cell and is almost independent of the flow rate. But it increases from 0.08 Watt to 0.16 W when the flow rate increases from 1.67 lit/hour to 3.33 lit/hour. This is an indication of the effect of the flow rate on the thermal efficiency of the system. For purpose of the explanation red and violet dotted lines showing cell wattage of 2.806 Wattage at the temperature of 53.83^{0}C for not cooled system (stagnation).

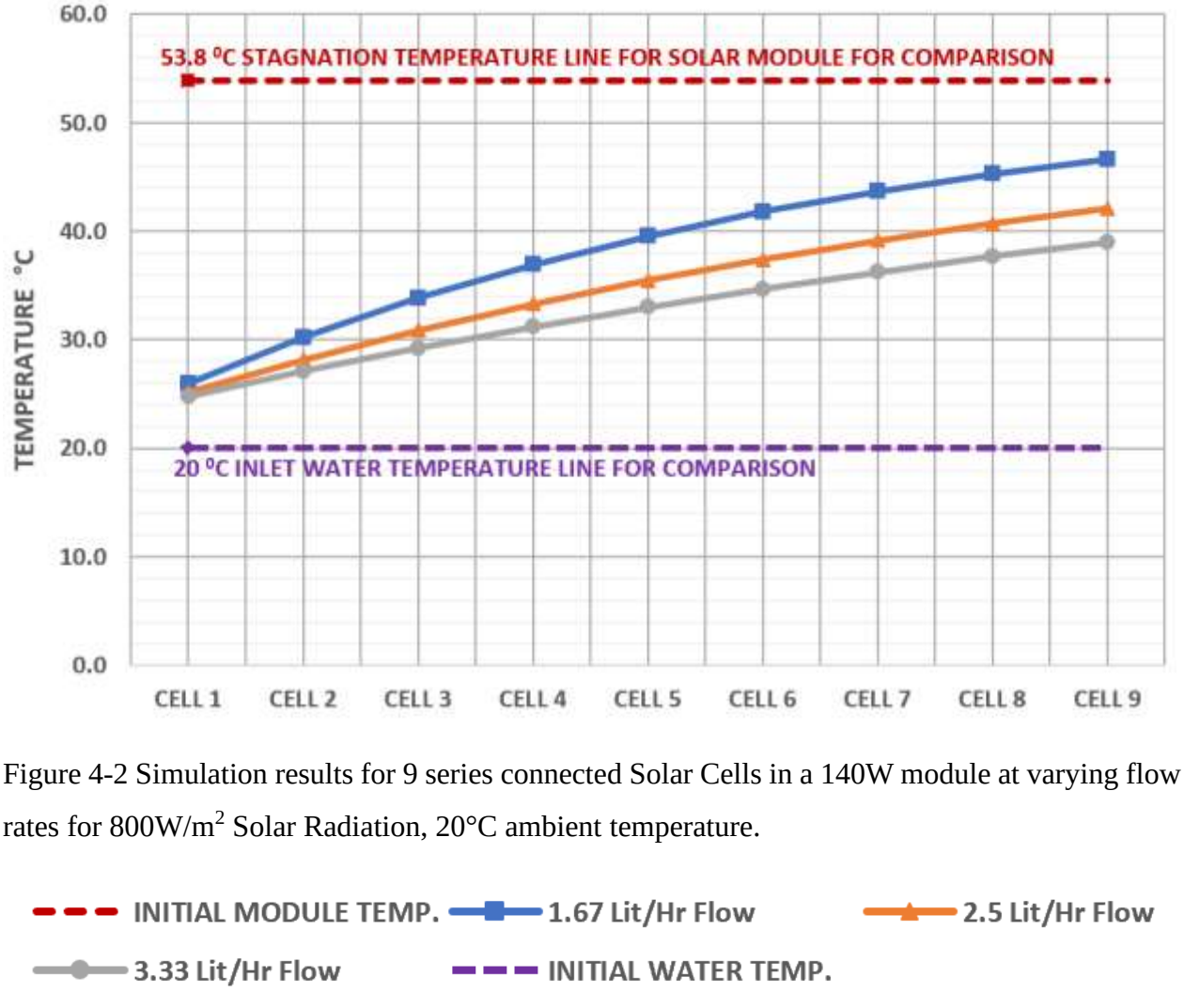

Figure 4-2 Simulation results for 9 series connected Solar Cells in a 140W module at varying flow rates for 800W/m^2 Solar Radiation, 20°C ambient temperature.

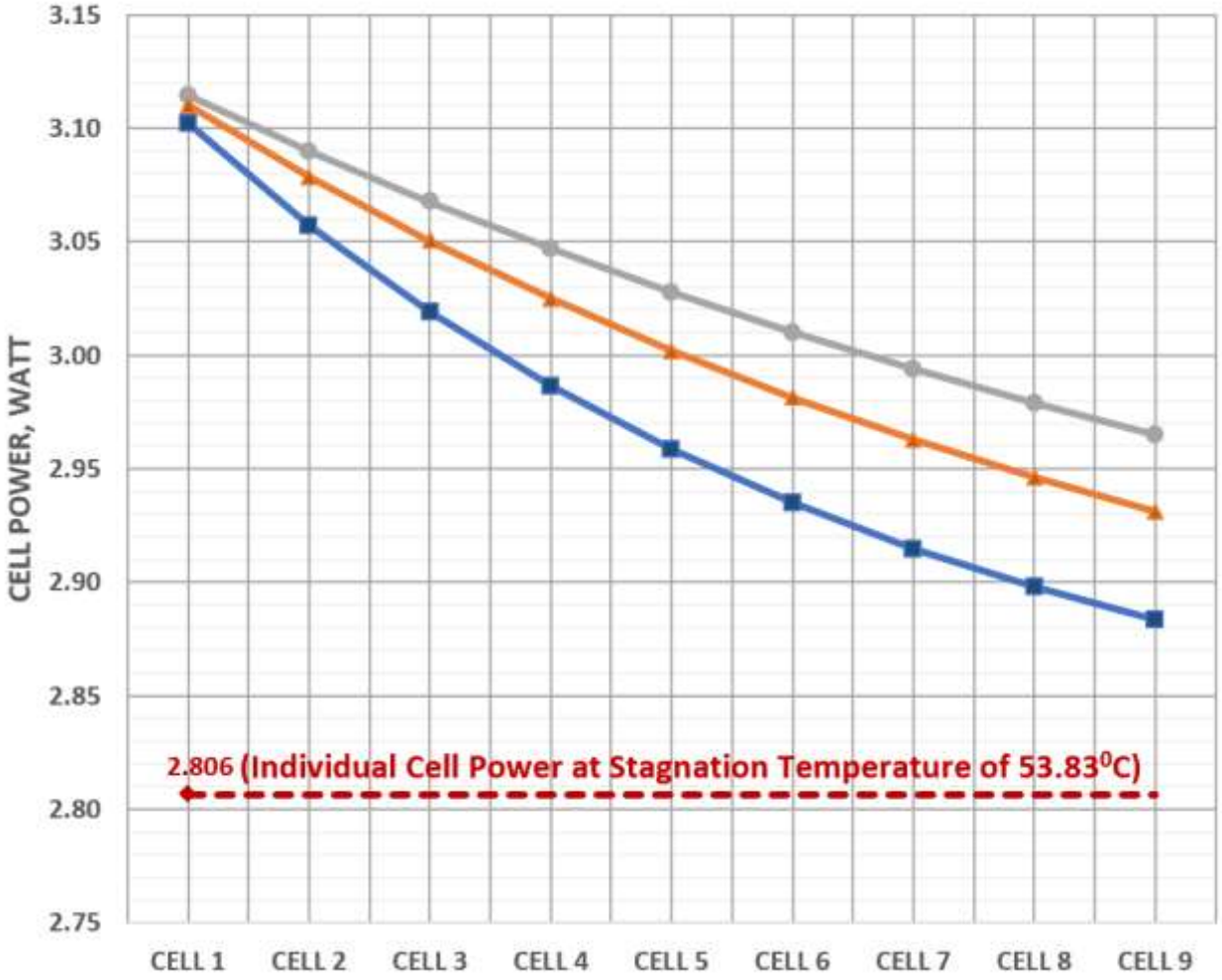

Figure 4-3 Simulation results of individual wattage of nine series connected Solar Cells at varying cooling water flow rates for 800W/m^2 solar radiation and 20°C ambient temperature

Simulation of the variation of the wattage power with the number of the cell for a created for a 36-cell 140W polycrystalline module. Figure 4-3 shows the wattage of 9 individual cells connected in series. Each cell will operate at different wattages mainly because voltage of solar cells drops as the temperature of cells rises. For reference, the power output of solar cell at stagnation temperature is shown in red.

4.4.2 Concept and New Design of Cooling Water Circuit

In order to understand the new concept refer to graphical performance shown in Figure 4-4, Table 4.2 and Table 4.3 below.

As seen in Figure 4-5, a sub header 2 water input pipe is placed along the length of 9 cells to feed cooling water in individual cells. On the other side of cells width another outlet header pipe 2 is used to collect hot water after water picks up heat from each solar cells. This design requires additional feeder(inlet) and outlet pipes to feed the sub-header pipes along the cells. Similarly, additional sub-header pipe for taking out the heated water is connected to main hot water outlet header pipe. It is made sure, header pipes do not touch any solar cells to transfer heat.

The analysis clearly indicates that if all solar cells in a BIPV-T or PV-T modules are cooled uniformly at same temperature we can get achieve high module output. At higher cooling water flow rate the cell temperatures are lower and temperature rises at lower flow rates. Also noticeable is that higher or lower cooling water flow rates there is insignificant variation in temperature and output gain. The main advantage of new cooling pipe configuration is that even at higher temperatures all solar cells can be maintained at uniform temperature.

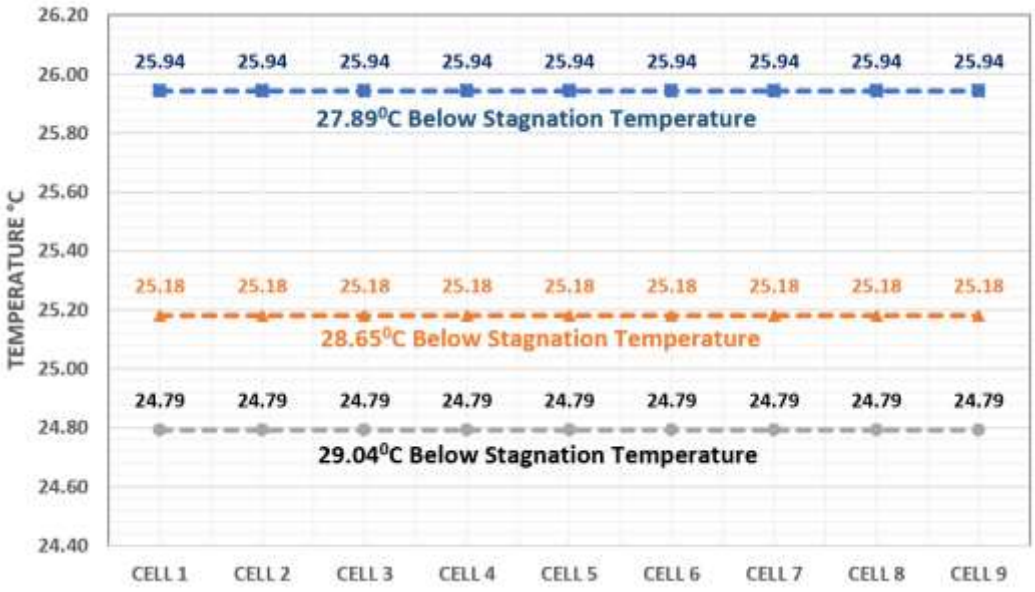

Figure 4-4 Individual Cell Cooling of 9 series cells using novel water cooling pipe layout.

Figure 4-4 graph shows the cooling effect of different water flow rates. A BIPV-T solar module will operate 28 to 29°C below the stagnation temperature of solar cells. The power and efficiency gains are shown in Table 4.2 and Table 4.3.

Figure 4-2 show the variation of the cell temperature with the number of cells for the same water cooling flow rates as for Figure 4-3. A same constant temperature of the cell is obtained from the first to the last cell. For the same flow rate. This indicated that each cell of the panel has the same temperature prior to the individual cooling.

Figure 4-4 depicts lowest cell temperature for all cells if cooling water enters and exits from individual cells. Combining Figure 4-3 and Figure 4-4. shows if all solar cells have same temperature as the first cell then we can get highest power output from each cell. For example, at 1.67lph flow rate all cells will deliver 3.102W (1^{st} Cell) x 9 cells = 27.92W if they operate at uniform temperature same as first cell. For non-uniform cooling combining the strings of 9 will deliver 2.883W (9^{th} Cell) x 9 cells = 25.95W. The higher power generated by other 8 cells will be dissipated in the 9^{th} cells until the current output of all cells become equal. Therefore, uniformly cooled individual cells will deliver 7.6% higher power.

Table 4.2 Performance of PV module at varying cooling water flow rates. The cooling is based on flowing cooling water over nine cells in a row versus individual solar cells using at 800W/m^2 & 20°C ambient.

Flow rate lit/hr	140W, 36 cell module wattage			Individual cell gain %	Gain over Stagnation %
	Series cooling	Individual cell uniform cooling	Gain over series cells		
1.67	107.02	111.68	4.66	4.35%	10.53%
2.50	108.35	111.96	3.61	3.34%	10.82%
3.33	109.18	112.11	2.93	2.69%	10.96%
0.00	101.03	101.03	0.00	0.00%	0.00%

NOTE: cooling water inlet temperature 20°C

Table 4.2 and Table 4.3 show clearly an important wattage gain over the series cooling and individual cell gain of 4.35 % for a flow rate of 1.67 lit/hr and a gain over stagnation about 10.5% for the same flow rate. There is not a significant gain over stagnation with the flow rate increases.

Table 4.3 Electrical & thermal efficiency of BIPV-T module for cooling by passing water over nine cells in a row versus individual cell cooling.

Flow Rate	Series Cooling of Solar Cells		Uniform Cooling of Individual Cells	
lit/hr	PV Efficiency %	Thermal Eff. %	PV Efficiency %	Thermal Eff. %
1.67	13.38	25.22	13.96	45.21
2.50	13.54	30.44	14.00	46.36
3.33	13.65	33.60	14.01	46.95
0.00	12.63	0.00	12.63	0.00

Based on the improved performance results for individual cell cooling in a module, a novel cooling coil layout was designed as shown in Figure 4-5.

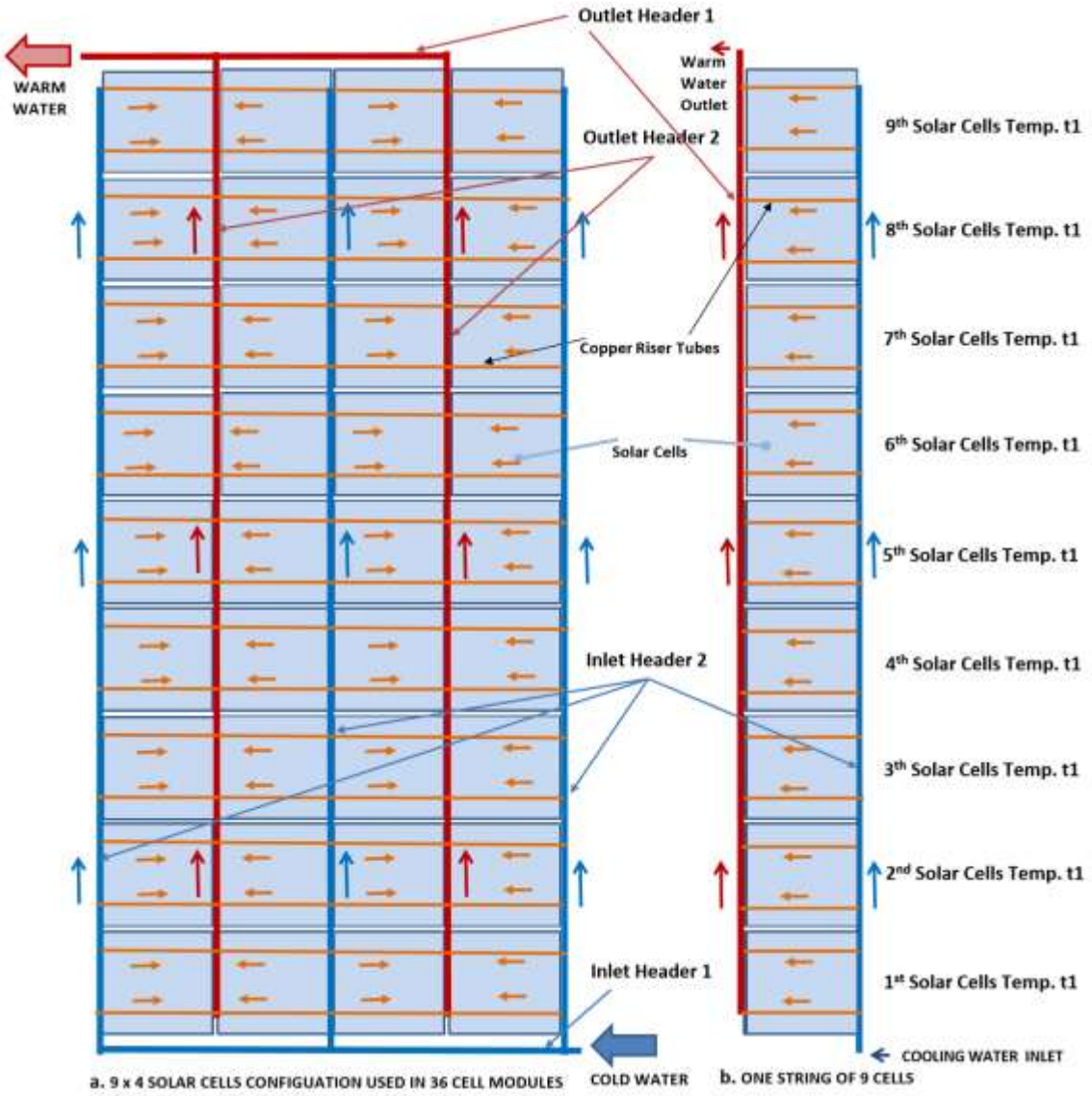

Figure 4-5 Design of a 36 cell BIPV-T solar module with a novel cooling pipe layout. This individual cooling system has never been developed before and it better perfornace than previous cooling system are not individually cooled.

Figure 4-5 Shows our proposal for a new design of a 36 cell BIPV-T solar module with novel cooling pipe layout. In the actual prototype a copper sheet attached to cooling water tube is pasted at the back of standard commercially available solar module. The cold and hot water headers (depicted in blue and red in Figure 4-5) are higher than riser pipes (depicted in orange) to prevent the former from touching the solar cells.

In this case as shown in Figure 4-5 we have main input header pipe 1 where cooling water enters and distributes cooling water to three input sub-headers 2. Each sub-header pipe 2 then feeds cooling water to riser tubes (Figure 4-5) to cool individual cells. The outlet sub-header pipe 2 is provided on the other side of individual cells to collect warm fluid which picks up heat from each cell. This cooling pipe configuration ensures uniform temperature of individual solar cells in the modules. The two outlet sub-headers pipe 3 connects to main header pipe 1 for warm water to exit from the module. The results obtained from the TRNSYS and experimental measurements made on a protype based on individual cell cooling we will fabricate to show an important improvement of the cooling system in comparison of the other previous cooling system.

The fabricated BIPV-T prototype is expected to have following improvements over water cooling pipe configurated used by other researchers:

1. All 36 solar cells in BIPV-T module will operate at uniform temperature with minimum variation.
2. The mismatching of solar cells electrical output will be minimised which will improve efficiency.
3. The even cooling will prevent overheating of any solar cells that causes premature failure of modules.
4. The overall efficiency will increase due to heat gain in cooling water. The combined thermal and electrical efficiency will boost overall efficiency of BIPV-T module.

4.5 Conclusion

The TRNSYS simulation results shows approximately 10.5% to 11% improvements in performance of BIPV-T modules using novel water-cooling circuit over conventional BIPV modules. In addition, the simulation indicates that novel cooling circuit layout will have 3.2% to 4.3% improvement over BIPV-T modules with series cooling proposed by some researchers and commercially available from some manufacturers. Additionally, thermal efficiency between 45% to 47% is achieved by collecting heat in cooling water.

The novel design prevents negative effect of non-uniform cooling of solar cells in a module. In conventional cooling pipe configuration used in other studies will generated highest current by hottest cells at the outlet. Since all cells in modules are connected in series, the cells at the inlet will operate at lowest temperature and higher current generated by cells at higher temperature will get absorbed this cell. This can cause overheating of cell/cells that generate lower current. As PV technology is progressing fast, solar cells are generating higher currents year after year. This means current mismatching can have more severe effect.

The uniform cooling of individual cells proposed here will ensure mismatching of current does occur.

Infact, BIPV-T modules with glazing will have more severe effect in mismatching as the solar cell operate at even higher temperature. The uniform cooling even at higher water temperature, as shown in graph Figure 4-4 and novel cooling pipe layout shown in Figure 4-5, will have major advantage in keeping the solar cells at uniform temperatures.

Though this study was conducted for water based cooling system same concept of uniformly cooling individual cell could be applied to air cooling system in BIPV-T modules.

A BIPV-T module design based on cooling of individual solar cells was constructed and tested outdoors in natural sunlight. In next paper, complete design and fabrication details as well as test result of prototype is discussed.

4.6 References

[1] M. K. Fuentes, "A simplified thermal model for flat-plate photovoltaic arrays," Sandia National Labs., Albuquerque, NM (USA), 1987.

[2] M. Y. Othman, A. Ibrahim, G. L. Jin, M. H. Ruslan, and K. Sopian, "Photovoltaic-thermal (PV/T) technology–the future energy technology," *Renewable Energy,* vol. 49, pp. 171-174, 2013.

[3] "Hybrid PV-Thermal Data Sheet," ed: Solimpeks, 2013.

[4] T. T. Chow, "A review on photovoltaic/thermal hybrid solar technology," *Applied energy,* vol. 87, no. 2, pp. 365-379, 2010.

[5] "Test Report M1.11.NRG.0320/43724: Volther Powervolt," Eurofins, Italy, August 2011.

[6] "Test Report 21222892_E: DualSun 250M," TUV Reinland Energie und Umwelt GmbH, November 2013.

[7] V. Tyagi, S. Kaushik, and S. Tyagi, "Advancement in solar photovoltaic/thermal (PV/T) hybrid collector technology," *Renewable and Sustainable Energy Reviews,* vol. 16, no. 3, pp. 1383-1398, 2012.

[8] J. A. Duffie and W. A. Beckman, *Solar engineering of thermal processes*. John Wiley & Sons, 2013.

[9] Stine, W. B., and G. Michael, "Power from the Sun," ed, 2001.

[10] T. N. Anderson, M. Duke, G. L. Morrison, and J. K. Carson, "Performance of a building integrated photovoltaic/thermal (BIPVT) solar collector," *Solar Energy*, vol. 83, no. 4, pp. 445-455, 2009.

[11] T. N. Anderson, S. K. Bura, M. Duke, J. K. Carson, and M. C. Lay, "Development of a building integrated photovoltaic/thermal solar collector based on steel roofing," *4th New Zealand Metals Industry Conference*, 2008.

[12] Y. Tripanagnostopoulos, "Aspects and improvements of hybrid photovoltaic/thermal solar energy systems," *Solar energy*, vol. 81, no. 9, pp. 1117-1131, 2007.

[13] M. Bosanac, B. Sorensen, K. Ivan, H. Sorensen, N. Bruno, and B. Jamal, "Photovoltaic/thermal solar collectors and their potential in Denmark," *Final Report, EFP Project, www. solenergi. dk/rapporter/pvtpotentialindenmark. pdf*, 2003.

[14] V. J. Fesharaki, M. Dehghani, J. J. Fesharaki, and H. Tavasoli, "The effect of temperature on photovoltaic cell efficiency," in *Proceedings of the 1stInternational Conference on Emerging Trends in Energy Conservation–ETEC, Tehran, Iran*, 2011, pp. 20-21.

[15] T. Matuska, "Theoretical analysis of solar unglazed hybrid photovoltaic-thermal liquid collector," in *Proceedings of the Eurosun*, 2010.

[16] H. A. Zondag, D. d. de Vries, W. Van Helden, R. C. van Zolingen, and A. Van Steenhoven, "The thermal and electrical yield of a PV-thermal collector," *Solar energy*, vol. 72, no. 2, pp. 113-128, 2002.

CHAPTER 5 ARTICLE 2: DEVELOPMENT OF A NEW BUILDING INTEGRATED PV-THERMAL SOLAR MODULE

A. Samson Myles* and O. Savadogo* and Kentaro Oishi

Laboratory of New Materials for Energy

Département de Génie Chimique

École Polytechnique de Montréal

*Correspondence to:

austin-samson.myles@polymtl.ca

and

osavadogo@polymtl.ca

Submitted to Applied Energy on July 24, 2019

5.1 Abstract

A photovoltaic thermal module for building integration was designed with novel individual solar cells cooling pipe circuit. This new design has never been developed before. In the first step, the design, fabrication and testing of a field model of a 140W, 36 cells photovoltaic module with the novel cooling pipe circuit is discussed and their performances evaluation in indoor and outdoor condition have been presented. The outdoor performance shows uniformity in cooling of individual solar cells and improvement in the electrical performance of the PV module.

In the second step, the design developed in the first step was used to fabricate a new commercial prototype with improved performances by using a better conductive bond between the tube and sheet by bracing/soldering than using conductive silicone glue used in the first step prototype. Accordingly, a BIPV-T prototype using four high efficiency solar cells was fabricated and tested in outdoor natural sunlight. The result shows marked improvement in module efficiency when cooled by water circulation. Even the efficiency of the most efficient existing commercial solar cells used for this model drops at elevated operating conditions. The improvement in design of novel cooling pipe configuration reduces the cost by a factor of six making it attractive for commercial production.

5.2 Introduction

The integration of photovoltaic (PV) module into the roof or façade of building affects the heat flow out of the PV module, thereby elevating its operating temperature. This increases in the module temperature have a major impact on its performances by reducing its power, thereby lowering the efficiency. In addition, higher operating temperatures accelerate the degradation and the failure of the photovoltaic modules. The performance of the photovoltaic module is further affected if the cells within a PV module operate at different temperatures causing mismatching [1-5].

PV modules are rated at 25°C solar cell temperature; however, in field conditions the normal operating cell temperature (NOCT) is 20°C above ambient temperature [6-9] i.e. 45°C. For this case, power output of the PV module decreases by 0.4%/°C; that means the module will deliver

8% lower power when the ambient temperature is 25°C. In warmer climates the solar cells temperature is even higher, say 65°C. In this case the power output of the PV modules may decrease by 16%.

Effectively, when the PV modules are integrated in building to form roof or façade, the solar cells temperature is elevated further as the natural cooling from back of the PV module is impeded [6-8]. Then the Installed Normal Operating Cell Temperature (INOCT) increases by an additional 18°C at least. At an ambient temperature of 25°C, the solar cell temperature is denominated as INOCT = NOCT + 18°C = 63°C. Furthermore, in warmer climates or summer months when ambient temperature is higher than 25°C, the INOCT will rise, thereby reducing the power output substantially.

On the other hand, commercial PV module manufacturing lines start by sorting solar cells with matching current output to ensure highest output or efficiency and to ensure reliability. If one solar cell connected in series in a solar module delivers lower current than other cells, then the net current output is equal to the lowest output delivered by any solar cell. If one cell's current is lower than the others, then it will absorb current from higher output cells and this may result in the damage or the delamination of the module. It may also cause fire of large PV module installations. Accordingly, cooling all cells uniformly in a PV module is very important.

The classical idea is to cool the PV module by circulating water in a pipe circuit under the PV module to improve electrical power output. The heat extracted from a solar panel can be used for hot water supply for domestic use, space heating, swimming pool heating and as process heat in industry for large BIPV-T installations. Further, the combined electrical and thermal output will increase overall efficiency of BIPV-T module substantially. Since at different locations across the World the solar radiation intensity and the ambient temperatures vary. Therefore, a method must be developed to predict performance of BIPV-T module at any given location at various temperatures.

While there are several designs of BIPV-T and PV-T modules proposed, these have inherent disadvantage of non-uniform cooling of individual solar cells in a module [1, 4, 6, 7, 10-23]. Unfortunately, the design of the classical BIPV-T is not effective because it does not allow uniform cooling of individual cells in a BIPV-T and PV-T modules. Therefore, the aim of this work is to

develop a new design of the BIPV-T design which will use a novel cooling pipe configuration that will ensure uniform cooling of individual solar cells in a PV module.

In near future, this concept can be used to fabricate the BIPV-T module will be developed to use as building façade or roof to replace conventional building material to save cost. The BIPV-T collector can also be integrated in existing buildings by using suitable support structure.

5.2.1 Classical considerations of thermal performance of BIPV-T module

The appropriate aperture irradiance is the global (total) irradiance falling on the collector aperture (I_a) is given by [24]:

$$I_a = G_T \quad \left(\frac{W}{m^2}\right) \qquad (1)$$

Where, G_T is the global irradiance on a collector aperture.
Equation (1) includes both direct (beam) and scattered and reflected energy.

For Flat-plate thermal collectors , the thermal and photovoltaic collector/module efficiency may be calculated as follows by [24]:

$$\eta_{\mathrm{TH}} = \frac{\dot{m} C_p (T_{\mathrm{o}} - T_{\mathrm{i}})}{G_T A_c} \qquad (2)$$

Where, $\dot{m}$ is mass flow rate of fluid in lit/hr, C_p is specific heat of water 1calories/gram/°C or 4.1813 joules/g/°C, T_o is the outlet temperature of fluid, T_i is the inlet temperature of fluid and A_c is solar collector area.

For a PV module with flat-plate collector configuration, the electric energy conversion of the solar irradiance is given by [24]:

$$\eta_{\mathrm{PV}} = \frac{IV}{G_T A_c} \qquad (3)$$

Where, I is the output current, V the output voltage and A_c is the aperture area of the solar module.

The thermal performance of BIPV-T is done outdoors in natural sunlight above 700W/m^2 and measure the fluid inlet and outlet temperatures and fluid flow rate.

The useful thermal energy (Q_u) gain is expressed as [8, 24-26]:

$$Q_u = \dot{m}C_p(T_o - T_i) \quad (4)$$

Where the parameters of equation (4) are defined in equations (2) above.

The thermal performance of a collector operating under steady condition is expressed as [26]

$$Q_u = A_c F_R[G_T(\tau\alpha)_{\text{av}} - U_L(T_i - T_a)] \quad (5)$$

Where, $(\tau\alpha)_{\text{av}}$ is a transmittance-absorptance product, A_c is the collector area, F_R is the heat removal factor, U_L is the overall loss coefficient, G_T is the total solar radiation incident upon the collector surface, T_i is the inlet water temperature and T_a is the ambient temperature. The outdoor testing is done on a clear day near solar noon time. The (τα) determined for conditions under which a collector provides most of its output.

The above equation 1 & 2 above can be used to define an instantaneous efficiency (η_i) [26]:

$$\eta_i = \frac{Q_u}{A_c G_T} = F_R(\tau\alpha) - \frac{F_R U_L(T_i - T_\alpha)}{G_T} \quad (6)$$

$$\eta_i = \frac{\dot{m}C_p(T_o - T_i)}{A_c G_T} \quad (7)$$

The above equations are the basis of the ASHRAE standard test methods used in North America. The European practice is to base collector results on T_m the arithmetic average of the fluid inlet and outlet temperature. Therefore,

$$\eta_i = F_{\text{av}}(\tau\alpha) - \frac{F_{\text{av}} U_L(T_{\text{m}} - T_a)}{G_T} \quad (8)$$

where F_{av} is the average heat removal factor and T_m is the average of the outlet and inlet fluid temperatures. The thermal performance for BIPV-T collector is measured in nearly steady state conditions. We measure $\dot{m}$, T_o and T_i to determine Q_u from equation 4 mentioned above. We also

measure G_T, and T_a, which are needed for the analysis based on equation 3 and 7 above. The outdoor tests are done in the midday hours on clear days when the beam radiation is high and usually with the beam radiation nearly normal to the solar collector. The transmittance-absorptance product for these test conditions is approximately the normal-incidence value and is written as $(\tau\alpha)_{\mathrm{n}}$.

To minimize effects of heat capacity of collectors, we make the tests should be usually made in nearly symmetrical pairs, one before and one after solar noon, we consider the results of the pairs averaged. We determine the instantaneous efficiencies are determined from $\eta = \dot{m}C_p(T_o - T_i)/A_cG_T$ and are plotted as a function of $(T_i - T_a)/G_T$ or as in European Union $(T_{\mathrm{m}} - T_a)/G_T$.

Where, T_i is the inlet temperature of water, T_a is the ambient temperature, T_{m} is the average of inlet and outlet temperature of water and G_T is the total solar radiation (beam + diffuse) incident upon the collector surface.

If $\mathrm{U_L}$, $\mathrm{F_R}$, and $(\tau\alpha)_n$ were all constant, the plots of η_i, versus $(T_i - T_a)/G_T$ would be straight lines with intercept $F_R(\tau\alpha)_n$ and slope – F_RU_L. However, they are not, and the data scatter. The $\mathrm{U_L}$ is a function of temperature and wind speed. Also, F_R is a weak function of temperature. Thus, scatter in the data are to be expected, because of temperature dependence, wind effects, and angle of incidence variations. The long-term performance estimates of BIPV-T module can be characterized by the intercept and slope i.e., by $F_R(\tau\alpha)_n$ and F_RU_L.

To determination of heat capacity of BIPV-T module time constant method is used. The time constant is defined as the time required for a fluid leaving a collector to change through $(1 - 1/e) = (0.632)$ of the total change from its initial to its ultimate steady value after a step change in incident radiation or inlet fluid temperature. The ASHRAE outlines two procedures for estimating time constant. The first is to operate a solar collector at nearly steady state conditions with inlet fluid temperature controlled at or very near ambient temperature. The solar radiation is abruptly shut off by shading or repositioning the collector and the decrease in outlet temperature (with the pump running) is noted as function of time. The time t at which the equality is reached is the time constant of the collector:

$$\frac{T_{o,t} - T_i}{T_{o,\text{init}} - T_i} = \frac{1}{e} = 0.368 \quad (12)$$

Where, $T_{o,t}$ is outlet temperature of fluid after lapsed time t and $T_{o,\text{init}}$ is initial outlet temperature. The number e is a mathematical constant that is based on the natural logarithm and its value is approximately 2.717.

The second method for measuring time constant is to test collector not exposed to radiation (i.e., at night, indoors, or shaded) and impose a step change in the temperature of the inlet fluid from a value well above ambient (e.g. 30℃) to a value very near ambient. The equation 12 mentioned above also applies to this method. This method was used for determining the time constant of BIPV-T module.

The aim of this work is:

i) To measure parameters that are required to determine the electrical and thermal performance of BIPV-T module.

ii) To size a BIPV-T system for various applications using software such as F-chart or PV F-chart.

5.3 Experimental procedure

5.3.1 BIPV-T module fabrication.

The test for thermal performance was conducted using European Union test standard EN 12975-2: 2006: Thermal solar systems and components - Solar collectors – Part2: Test methods which is same as ASHRAE test method used in North America [26].

Figure 5-3 and Figure 5-4 show the different components of the uniformly cooled of individual cells of a PV module. The components parameters also described in Table 5.1. A standard polycrystalline PV module rated at 140W under standard test condition was acquired from Solar Tech. This solar module came with 50 mm high aluminum frame fixed permanently to the module. A copper sheet of 0.2mm thickness with 380W/m.K conductivity was pasted at the back of PV

module using conductive adhesive. A copper cooling pipe of ¼" diameter readily available in the market was selected to fabricate a novel cooling pipe layout.

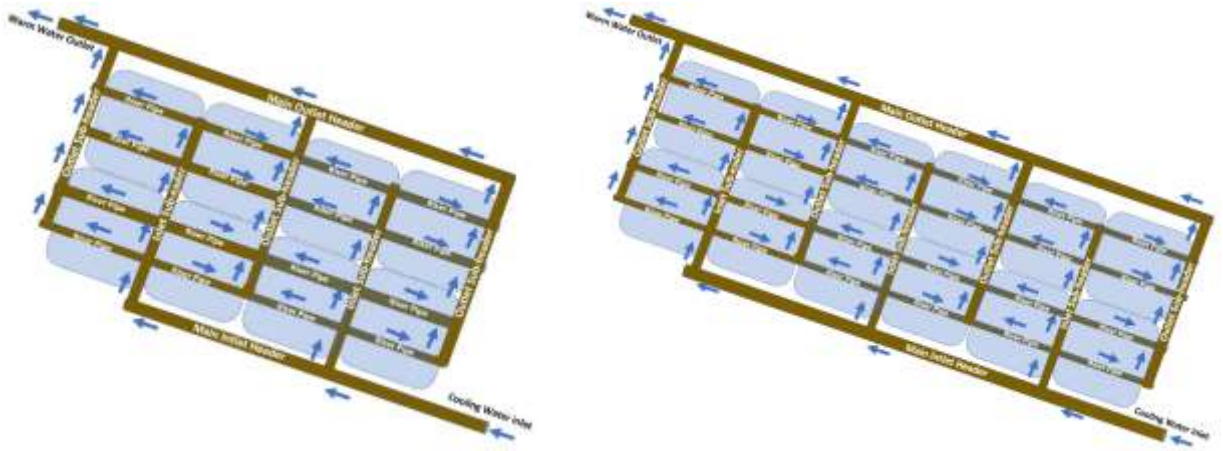

(a) (b)

Figure 5-1 Individual PV cell water cooling sketch (a) for 36 cell modules (b) for 60 and 72 cell modules (only two rows are shown for explanation for new concept)

Figure 5-1 shows the design of the individual PV cell cooling which we used to fabricate the 36 cell prototype shown in Figure 5-6 and Figure 5-7. The blue arrows in Figure 5-1 indicate the cooling water flow direction in the novel BIPV-T module. Each cell of the panel is fed by cooling water at the same temperature. This avoids an increase of the cooling water temperature from the first cell to the last cell in the conventional cooling system shown in Figure 5-2. In this new design the first cell of the panel where the cooling water is entering is at the same temperature as the last cell of the panel. What is new in our approach as shown in Figure 5-1 shows is: each cell of the panel is fed with cooling water at the same temperature; whereas in the classical cooling system (see Figure 5-2), the cooling water of the first cell will go through from the first to the second to the third until it gets through the last cell. Accordingly, the cooling water temperature in a such configuration will increase significantly from the first cell to the last cell. The temperature of the first cell where the cooling water is entering will be significantly less hot than the last cell. Thus, non uniformity in cell temperature will contribute to decrease in overall performance of the module and may damage the module prematurely.

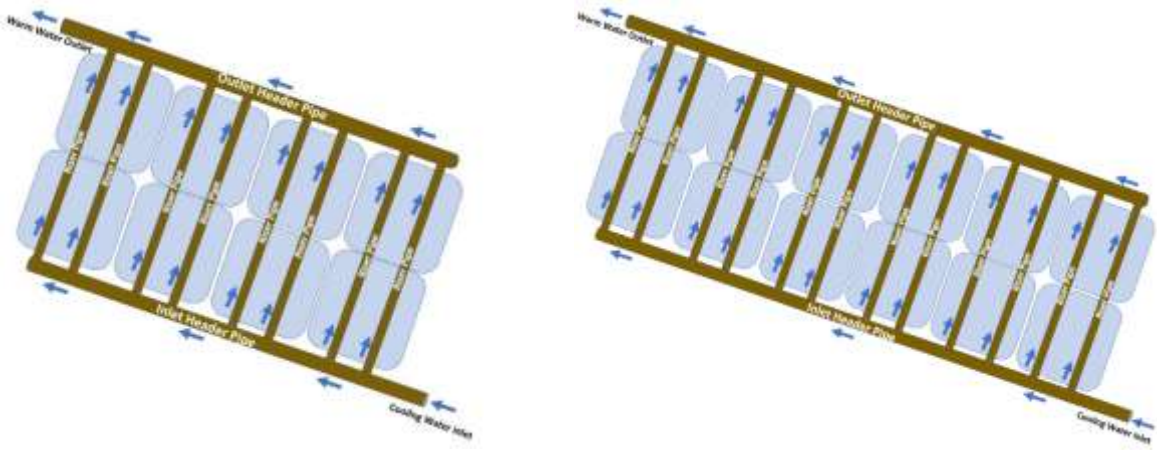

(a) (b)

Figure 5-2 Conventional water cooling pipe design for (a) for 36 cell modules (b) for 60 and 72 cell modules (only two row are shown for explanation))

To simplify the fabrication of our novel design, all bends and branches were created using tee's, elbows and reducers. Cut lengths of ¼" copper pipes were assembled like LEGO using tees and bends to make the novel cooling pipe layout. The joints were soldered (brazed) to make it leakproof.

(a) (b) (c)

Figure 5-3 Novel cooling pipe and attachment details at the back of PV module. It is well described below.

The pipes matrix in Figure 5-3(a) is pasted on a copper sheet for uniform distribution of temperature and the sheet is glued to back of PV module. Thermally conductive adhesive was used to attach the cooling pipe to the copper sheet and to glue to the back of module. See Figure 5-3(c) above.

A layer of environment friendly denim R6.7 insulation was placed over cooling pipe to reduce heat loss. The insulation used is 45 mm thick. The insulation was held in place using 8 mm thick reflective sheet. The sheet is anchored to PV module frame using Velcro strips. See Figure 5-4(b) below.

(a) (b) (c)

Figure 5-4 Rear Denim Insulation, Back and Front of BIPV-T Module with Novel Cooling Pipe Configuration

Table 5.1 Specification of BIPV-T Module Fabricated

S.N.	DESCRIPTION	SPECIFICATION	REMARKS
1.	40W Polycrystalline PV module	1466mm x 660mm x 50mm	Junction Box **Removed**
2.	Wire Output for PV Module	6mm^2, 1m each +ve and -ve	Electrical Performance
3.	Copper Absorber Sheet	0.2mm thick	Thermal
4.	Copper Riser Tubes	1/4” Outer diameter	0.030” wall thickness
5.	Copper Header Tubes	3/8” Outer diameter	0.032” wall thickness
6.	Copper Elbow 90^0	1/8” Inside diameter	Pipe Connection
7.	Copper Tee	1/4” Inside diameter	Pipe Connection
8.	Copper Reducer	¼” to 1/8” Inside diameter	Pipe Connection
9.	Conductive Adhesive SE4485	2.2W/m.K	Thermal Joints

10.	Denim insulation 45mm thick (R6.7)	K=0.037W/m.°C, R=1.08 m^2/W.°C	Thermal conductivity & thermal resistance
11.	Rear cover for insulation 5/16" (8mm) thick	R-1.08 m^2/W.°C	-60°F – 180°F
12.	12V, 14.5W DC Water Pump	10 lpm at 8m head	Suitable upto 70°C
13.	Electronic speed controller for pump	Water flow control	Flow rate control
14.	Sealed maintenance-free battery	12V, 12AH	Pump operation
15.	PV module tester with Cell for solar radiation measurement	100V, 20A	I-V curve, Solar intensity, temp.
16.	Thermal imaging camera	TG165	Surface temp.
17.	Digital and glass thermometer	0-200°C	PV/Ambient temp
18.	Graduated cylinder and stopwatch	2 litre cylinder	Flow rate

NOTE: The junction box from solar module was removed to aid cooling of solar cell below the junction box. The wire output is taken out through width side frame.

5.4 Outdoor Testing in Natural Sunlight

5.4.1 Test Set Up

An outdoor test rig for testing PV-thermal modules was created as shown below in Figure 5-5 and Figure 5-6.

The test rig consisted of a mounting structure to mount BIPV-T module. The angle of inclination of mounting structure could be adjusted. A reference solar cell to measure the solar intensity in the same plane as the top surface of the BIPV-T is mounted at the side of the structure.

The positive and negative wire output from PV module was connected to an automatic current and voltage tracer (miniKLA) for measuring electrical performance in natural sunlight. The output of reference cell with built-in temperature sensor is also plugged in the same device to automatically measure the solar radiation and electrical parameters simultaneously.

A 200-litre water tank is connected to a 12V battery operated pump. The 14.5W pump is rated to deliver 10 lpm to 8m head. The pump came with an electronic controller to control speed to vary flow rate. A 12V, 13AH deep cycle AGM battery was used for operating the pump. The inlet of the pump is connected the water tank while outlet of the pump is attached to the lower end of water-cooling pipes attached to the back of the BIPV-T module. A plastic tubing was used connecting the pump to the BIPV-T module.

On the exit of cooling pipe of BIPV-T module, a pressure gage with range of 0-7 bar was installed. A shut off valve was installed after the pressure gauge to increase pressure by choking the water outflow.

To measure the inlet and the exit water temperature, an alcohol in glass thermometer with range of -20°C to 50°C was used. The same thermometer was used for measuring ambient air temperature. The wind velocity recorded from nearest the weather station through iPhone APP in km/hr and converted to meters per second.

The temperature of the individual solar cells was measured with a digital infrared meter having laser pointer. The temperature was measured in the middle of each of 36 solar cells in the module.

The BIPV-T module was faced true south and inclination of the mounting structure was adjusted based on the solar azimuth and solar altitude at solar noon. The sun altitude, azimuth and solar noon is determined using Sun Surveyor APP. The inclination and orientation adjustment for mounting structure is done using orientation meter from Solar Consulting APP. All measurements are done 45 minutes before and 45 minutes after solar noon time. The BIPV-T was left in the sunlight for 12-15 minutes before measuring the electrical output and the cell temperature. It was ensured that there is no water inside the cooling pipe for taking readings in stagnation temperature. The readings taken during water cooling of BIPV-T was allowed 9 to 10 minutes to stabilize the solar cell temperature. This was done every time when cooling the flow rate was changed.

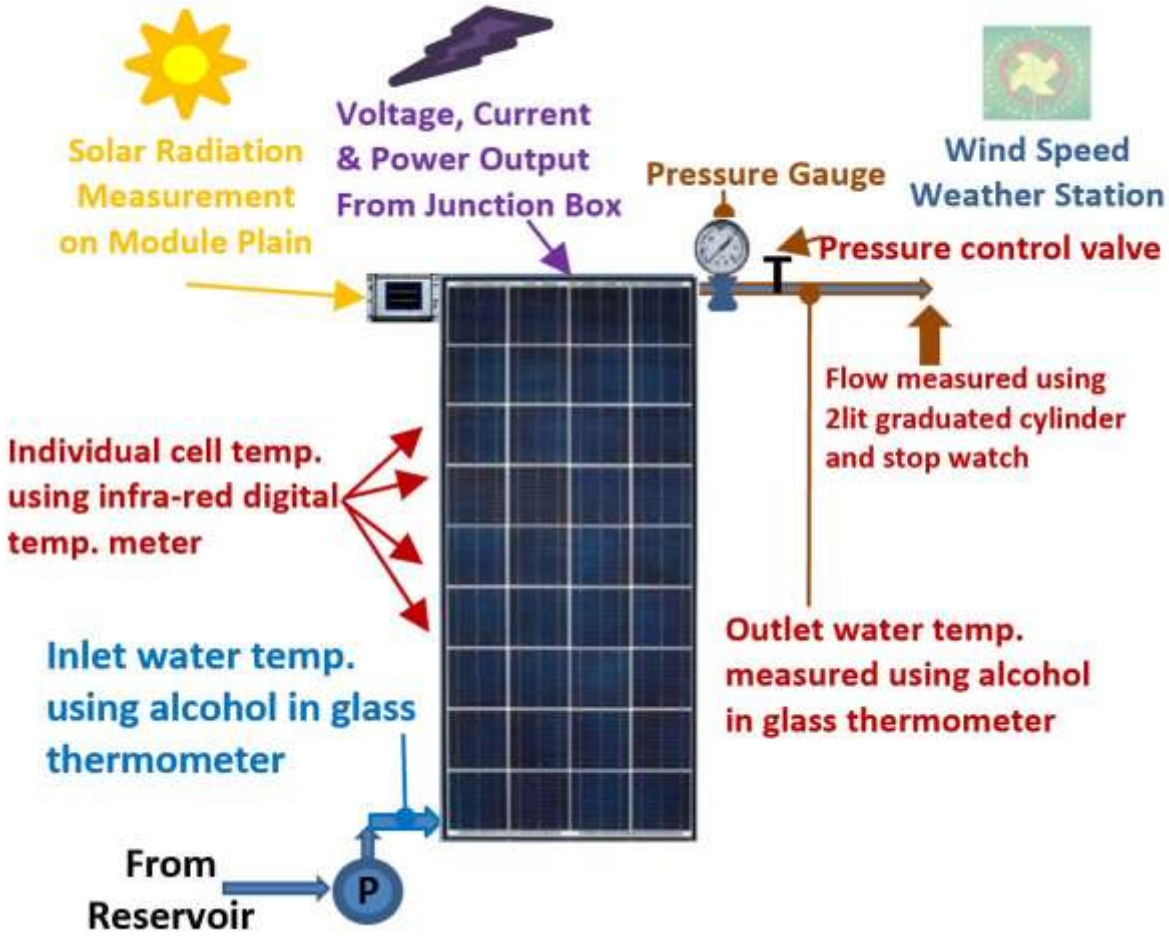

Figure 5-5 Test set-up for performance evaluation

Figure 5-6 Outdoor Test Setup showing BIPV-T Module

Figure 5-7 Measuring Temperature of Individual Solar Cells using Infra-red Temperature Meter

5.4.2 Methodology

The following sequence of testing was followed [26].

The testing of BIPV-T module was done 45 minutes before solar noon and 45 minutes after the solar noon. The module mounting rack was designed for 30˚ to 45˚ inclination. Since the tests were conducted from June to September the optimum inclination of 30˚ was selected. The BIPV-T module was oriented True South. The solar noon during the month of June is 12:51PM clock time during which the Sun reaches its highest point and aligned to the surface of the BIPV-T module. After about 15 minutes of exposure to sunlight the electrical performance of solar module was done in stagnation condition i.e. without circulating the cooling water. This way we could compare the improvement in performance when module was cooled by circulating the water. The temperature of individual cells in the BIPV-T modules is taken with the help of a handheld infra-red temperature meter as seen in Figure 5-7.

The ambient temperature and the wind velocity are also noted. After the stagnation temperature and the electrical performance are observed a battery-operated water circulation pump was switched ON to force the cooling water through cooling pipe attached at the back of BIPV-T module. Once the temperature of the water at the outlet of the BIPV-T module stabilize in 10-12 minutes, the inlet and the outlet temperature readings of the cooling water are measured. The temperature of each of 36 cells in the module is measured simultaneously using infrared temperature meter. Thereafter module electrical performance was recorded using the outdoor module tester (MiniKLA). The ambient temperature and the wind speed are also recorded. The above tests are conducted by varying the cooling water flow rates. For every flow rate, individual cell temperatures, solar radiation, wind speed, ambient, inlet and outlet water temperatures and module electrical output are recorded. The tests are conducted when the sunlight was above 700W/m^2 in clear sunny days. The cooling water flow rates is varied between 0.02 lit/sec to 0.04 lit/sec [26].

5.4.3 Measured and Derived Data

The measured experimental values of novel BIPV-T module are presented in Table 5.2. The measurements are done for ambient temperature (T_a), the global solar radiation in watt per square meter (G is net solar falling on the BIPV-T module area 0.968m^2), solar cell temperature of BIPV-T module (Av. BIPVT Temp is average temperature of 36 cells), the PV power (W) , the temperature of the cooling water inlet (T_{in}), the temperature of the cooling water outlet (T_o), the

flow rate of cooling water in lit/hr at the outlet of BIPV-T module, The pressure is measured at the outlet of BIPV-T module. The pressure is regulated with a shut of valve after the pressure gauge. The flow rate is adjusted both with shut of valve and electronic controller to control the speed of the pump.

In order to calculate the thermal efficiency of BIPV-T module, useful energy Q_u as described in equation 4 is used and derived data is presented in Table 5.3. In this equation (T_o – T_i) is temperature rise in cooling water. This parameter is dependent on flow rate, solar intensity, ambient temperature and wind speed. The temperature rise is higher if flow rate is lower, solar intensity is higher, ambient temperature is higher and wind speed is lower. However, efficiency at higher temperature rise is lower as compared to lower temperature rise due to increased convection and radiation losses from BIPV-T module. Consequently, at higher flow rates temperature gain in cooling water is lower but efficiency is higher due to reduced losses. Though prescribed flow rate for testing solar thermal collectors are between 0.02 lps (72lph) to 0.04 lps (144lph)[26], readings at lower and higher flow rates is also taken. Since BIPV-T is unglazed solar heat collector, we wanted to observe the extent to which outlet temperature will rise at higher and lower flow rates.

In order to compare thermal performance in novel cooling design shown in Figure 5-1 with classical BIPV-T cooling system as shown in Figure 5-2. To compare efficiencies η_{therm} versus $(T_m - T_a)/G$ graph is generated as shown in Figure 5-9. The novel design proposed by us produces approximately 56% thermal efficiency as compared to [11], where thermal efficiency is about 45.5%. The thermal efficiency is also dependent on conductivity and thickness rear insulation that effect the convection loss. Therefore, comparison of thermal performance of two different BIPV-T module is not perfect.

The electrical efficiency of BIPV-T was obtained using Equation 3 described earlier. The solar radiation is measured in watt/m^2 and net solar G is obtained by multiplying measured solar radiation in watts/m^2 by area of BIPV-T module which is length x width (1466mm x 660mm) given in Table 5.1. The electrical performance BIPV-T module is measured using an automatic module tester Mini-KLA which measures solar radiation intensity, voltage, current and power. Mini-KLA also provides I-V curve for each test as shown in Figure 5-13, Figure 5-14, Figure 5-15.

Table 5.2 Outdoor test data of BIPV-T module in natural sunlight and analysis

S.N.	MEASURED TEST CONDITIONS			SOLAR COLLECTOR MESUREMENTS				
	T_a ℃	G (Net Solar) W	Wind m/s	Av. BIPVT Temp ℃	PV Power W	T_i ℃	T_o ℃	Flow Rate lit/hr
1	23.0	955.0	2.22	44.92	126.5	-	-	0
2	22.0	965.6	2.22	41.68	128.2	27.0	35.0	39.46
3	22.5	947.3	2.22	38.79	127.8	30.0	37.0	50.57
4	23.0	940.46	2.22	37.29	128.9	26.0	32.0	67.67
5	25.0	969.5	2.22	41.75	129.7	27.0	34.5	74.20
6	25.0	962.7	2.22	39.54	129.8	28.0	33.2	88.17
7	23.5	918.2	2.22	33.43	128.9	25.0	29.5	105.00
8	23.2	963.7	2.22	37.22	131.4	28.5	33.0	120.64
9	23.5	900.8	2.22	34.63	123.1	24.5	28.5	140.50
10	22.0	955.0	2.22	35.28	131.1	28.5	32.4	156.93

Table 5.3 Derived results of outdoor test of BIPV-T module in natural sunlight and analysis

DERIVED TEST RESULTS						
S.N.	T_o - T_i K	T_m °C	Thermal Power W	$\frac{T_m - T_a}{G}$	Thermal Eff., η_{therm} %	PV Eff., η_{PV} %
1	-	-	-	-	-	13.24
2	8.0	31.00	314.93	0.00932	32.69	13.29
3	7.0	33.50	353.14	0.01161	37.41	13.52
4	6.0	29.00	405.05	0.00638	43.17	13.72
5	7.5	30.75	555.17	0.00593	57.40	13.39
6	5.2	30.60	458.48	0.00582	47.62	13.49
7	4.5	27.25	471.37	0.00395	51.46	13.99
8	4.5	30.75	542.88	0.00783	56.39	13.64
9	4.0	26.50	562.00	0.00333	62.39	13.67
10	3.9	31.00	612.00	0.00885	64.09	13.73

All data presented in Table 5.2 was measured and tabulated as described in Section 1.2.2 Methodology. The average BIPV-T temperature presented in Table 5.2 is the average temperature of all 36 solar cells in the module.

The derived data presented in Table 5.3 are obtained from equations described in Section 1.2.1 Classical considerations of thermal performance of BIPV-T module. As explained in section 1.2.3 PV power is obtained directly from automatic module tester whereas thermal power is obtained from Equation 4. The efficiencies of PV are calculated from Equation 3 and Thermal efficiencies are calculated from Equation 7 presented in section 1.2.1. T_m is the arithmetic average of the fluid inlet and outlet temperature. The efficiency of PV module is derived from Equation 3 where net solar $G = G_T$.

Figure 5-8 is representation of BIPV-T module efficiency with respect to cooling water flow rate. The data for plotting this graph is taken from Table 5.2 and Table 5.3. The graph shows increase in flow rate reduces the BIPV-T temperature and improves the efficiency. The scattering of points is common because performance is temperature dependent, wind effects, and angle of incidence variations[26].

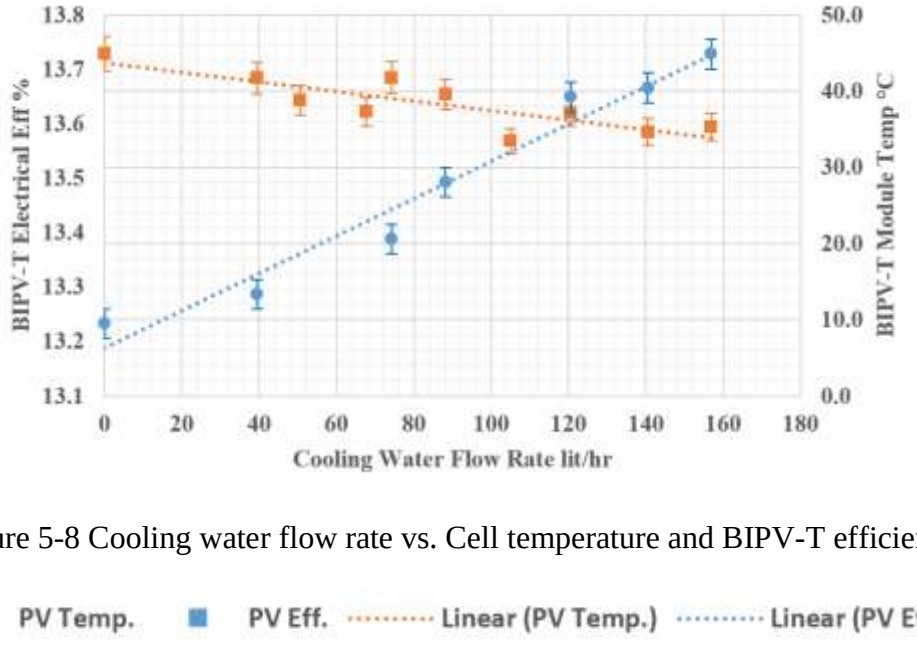

Figure 5-8 Cooling water flow rate vs. Cell temperature and BIPV-T efficiency

Using the data of Table 5.3, Figure 5-8 shows the variation of the PV efficiency with cooling water flow rate. The temperature of the BIVP-T increases as the flow rate decreases. The PV efficiency increases as the cooling water rate increases.

Table 5.9 shows thermal and electrical efficiencies $\eta_{therm}\ and\ \eta_{PV}$ with respect to inlet parameter $(\mathrm{T_m} - \mathrm{T_a})/\mathrm{G}$. The data for plotting the performance is taken from Table 5.3. This is a classical representation of thermal performance as per European standard. As explained in equation European method uses $\mathrm{T_m}$ mean temperature of inlet and outlet water temperature passing through BIPV-T collector. The performance estimates of solar thermal collectors can be characterized by intercept $F_{\mathrm{av}}(\tau\alpha)$ and slope $F_{\mathrm{av}}U_L$ as described in equation 8 [26].

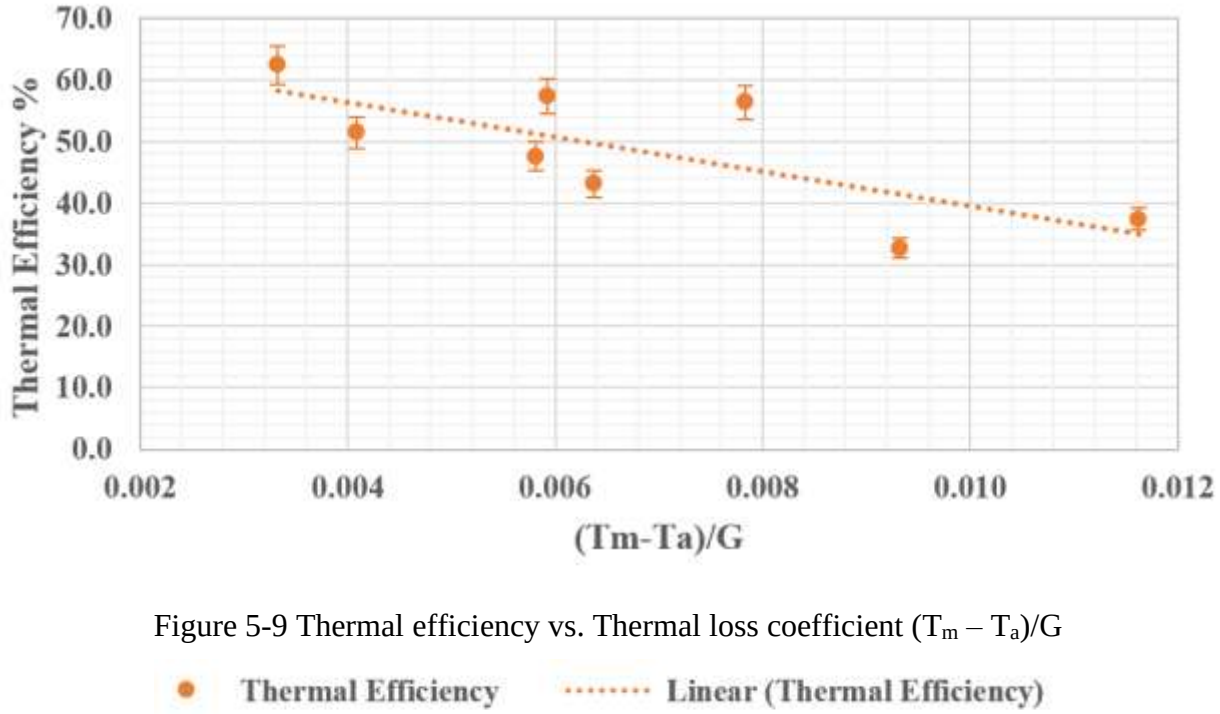

Figure 5-9 Thermal efficiency vs. Thermal loss coefficient $(\mathrm{T_m} - \mathrm{T_a})/\mathrm{G}$

5.5 Temperature Uniformity Testing of Novel Cooling Pipe Configuration for BIPV-T Module

5.5.1 Indoor testing by circulating preheated water

After fabricating the BIPV-T module a series of indoor testing was conducted to evaluate the performance at various cooling water temperatures and flow rates. The objective of indoor testing was to eliminate the effect of wind velocity and shading.

The indoor test setup is exactly same as proposed for outdoor testing in natural sunlight except that preheated water at varying temperatures and flow rates is circulated in the cooling circuit. The temperature of all 36 solar cells is measured to determining the temperature variation.

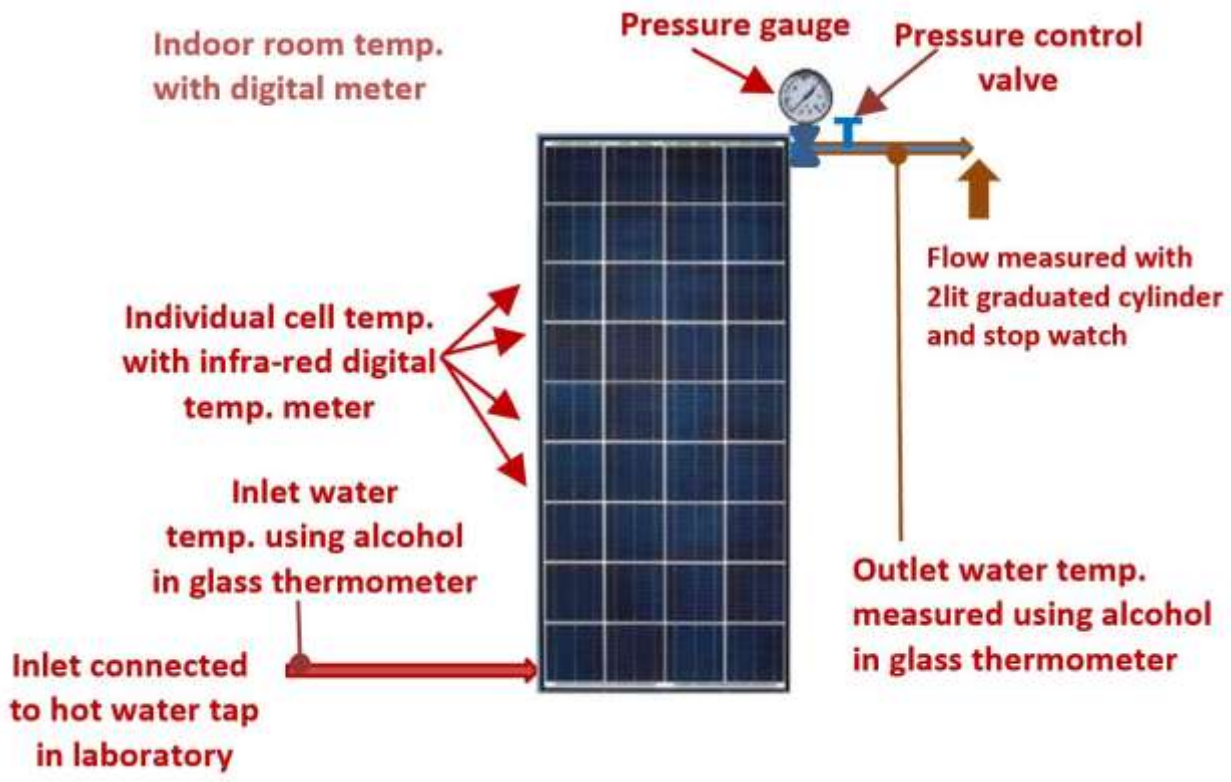

Figure 5-10 Indoor testing of novel water-cooling pipe configuration for temperature uniformity

The variation in cell temperature in indoor testing with respect to varying cooling water flow rate is shown in Table 5.4 and Table 5.5. The testing was conducted for two flow rates 118 liters per

hour and 74.66 liters per hour respectively. The performance of cell temperature uniformity was done by circulating hot water at 47°C. The temperature of each cell (36) was measured using infra red temperature meter. The cell temperature for novel BIPV-T is remarkable uniform within 2.1°C at 118litres per hour flow rate. Even at low flow rate of 74.66litres per hour the temperature uniformity is within 2.5°C.

Table 5.4 Experimental results of the cell temperature of indoor testing of BIPV-T module with novel cooling pipe circuit at high cooling water flow rate

Flow Rate (LPH)	118 LPH	Individual Cell Temperature (°C) Variation with Solar Cell number								Row Temp. Diff. °C
		Cell	Temp	Cell	Temp	Cell	Temp	Cell	Temp	
Date	18-Apr-18	1	36.3	10	36.5	19	36.2	28	35.8	0.7
T_{amb} , °C	22.1	2	35.8	11	36.5	20	36.3	29	36.8	1
Av. Module Temp., °C	36.50	3	35.1	12	35.7	21	36.3	30	36.7	1.6
Max Cell Temp., °C	37.6	4	35.0	13	36.1	22	37.1	31	36.2	2.1
Min Cell Temp., °C	35.0	5	35.8	14	36.7	23	37.5	32	37.1	1.7
(Max - Min) Temp., °C	2.6	6	36.5	15	36.5	24	37.2	33	36.2	1
(Max - Av) Temp., °C	1.10	7	36.3	16	35.6	25	37.2	34	37.0	1.6
(Av. - Min) Temp., °C	1.50	8	36.5	17	37.1	26	37.3	35	37.5	1
Water (In - Out) °C	3.0	9	36.8	18	35.9	27	37.2	36	37.6	1.7
Column-wise Temp Diff., °C ->		1.8		1.5		1.3		1.8		
$Water_{in}$ Temp., °C	47.0	$Water_{out}$ Temp., °C						44.0		
Wind Speed, m/s	0	($Water_{out}$ - Av. Module Temp), °C						7.50		

The Vertical Column-wise Column 1: Cells 1-9; Column 2: Cells:10-18; Column 3: Cells 19-27 and Column 4: Cells 28-36); Horizontal Row-wise (Row 1: Cell 1,10,19 and 21); (Row 2: Cell 2,11,20,29); (Row 3: Cell 3,12,21,30); (Row 4: Cell 4,13,22,31); (Row 5: Cell 5,14,23,32); (Row 6: Cell 6,15,24,33); (Row 7: Cell 7,16,25,34); (Row 8: Cell 8,17,26,35); (Row 9: Cell 9,18,27,36).

Table 5.5 Experimental results of the cell temperature of indoor testing of BIPV-T module with novel cooling pipe circuit at low cooling water flow rate

Flow Rate (LPH)	74.66 LPH	Individual Cell Temperature (°C) Variation with Solar Cell number								Row Temp. Diff. °C
		Cell	Temp	Cell	Temp	Cell	Temp	Cell	Temp	
Date	18-Apr-18	1	37.0	10	36.9	19	36.3	28	36.4	0.7
T_{amb} , °C	21.6	2	36.0	11	36.7	20	36.2	29	36.9	0.9
Av. Module Temp, °C	36.85	3	35.6	12	35.5	21	36.3	30	36.7	1.2
Max Cell Temp, °C	38.1	4	35.0	13	36.0	22	37.3	31	36.5	2.3
Min Cell Temp, °C	35.0	5	36.0	14	36.9	23	37.6	32	37.9	1.9
(Max - Min) Temp, °C	3.1	6	36.9	15	37.4	24	37.5	33	37.3	0.6
(Max - Av) Temp., °C	1.25	7	37.0	16	36.1	25	37.5	34	37.5	1.4
(Av. - Min) Temp., °C	1.85	8	37.3	17	37.9	26	37.5	35	38.1	0.8
Water $_{(In - Out)}$, °C	2.0	9	37.5	18	36.1	27	37.4	36	37.9	1.8
Column-wise Temp Diff., °C ->		2.5		2.4		1.4		1.7		
$Water_{in}$ Temp., °C	47.0	$Water_{out}$ Temp., °C						45.0		
Wind Speed, m/s	0	($Water_{out}$ - Av. Module Temp.), °C						8.15		

The vertical column-wise and horizontal row wise cell configuration for measuring cell temperature for 74.66 litres per hour flow rate is exactly same as for 118 litres per hour flow rate described below Table 5.4. The water is circulated at 3 bar pressure.

Temperature variation with solar cell number for BIPV-T module in indoor testing is shown in Figure 5-11 and Figure 5-12. The pattern in cell temperature at flow rate of 118 litres per hours and 74.66 litres per hour is almost same.

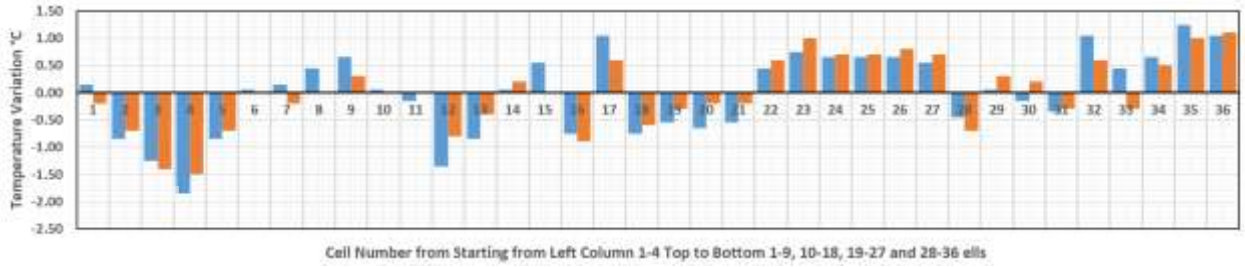

Figure 5-11 Vertical column-wise temperature variation in solar cells for BIPV-T module in indoor testing

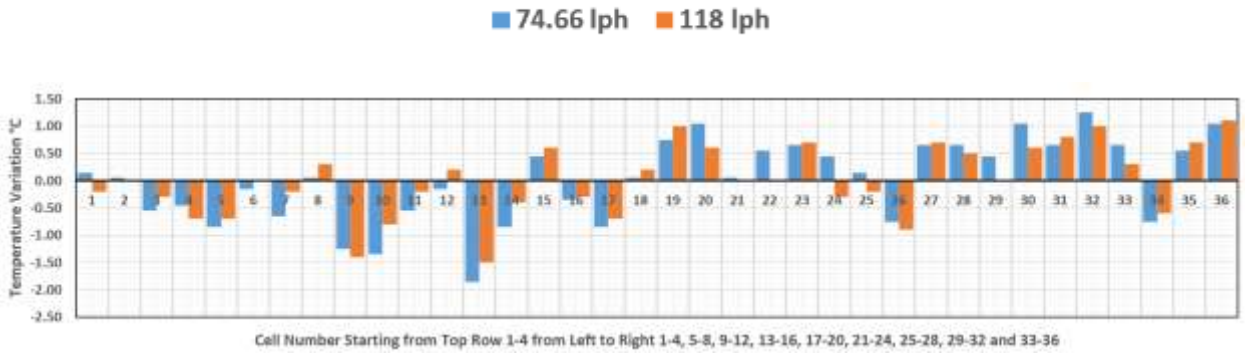

Figure 5-12 Horizontal row-wise temperature variation with solar cell number for BIPV-T module in indoor testing (for 36 cell module)

5.5.2 Testing of uniformity in cooling of BIPV-T module in outdoor in sunlight

Earlier tests were conducted indoors to check the uniformity of cooling with novel cooling pipe configuration. The indoor testing was done without Sunlight. It is important to check how effective is the novel cooling pipe configuration in cooling all 36 solar cells uniformly in outdoor conditions.

Figure 5-13, Figure 5-14 and Figure 5-15 are the current voltage curves obtained from three tests respectively, in stagnation condition or without cooling, low (74.20 lit/hour) and high (120.64 lit/hour) flow rates under pressurized 0.6 bar conditions.

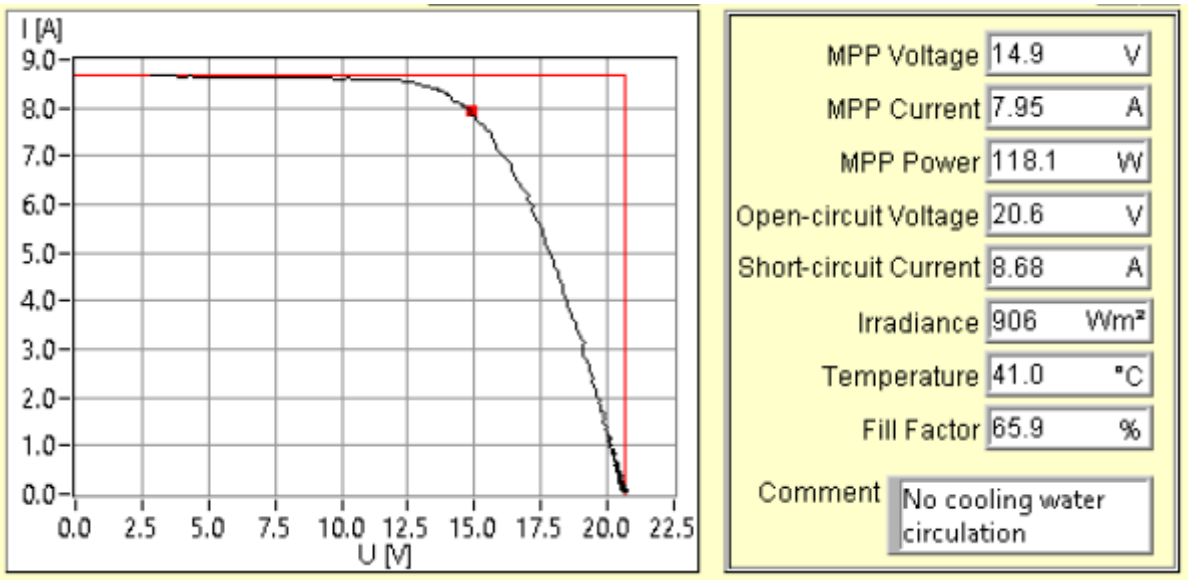

Figure 5-13 BIPV-T module outdoor electrical performance in stagnation state (without water cooling)

Table 5.6 Experimental outdoor data of BIPV-T module output, module temperature and temperature uniformity tests without cooling

Flow Rate, lph	**0**	**INDIVIDUAL CELL TEMPERATURES**				**Temp Diff. Rows**
Wind Speed	**2.22 m/s**	**42.8**	**45.7**	**44.4**	**43.0**	**2.9**
T_{amb} (20^0C)	**23.5**	**44.7**	**46.9**	**45.9**	**45.3**	**2.2**
BIPVT Temp. ^{0}C	**45.99**	**46.1**	**47.9**	**47.5**	**46.7**	**1.8**
V_{oc}, Volt	**20.7**	**45.7**	**48.4**	**47.8**	**47.7**	**2.7**
I_{sc}, Ampere	**8.65**	**45.8**	**48.5**	**47.6**	**47.1**	**2.7**
P_{mpp}, Watt	**118**	**45.7**	**48.2**	**47.6**	**46.6**	**2.5**
V_{mpp}, Volt	**14.8**	**44.7**	**47.6**	**47.5**	**45.1**	**2.9**
I_{mpp}, Ampere	**7.95**	**44.7**	**47.0**	**47.2**	**44.9**	**2.5**
Solar, Watt/m^2	**906**	**41.8**	**45.0**	**44.8**	**41.7**	**3.3**
Temp. Difference Columns >		**4.3**	**3.5**	**3.4**	**6.0**	
$WATER_{in}$ TEMP	**-**	**$WATER_{out}$ TEMP >**		**-**		

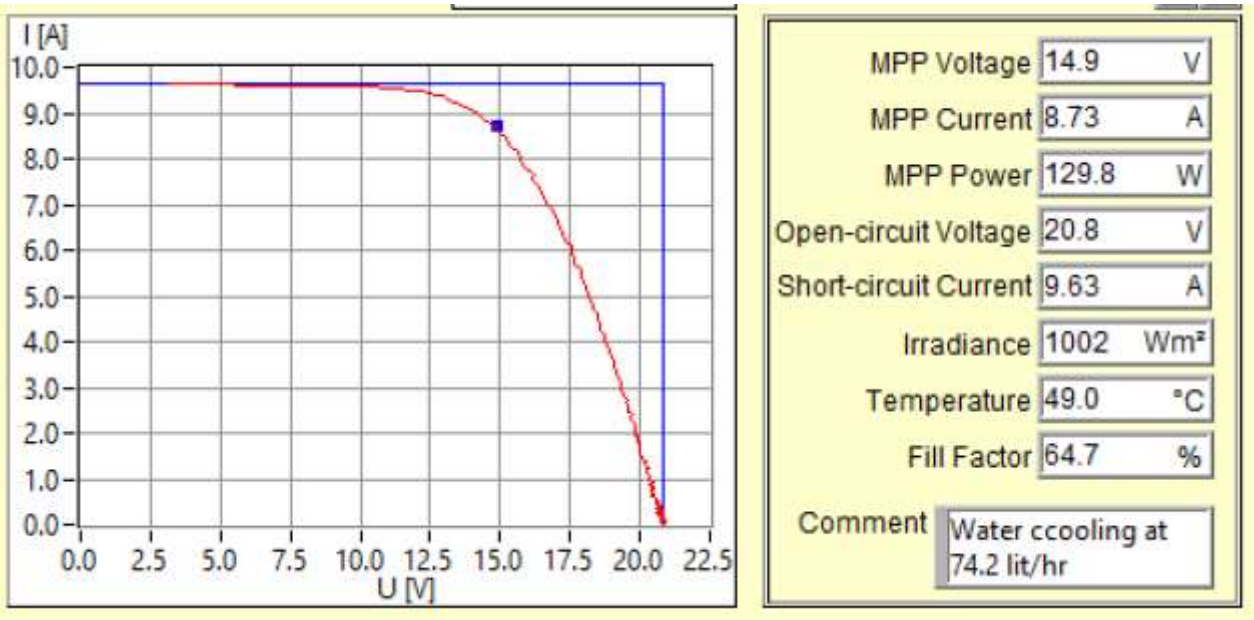

Figure 5-14 Experimental results of BIPV-T module electrical performance at low water cooling rate (74.2 litres/hour)

Table 5.7 BIPVT module electrical performance with 74.2 lit/hr cooling water circulation

Flow Rate lph	74.2	INDIVIDUAL CELL TEMPERATURES				Temp Diff. Rows
Wind Speed	2.22 m/s	37.0	42.0	38.8	42.8	5.0
T_{amb} °C	25.0	37.2	42.5	38.5	42.1	4.9
BIPVT Temp.°C	41.75	44.1	44.3	44.3	38.4	5.9
V_{oc}, Volt	20.8	44.1	45.0	45.0	42.9	2.1
I_{sc}, Ampere	9.63	40.4	44.5	41.9	39.7	4.8
P_{mpp}, Watt	129.8	44.0	42.3	44.5	39.1	4.9
V_{mpp}, Volt	14.9	43.8	42.2	41.5	40.6	3.2
I_{mpp}, Ampere	8.71	43.2	44.4	44.3	38.8	5.6
Solar Intensity	1002	36.9	43.3	41.0	37.6	5.7
Temp. Difference Columns>		6.9	1.9	5.8	4.5	
$WATER_{in}$ TEMP	27	$WATER_{out}$ TEMP		34.5		

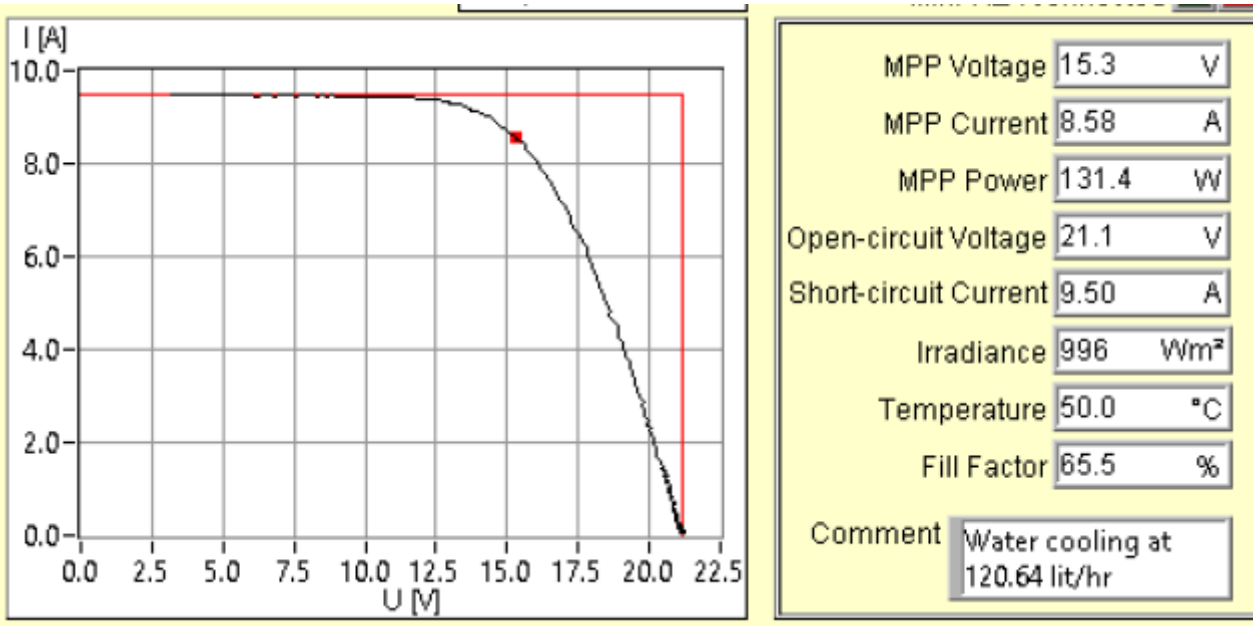

Figure 5-15 Experimental BIPVT module electrical performance at high cooling water circulation rate (120.64 litres/hour)

Table 5.8 BIPVT Module Electrical Performance with 120.64 lit/hr cooling water circulation

Flow Rate, lph >	**120.64**	**INDIVIDUAL CELL TEMPERATURES**				**Temp. Diff. Rows**
Wind Speed, m/s	**2.22**	**33.8**	**34.5**	**37.3**	**34.5**	**3.5**
T_{amb} °C	**23.2**	**35.5**	**38.4**	**37.3**	**37.2**	**1.2**
BIPVT Temp. °C	**37.22**	**38.2**	**39.9**	**39.6**	**37.4**	**2.5**
V_{oc}, Volt	**21**	**39.4**	**39.7**	**39.5**	**40.3**	**0.2**
I_{sc}, Ampere	**9.5**	**39.9**	**37.5**	**36.7**	**39.5**	**0.4**
P_{mpp}, Watt	**131.3**	**35.6**	**38.3**	**37.5**	**37.8**	**2.7**
V_{mpp}, Volt	**15.3**	**34.6**	**38.9**	**38.4**	**39.3**	**3.8**
I_{mpp}, Ampere	**8.58**	**35.1**	**36.4**	**36.2**	**39.9**	**4.8**
Solar, Watt/m²	**995**	**33.8**	**35.3**	**33.5**	**33.3**	**2.0**
Temp. Difference Columns >		**6.1**	**5.4**	**6.1**	**3.1**	
$Water_{in}$ Temp. °C >	**28.5**	**$Water_{out}$ Temp. °C >**		**33**		

Figure 5-13, Figure 5-14 and Figure 5-15 electrical performance of BIPV-T for uncooled and cooled at low and high water flow rates. The temprature distribution is fairly uniform from one cell to another cell for the 36 cells module as shown in highlighted section of Table 5.6, Table 5.7 and Table 5.8. For a given cell, the cell temperrature is higher in stagnation condition than when the cell is cooled at 74.2 or 120.64 litres per hour. The cell temperature (41.77°C) is higher at low cooling flow rate (74.2 litres/hour) than its temperature at high cooling flow (120.64 litres/hour).

Using data of Figure 5-13, Figure 5-14 and Figure 5-15, the normalized of the MPP current in A/Wm^2 of irradiance, MPP short circuit current/ Wm^2 of irradiance and the MPP POWER/ Wm^2 of irradiance are shown in Table 5.9. It seems that there is no fundamental difference in electrical performance of module at varying water-cooling flow rates.

Table 5.9 Normalized of the MPP current in A/Wm^2 of irradiance, MPP short circuit current/ Wm^2 of irradiance and the MPP POWER/ Wm^2 of irradiance are shown.

	MPP current/ Wm^2 of irradiance	MPP short circuit current/Wm^2 of irradiance	MPP POWER/ Wm^2 of irradiance
Stagnation	0.008775	0.00955	0.130
Cooling at 74.2 lit/hr.	0.00869	0.00961	0.131
Cooling at 120.64 lit/hr.	0.00862	0.00955	0.132

Figure 5-16 and Figure 5-18 show the comparative variation of cell temperatures for uncooled and cooled BIPV-T module at 120.64lph per hour and 74.2lph per hour respectively. Figure 5-16 is vertical column wise cell temperatures and Figure 5-18 is horizontal row wise cells in the BIPV-T module.

Figure 5-17 and Figure 5-19 show temperature differential between each cell with respect to average temperature of all 36 cells. Figure 5-17 is vertical column wise cell temperatures and Figure 5-19 is horizontal row wise cells in the BIPV-T module. Some cells are operating at higher than average and some at lower than average cell temperatures. Generally, solar cells in the middle

of module show higher temperature. This may be due to poor contact of cooling sheet at the back of module.

5.5.3 Graphical performance of temperature uniformity of 36 cells in a BIPVT module with novel cooling circuit

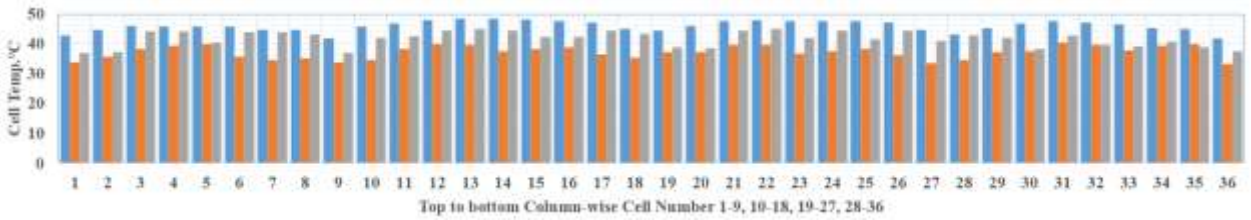

Figure 5-16 Vertical column-wise temperature of solar cells at various flow rates in BIPVT module

Figure 5-16 shows the temperature of each of 36 cells. The cells are counted top to bottom 1-9 cell, 10-18 cell, 19-27 cell and 28-36 cell. The comparison of cell temperature without cooling, cooling @74.20lph and @120.64lph presented for all 36 cells in new BIPV-T module.

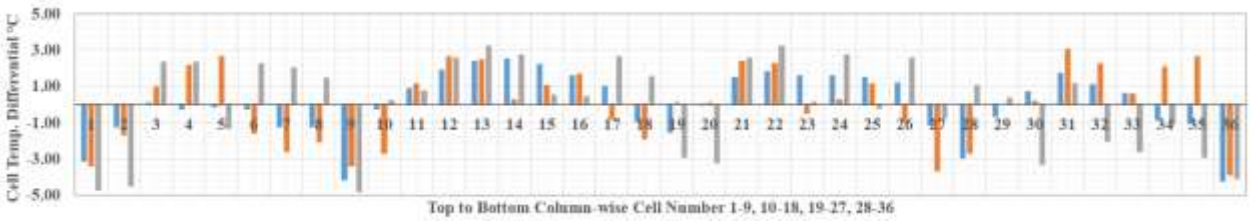

Figure 5-17 Vertical column-wise temperature differential of solar cells at various flow rates in BIPVT module

Figure 5-17 shows the temperature differential of each 36 cells. The cells are counted top to bottom 1-9 cell, 10-18 cell, 19-27 cell and 28-36 cell. The comparison of cell temperature without cooling, cooling @74.20lph and @120.64lph presented for all 36 cells in new BIPV-T module.

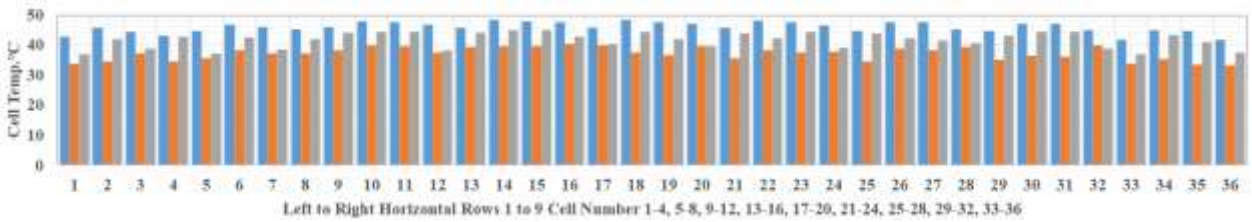

Figure 5-18 Horizontal row-wise temperature of solar cells at various flow rates in BIPVT module

Figure 5-18 shows the temperature of each of 36 cells. The cells are counted left to right starting with top horizonal row and ending at bottom horizontal row 1-4 cell, 5-8 cell, 9-12 cell, 13-16 cell, 17-20 cell, 21-24 cell, 25-28 cell, 29-32 cell and 33-36 cell. The comparison of cell temperature without cooling, cooling @74.20lph and @120.64lph presented for all 36 cells in new BIPV-T module.

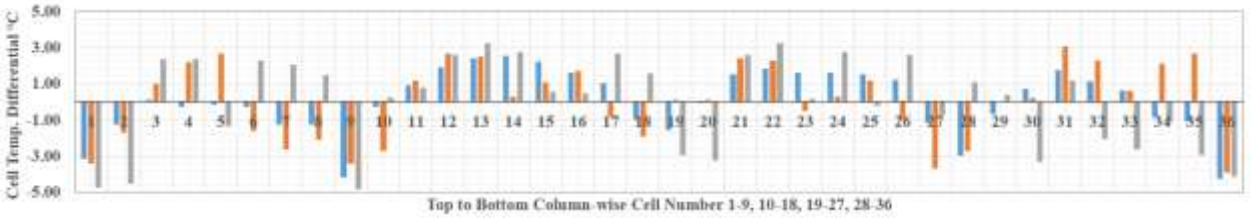

Figure 5-19 Horizontal row-wise temperature differential of solar cells at various flow rates in BIPVT module

Figure 5-19 shows differential temperature of cells about zero axis which is the average temperature of 36 cells. The graph shows which of 36 cells are heating above average and which below average for uncooled and cooled at low and high water flow rates. Figure 5-18 shows the temperature of each of 36 cells. The cells are counted left to right starting with top horizonal row and ending at bottom horizontal row 1-4 cell, 5-8 cell, 9-12 cell, 13-16 cell, 17-20 cell, 21-24 cell, 25-28 cell, 29-32 cell and 33-36 cell. The comparison of cell temperature without cooling, cooling @74.20lph and @120.64lph presented for all 36 cells in new BIPV-T module.

5.6 Improvement in Design of Novel BIPV-T Cooling Pipe

(a) To simplify and improve the fabrication of BIPV-T module with novel cooling pipe configuration a second working model of size 335mm x 335mm was made and tested. For making this module 125mm x 125mm Sun Power cells was used and cooling circuit was made to fit the cell area. The thermal absorber and novel cooling pipe configuration are shown with water flow direction Figure 5-20(a).

(b) Improved cooling pipe attached to copper cooling sheet shown in Figure 5-20(b).

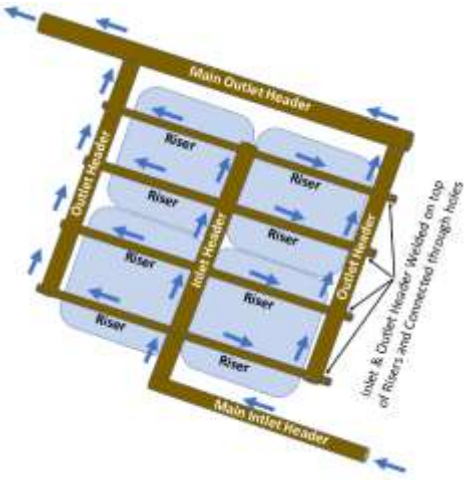

(c) Water flow direction (b) Improved cooling pipe attached to copper cooling sheet

Figure 5-20 View of novel cooling pipe configuration attached to copper plate

The cooling water flow direction and tube and sheet fabricated by bracing with Sn/Ag solder to improve thermal conductivity between copper tube and sheet.

(a)

(d)

(c)

Figure 5-21 Picture of front and back of BIPV-T module model

Figure 5-21(b) shows how copper tube and sheet heat exchanger is inserted at the back of PV module and held in place with tape instead of pasting with conductive glue. Since PV modules carry 25year warranty it is not advisable to make any physical changes. Moreover, solar water heating collectors usually carry only 5-year warranty and its life is limited to 15 years. The attachment of cooling sheet is therefore kept flexible to replace and repair when needed. The sheet and tube cooling sheet cover solar cell area 0.253m x 0.253m. During the outdoor testing, area around four solar cells as seen in Figure 5-21(b) is masked with opaque tape to ensure heat from excessive width of empty space does not get transferred to the solar cells. This is because the cooling pipe and copper plate is made to the size of four laminated solar cells.

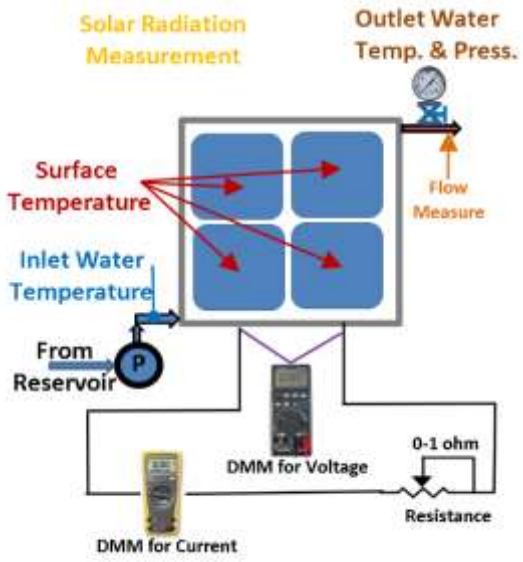

Figure 5-22 Set-up for outdoor testing of small BIPV-T module

The outdoor test setup is shown in Figure 5-22. All outdoors measurements for ambient temperature, wind speed, water pressure, cooling water inlet and outlet temperatures are done as described earlier for 1st prototype. The solar radiation measurement is done with Mini-KLA but current and voltage measurements are done with two multimeters. For collecting multiple current and voltage data for drawing I-V characteristics 1ohm variable resistance is used.

The electrical, thermal and weather data collected from testing is tabulated in

Table 5.10 below. The derived data is also presented in the same table. The table below shows the measured and derived data for improved novel BIPV-T module. This data is used for drawing performance curves in Figure 5-24 and Figure 5-25.

Table 5.10 Outdoor Performance of BIPV-T Module with Improvements in Cooling Pipe Fabrication Methodology

S.N.	MEASURED TEST CONDITIONS			BIPV-T MEASUREMENTS					DERIVED RESULTS					
	Ambient	Radiation	Wind	PV Temp	Power	T_i	T_o	Flow	ΔT	T_m	Therm Pwr		η_{therm}	η_{PV}
	°C (T_a)	*G* (net)	m/s	°C (mean)	watts	°C	°C	lit/hr	k	°C	W	$\frac{T_m - T_a}{G}$	%	%
1	21.0	49.60	1.39	47.05	7.94	0.00	0.00	0.00	0.00	0.00	0.00	0.00	0.00	16.01
2	21.0	56.65	1.39	39.45	9.43	29.50	34.00	6.85	4.50	31.75	30.83	0.18976	54.95	16.64
3	25.7	60.30	1.39	39.30	10.10	29.50	33.80	7.85	4.30	31.65	33.76	0.09867	55.98	16.75
4	27.5	60.36	1.39	38.10	10.22	29.50	32.30	12.37	2.80	30.90	34.64	0.05633	57.38	16.93

Where, T_i is inlet temperature of cooling water, T_o is outlet temperature of cooling water, ΔT is temperature difference between outlet and inlet temperature of cooling water, T_m is the mean temperature of outlet and inlet temperature of cooling water and ***G*** is the net solar radiation falling on the surface of PV module aperture which is **0.064 m^2**(0.253m x 0.253m).

Table 5.11 Outdoor performance of BIPV-T before incorporating cooling pipe and insulation

Solar Radiation:	775 W/m^2		Module Size for Measurements:	0.253m x 0.253m
Temperature of PV Module:	48.80°C		Solar Cell Size (Pseudo Square):	125mm x 125mm
Open Circuit Voltage:	2.40 V		Number of Cells in Module:	4 Solar Cell
Voltage at Peak Power:	1.99 V		Make of Cells:	Sun Power
Short Circuit Current:	4.87 Amp		Module Frame Height	50mm
Current at Peak Power:	3.99 Amp		Module Backsheet	TPT Black
Peak Power:	7.94 W		Encapsulation	EVA
Note: Since the module voltage is too low for using automatic module tester a variable resistance and multimeters for voltage and current measurements were used.				

The Table 5.11 presents the physical and electrical specification of improve BIPV-T module. The electrical performance of uncooled BIPV-T module measured as described in Figure 5-22.

Figure 5-23 below shows current, voltage and power characteristics for improved BIPV-T module without cooling.

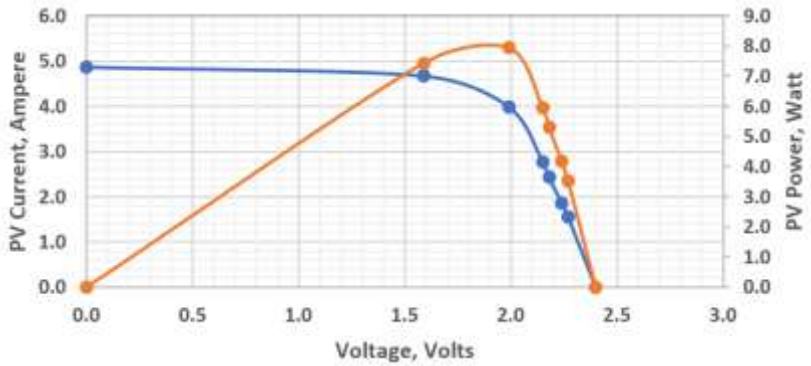

Figure 5-23 Voltage, current & power curve of BIPV=T in Natural Sunlight without cooling

Figure 5-24 below shows electrical efficiency of improved novel BIPV-T increases at higher flow rate due to drop in cell operating temperature.

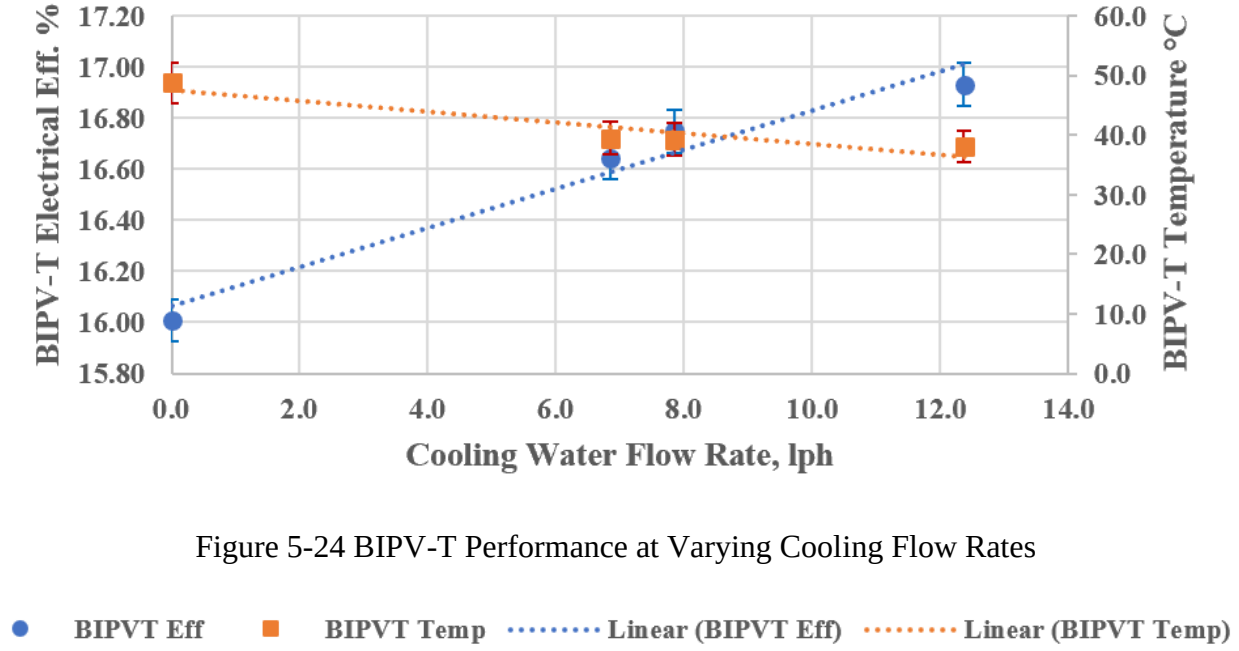

Figure 5-24 BIPV-T Performance at Varying Cooling Flow Rates

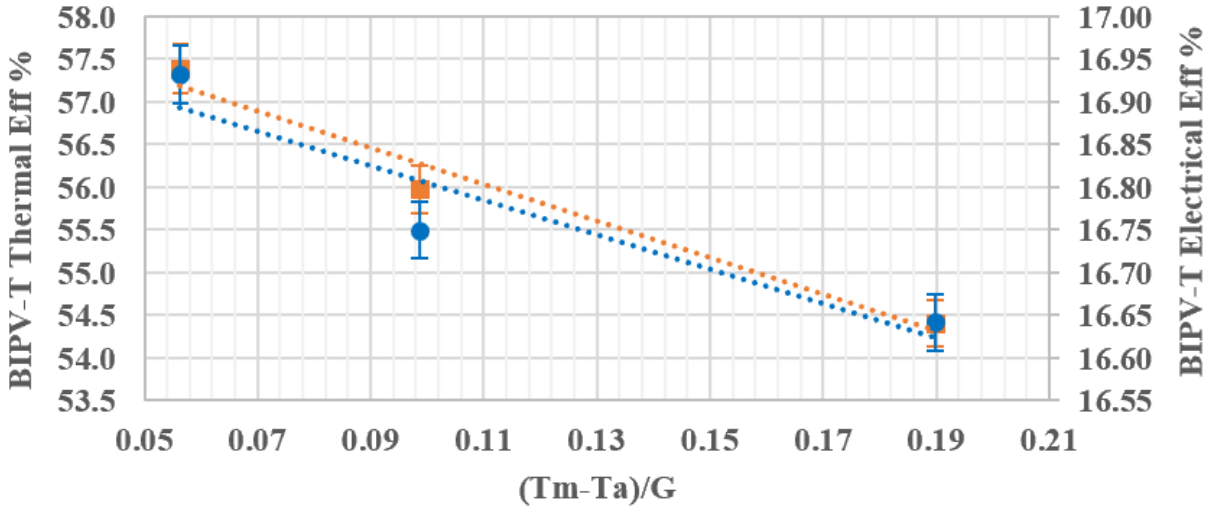

Figure 5-25 Thermal and electrical efficiencies versus Thermal loss coefficient [$(T_m - T_a)/G$, $K.m^2/W$]

Table 5.12 Solar Cell temperature uniformity in BIPV-T module at various flow rates and weather conditions

Stagnation (no cooling)			
Solar Radiation, W/m^2:	933	Cell1	Cell3
Ambient Temp., °C:	24.0	47.4 °C	48.1 °C
Input Water Temp., °C:	N/A	Cell2	Cell4
Output Water Temp., °C:	N/A	45.7 °C	47.0 °C
Wind Speed, kmph:	11.0	Av. Temp:	47.05 °C

Cooling Water Flow Rate 6.85 lit/hour (0.75 bar)			
Solar Radiation, W/m^2:	885	Cell1	Cell3
Ambient Temp., °C:	21.0	38.8 °C	43.0 °C
Input Water Temp., °C:	29.5	Cell2	Cell4
Output Water Temp., °C:	34.0	39.3 °C	42.7 °C
Wind Speed, kmph:	5.0	Av. Temp:	40.95 °C

Cooling Water Flow Rate 7.85 lit/hour (0.75 bar)			
Solar Radiation, W/m^2:	885	Cell1	Cell3
Ambient Temp., °C:	25.7	38.0 °C	39.9 °C
Input Water Temp., °C:	29.5	Cell2	Cell4
Output Water Temp., °C:	33.8	38.7 °C	40.6 °C
Wind Speed, kmph:	5.0	Av. Temp:	39.30 °C

Cooling Water Flow Rate 12.37 lit/hour (0.75 bar)			
Solar Radiation, W/m^2:	845	Cell1	Cell3
Ambient Temp., °C:	21.0	37.9 °C	38.5 °C
Input Water Temp., °C:	29.5	Cell2	Cell4
Output Water Temp., °C:	31.0	38.1 °C	39.2 °C
Wind Speed, kmph:	5.0	Av. Temp:	38.43 °C

Note: Cooling plate and pipe is not glued to the back of solar module.

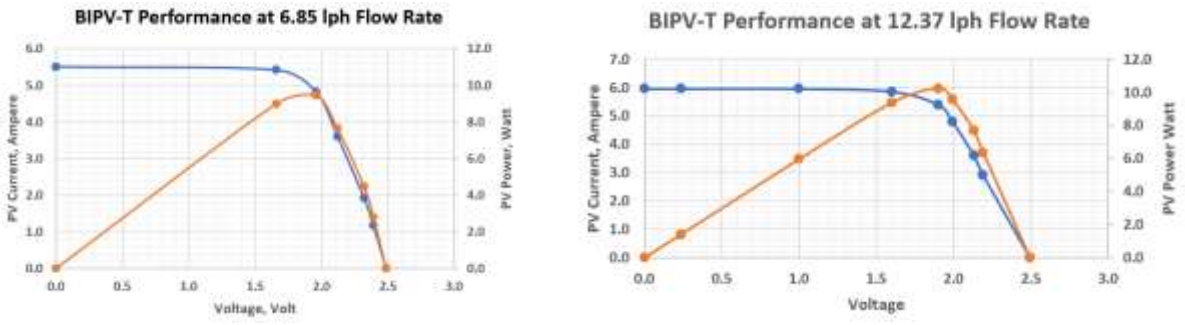

Figure 5-26 Electrical performance of BIPV-T module at various cooling-water flow rates

5.7 Results & Discussion

5.7.1 First BIPV-T prototype with novel cooling pipe configuration

The first article is on the simulation of the performance of BIPV-T based on TRNSYS software. Accordingly, the effect of various parameters as for example cooling water flow rates, cooling water temperature, ambient temperature, solar radiation intensity etc. on the performance of the BIPV-T e.g. PV efficiency, thermal efficiency, individual cell temperature uniformity have been determined. It was shown, our approach of using multiple sub-header design exhibit significantly better individual cell temperature uniformity than that has been obtained until now. Based on the simulation results two types of prototypes has been fabricated and tested using the same parameters as the simulation process. The results are in agreement with those of the simulation. In particular we obtained the following results.

The electrical and thermal performance of BIPV-T module tabulated in Table 5.2, Table 5.3 and Figure 5-8 and Figure 5-9 show an increase in electrical and thermal efficiencies with cooling water flow rate. The increase in electrical efficiency obtained is upto 0.75% (5.7% improvement) over uncooled cells. The thermal efficiency based on heat collection in cooling water obtained is upto 57.4%. These improvements are significant when compared to widely produced polycrystalline cells and modules efficiency increase of only 4% from year 2009 to 2019 (0.4%/year)[27].

The indoor uniformity test shows cell temperatures of novel BIPV-T are within 2.1°C at 118lph flow rate which is close to our target. However, in outdoor uniformity test the cell temperature uniformity increases to 6.1°C at 120.64 lph flow rate. The variations in temperature uniformity of 36 solar cell is likely due to variation in wind speed, ambient temperatures and angle of incidence of solar radiation during the course of observation. These improvements are related to the fundamental effect of temperature on the PV module performance. It is well established that the temperature coefficient on cell power is in the range of – 0.3 to -0.6%/°C depending of the cell and module technologies. Cooling of cells helps to overcome reduction in power output.

The Figure 5-8 shows electrical performance of BIPV-T module where scattering of readings is result of variation in atmospheric conditions during outdoor testing. In order to arrive at streamline, result a linear trend line was drawn on the graphical performance. The graph shows improvement in efficiency of BIPV-T module as the cooling water flow rate increases and temperature of module drops.

The Figure 5-9 shows thermal performance of BIPV-T module with respect to inlet parameter $(T_m-T_a)/G$. This is the most standard way of representing thermal performance as per European Union methods of testing [26]. The scattering of points shown in Figure 5-9 is common for outdoor testing. A linear trendline is shown with equation for use in software like TRNSYS and F-Chart for designing a solar water heating system. Accordingly, these results can be used to design our new water-cooling system with uniform cooling of each cell. The experimental results obtained for fabricated prototype indicate it is possible to cool individually each cell of a BIPV-T with novel concept of cooling pipe configuration.

The purpose of indoor test was to check if the fabricated BIPV-T module with Novel water-cooling configuration can provide uniform temperature for all solar cells as envisaged. The indoor testing observation will show any shortcoming in fabrication of BIPV-T module with novel cooling circuit that was designed to cool individual solar cells uniformly. For this purpose, hot water was circulated in the cooling pipe at various flow rate and pressure. The temperature of individual solar cells was noted using infrared thermometer. The result showed fairly uniform distribution from 0.7°C to 2.5°C which is satisfactory for a product made with minimum facility using low conductivity conductive silicone for bonding.

The outdoor performance for the uniform cooling in natural sunlight is presented in Table 5.7 and Table 5.8. As compared to indoor results, the outdoor results show more temperature variation in solar cells. The highest variation recorded was 6.5°C and the variation ranged from 0.2°C to 6.5°C. There are several reasons may be attributed to higher variation in cell temperature as compared to indoor testing. First, in the outdoor testing temperature recording of individual cell with infrared temperature meter was a challenge. The laser beam was not very visible in sunlight to focus exactly on the center of each solar cells. Secondly, coming too close to the module caused shadowing. Thirdly, during the temperature reading for 36 cells the periodic wind gust would change the temperature. Fourthly, the cooling water tank capacity was limited to allow long duration cooling as the BIPV-T was tested in single pass method. Fifthly, the cooling water could not be pressurized as much as in indoor testing due to pump limitations. The pressure ranged from 0.6bar to 0.8bar whereas indoor the pressure could be increased up to 3bar. The sixth but most important observation that graphical distribution and variation of cell temperatures in columns and rows shows that temperature variation is following sinusoidal pattern. That means center of the BIPV-T module is operating at higher temperature than edges. This may be attributed to improper contact of copper plate and cooling water pipe in the center of BIPV-T module.

5.7.2 Second improved BIPV-T with novel cooling pipe configuration

The objective of fabricating and testing an improved model of BIPV-T module is to make a more compact cooling pipe configuration and to improve the conductivity of water pipe to copper plate. In first prototype cooling pipe design the height of inlet and outlet headers pipes was very close to the frame height of the solar module due to use of Tee and Elbow joints. This resulted in difficulty in filling the insulation properly at the back of BIPV-T module. In addition, cost of material and labor was too high, the conductivity of thermally conductive adhesive used to attach cooling pipe to plate was very low 2.2W/m.K.

With the improved design proposed in this paper, the copper plate was braced to copper plate providing far better conductivity of 78 W/m.K (SnAg 96.5/3.5). The height of inlet and outlet header pipes reduced to $1/4^{th}$ of earlier design.

Since the copper cooling plate attached to cooling pipe was fabricated as same size as 4 solar cells the extra space around the solar cells was masked with tape for testing. The solar cells used are the highest efficiency solar cells available in market. The test results show that even for high efficiency solar cells the output power and efficiency drop substantially at high operating temperatures. As the solar cells are cooled the efficiencies increases. The test data in

Table 5.10 and Figure 5-24 shows that at cooling water flow rate of 12.37 liters per hour the electrical efficiency increases to 16.9% from 16.01% without cooling. An increase of 0.89% (8.8% over uncooled) in electrical efficiency and additional 57.38% thermal efficiency is good achievement. At this flow rate the output water gains 2.8°C temperature. The electrical and thermal efficiency obtained is good considering the fact that cooling plate is not glued to the back of BIPV-T module. The outlet water temperature of 32.3°C is obtained in single pass cooling which is additional thermal energy as compared to uncooled BIPV-T modules. This enhances the overall efficiency of BIPV-T system.

One of the main objectives of the novel cooling pipe configuration was to achieve uniform cell temperature in a PV module. In this case the uniformity is shown in Table 5.14. At highest flow rate the temperature difference between highest to lowest cell temperature is 1.3°C where as for lowest cooling water flow the difference increases to 4.2°C. Considering that copper plate attached to cooling water pipe is not pasted to the back of PV module this temperature uniformity is satisfactory. It is expected to achieve much better uniformity if cooling plate is laminated to the back of PV module.

5.8 Conclusion

5.8.1 First BIPV-T prototype with novel cooling pipe configuration

A BIPV-T module with novel water-cooling pipe configuration performs well. It improves electrical performance of BIPV-T module and delivers extra thermal energy thereby increasing overall efficiency of BIPV-T module. The water output temperature reaches 37°C at low flow rates which is good for space heating. To improve electrical performance flow rate can be increased and a booster thermal panel can be used for pre-heat water from BIPV-T module for higher temperature. Also, this BIPV-T uses very low insulation of 50mm, 6.7R whereas most other PV-T and BIPV-T

modules use 100mm thick glass wool insulation that causes module temperature to increase. So far none of the publications has shown individual cell temperature in a PV-T or BIPV-T modules. One reference [10] has shows highest and lowest temperature of PV-T module (non uniform module temperature) is indicated as 10°C while another study [23] shows cell temperature difference of 32°C. The cell uniformity in BIPV-T module with novel cooling pipe layout shows only 6.1°C as presented in Table 5.8.

5.8.2 Second improved BIPV-T with novel cooling pipe configuration

The improved design using new method of fabricating low height, high conductivity design for novel cooling pipe for cooling individual solar cells is successful. The bracing of the cooling pipe to copper plate improved the heat transfer between by a factor of 35 as compared to conductive adhesive. Since the copper plate is very thin only low temperature bracing was possible for which Sn/Ag alloy was used for bracing. Even at low bracing temperature the copper plate developed waviness which cause non uniform contact at the back of PV module. Instead of bracing ultrasonic welding will prevent waviness and improve the heat transfer further due to copper to copper contact. Inspite of imperfections the electrical efficiency in 2nd prototype is much better than 1st prototype.

Another significant achievement in improved fabrication technique is in the cost reduction in which dropped from Cad$ 2,500 /m^2 from 1st prototype to Cad$ 400/m^2 for the second one.

Further reduced height of cooling pipe provides flexibility of laminating the cooling pipe at the back of PV module under vacuum to improve thermal contact with copper plate. By making positive contact at the back of PV module instead of allowing air gap will improve the performance further.

5.9 References

[1] Y. Hu, W. Cao, J. Ma, S. J. Finney, and D. Li, "Identifying PV module mismatch faults by a thermography-based temperature distribution analysis," *IEEE Transactions on Device and Materials Reliability,* vol. 14, no. 4, pp. 951-960, 2014.

[2] D. C. Jordan, T. J. Silverman, B. Sekulic, and S. R. Kurtz, "PV degradation curves: non-linearities and failure modes," *Progress in Photovoltaics: Research and Applications,* vol. 25, no. 7, pp. 583-591, 2017.

[3] P. Manganiello, M. Balato, and M. Vitelli, "A survey on mismatching and aging of PV modules: The closed loop," *IEEE Transactions on Industrial Electronics*, vol. 62, no. 11, pp. 7276-7286, 2015.

[4] M. Rosa-Clot, P. Rosa-Clot, and G. M. Tina, "TESPI: thermal electric solar panel integration," *Solar Energy*, vol. 85, no. 10, pp. 2433-2442, 2011.

[5] K. Wilson, D. D. Ceuster, and R. A. Sinton, "Measuring the effect of cell mismatch on module output," *2006 IEEE 4th World Conference on Photovoltaic Energy Conference*, vol. 1, pp. 916-919, 2006.

[6] M. K. Fuentes, "A simplified thermal model for flat-plate photovoltaic arrays," Sandia National Labs., Albuquerque, NM (USA), 1987.

[7] J. W. Stultz, "Thermal and other tests of photovoltaic modules performed in natural sunlight," *Journal of Energy*, vol. 3, no. 6, pp. 363-372, 1979.

[8] T. Matuska, "Theoretical analysis of solar unglazed hybrid photovoltaic-thermal liquid collector," in *Proceedings of the Eurosun*, 2010.

[9] H. A. Zondag and W. G. J. V. Helden, "Stagnation temperature in PVT collectors," *PV in Europe, Rome (Italy)*, 2002.

[10] I. L. Alboteanu, C. F. Ocoleanu, and C. A. Bulucea, "Cooling system for photovoltaic module," *Recent Researches in Enviromental and Geolegical Sciences*, pp. 133-138, 2012.

[11] K. Touafek, M. Haddadi, and A. Malek, "Experimental study on a new hybrid photovoltaic thermal collector," *Applied solar energy*, vol. 45, no. 3, p. 181, 2009.

[12] K. A. Moharram, M. Abd-Elhady, H. Kandil, and H. El-Sherif, "Enhancing the performance of photovoltaic panels by water cooling," *Ain Shams Engineering Journal*, vol. 4, no. 4, pp. 869-877, 2013.

[13] K. Sopian, G. L. Jin, M. Y. Othman, S. H. Zaidi, and M. H. Ruslan, "Advanced absorber design for photovoltaic thermal (PV/T) Collectors," *Recent Researches in Energy, Environment, and Landscape Architecture*, 2011.

[14] K. Toufek, M. Haddadi, and A. Mk, "Experimental comparison of two configurations of hybrid photovoltaic thermal collectors," *Applied Solar Energy*, vol. 47, no. 3, pp. 189-194, 2011.

[15] M. Bakker, H. Zondag, and W. Van Helden, *Design of a dual flow photovoltaic/thermal combipanel*. Stan Ackermans Institute, 2002.

[16] M. Bosanac, B. Sorensen, K. Ivan, H. Sorensen, N. Bruno, and B. Jamal, "Photovoltaic/thermal solar collectors and their potential in Denmark," *Final Report, EFP Project, www. solenergi. dk/rapporter/pvtpotentialindenmark. pdf*, 2003.

[17] M. Y. Othman, A. Ibrahim, G. L. Jin, M. H. Ruslan, and K. Sopian, "Photovoltaic-thermal (PV/T) technology–the future energy technology," *Renewable Energy*, vol. 49, pp. 171-174, 2013.

[18] P. Dupeyrat, C. Ménézo, M. Rommel, and H.-M. Henning, "Efficient single glazed flat plate photovoltaic–thermal hybrid collector for domestic hot water system," *Solar Energy*, vol. 85, no. 7, pp. 1457-1468, 2011.

[19] R. Hosseini, N. Hosseini, and H. Khorasanizadeh, "An experimental study of combining a photovoltaic system with a heating system," in *World Renewable Energy Congress-Sweden; 8-13 May; 2011; Linköping; Sweden*, 2011, no. 057: Linköping University Electronic Press, pp. 2993-3000.

[20] T. T. Chow, "A review on photovoltaic/thermal hybrid solar technology," *Applied energy*, vol. 87, no. 2, pp. 365-379, 2010.

[21] A. Ibrahim *et al.*, "Performance of photovoltaic thermal collector (PVT) with different absorbers design," *WSEAS Transactions on Environment and Development*, vol. 5, no. 3, pp. 321-330, 2009.

[22] A. Popescu, C.-E. Panaite, and O.-V. Stadoleanu, "Combined Photovoltaic and Thermal Solar Panels-Enhanced Energy Conversion and Heat Transfer," *Termotehnica Supliment*, vol. 1, 2013.

[23] L. Brottier, J.-M. Hugo, and R. Bennacer, "An innovative PV-T collector: CFD and experimental results," vol. Research Gate, 2014.

[24] Stine, W. B., and G. Michael, "Power from the Sun," ed, 2001.

[25] D. Y. Goswami, F. Kreith, and J. F. Kreider, *Principles of solar engineering*. CRC Press, 2000.

[26] J. A. Duffie and W. A. Beckman, *Solar engineering of thermal processes*. John Wiley & Sons, 2013.

[27] "Best Research-Cell Efficiency Chart." NREL. https://www.nrel.gov/pv/cell-efficiency.html (accessed 2018).

CHAPTER 6 GENERAL DISCUSSION

The commercial production of photovoltaic cells and modules began about 4 decades ago. During this period many technologies were developed and tried but the crystalline technology remains to be the most popular. Even today crystalline technology occupies 95% of the production and sale worldwide. The theoretical maximum efficiency of crystalline solar cells stands at 30%. However, the efficiency of solar cells has increased at very low pace. Currently commercially available solar cells have reached between 20-22% under standard test conditions (STC). The efficiency of solar module ranges between 18-20% depending on the packing density. Another reason for drop in efficiency is caused by higher operating temperatures in field installation. The higher operating temperatures causes drop in power by 0.44% /°C.

The solar module rating is specified at standard test condition of 1000W/m^2, 25°C cell temperature and air mass 1.5. The rated test conditions are rarely achieved in field installations. The operating temperature of solar module usually reaches 47°C at 800W/m^2 and described as Normal Operating Cell Temperature (NOCT). In one field study conducted in 1978 shows that when solar modules are flushed with roof of the building the operating temperature rises by additional 18-20°C due to impeded cooling from the back of solar modules. By water cooling the solar module, an increase in efficiency was observed.

Over the years, researchers have proposed various water-cooling methods to improve the efficiency of solar modules. The water-cooling circuits like tube in sheet, direct flow, spiral flow, oscillatory flow, parallel serpentine flow, web flow, modified serpentine parallel flow, cavity flow, double pass top and bottom flow, drip flow over module glass etc. have been proposed and studied. All these water-cooling circuit are designed with the intention of reducing the operating temperature of solar module and increasing overall efficiency by recovering heat in cooling water. None of these designs addressed the requirement of cooling solar cells uniformly in a solar module. The PV industry makes serious effort to prevent mismatching of solar cells in a solar module. The cells operating at different temperature will result in different current outputs causing mismatching.

Some designs PV-T module use thick back insulation and a glazing on top to increase temperature of cooling water. The tests presented shows that stagnation temperature without glazing reaches 110°C and with glazing reaches 135°C. These designs have not considered that ethylene vinyl

acetate (EVA) encapsulate used for attaching the solar cells and backsheet to glass is cured at 120°C. This can cause damage to the module if the cooling of module accidently stops in bright sunlight. In addition, the solar modules as per IEC61215, IEC61730 and UL1703 are tested and certified to operate at a maximum of 85°C. The accelerated life test conducted in accordance with these test standards ensure the solar module will have long service life. All manufacturers offer 25-year product and power output warranty. The non-uniformity in cooling the solar cells on the other hand will result in much higher temperature difference in solar cells temperature within a solar module and strings of solar module. This will result in overheating of some solar cells that can result in premature failure of solar module.

Novel cooling pipe configuration for uniform cooling developed in this research work may be applied to other than BIPV-T applications.

CHAPTER 7 CONCLUSION AND RECOMMENDATIONS

7.1 Conclusion

This research work was undertaken to address the shortcoming of various water cooled BIPV-T modules proposed by other researchers. It was important to look at the design flaws in BIPV-T module (which is also applicable to PV-T modules) as a PV industry and design a novel cooling configuration to overcome the shortcomings. The basic approach in the past designs of BIPV-T modules (and PV-T module) have been to improve overall efficiency of modules by extracting heat in cooling fluid but not the detrimental effect of non-uniform cooling.

There is no doubt that overall efficiency of BIPV-T module improves considerably by combining both electrical and thermal efficiencies. But the most significant achievement of this research was to come out with a novel idea of cooling pipe configuration that will ensure uniform cooling of every solar cells in a solar module. The TRNSYS simulation reveals that cooling individual solar cells uniformly will improve the electrical efficiency of solar module at the same time heat collected in the form of hot water will increases overall efficiency.

It has taken nearly 40 years for commercially produced monocrystalline module efficiency to reach 20 - 22% commercial efficiency. This increase is mere 0.25% per year for mono crystalline technology and even lower for polycrystalline cells. Therefore, any fraction increase in efficiency by uniform cooling is an achievement.

Another important aspect of uniform cooling concept is related to PV industry. The photovoltaic industry makes effort in matching the current output of solar cells to make a module to prevent mismatching. The modern solar cell sorting machines can grade the solar cells within 10mA output. This is equivalent of temperature variation of only 2.1°C. In addition, photovoltaic industry uses EL testers to check mismatching of solar cells in production. The mismatching cause delamination due to localized heating and degrading in solar cell output. The PV industry brand it as grade C.

Therefore, it is important that BIPV-T or PV-T modules use uniform cooling of individual cells to ensure current mismatching does not occur.

A BIPV-T module with novel water-cooling pipe configuration was found to perform well. Considering that it was made with limited facility it provides uniform temperature of solar cells within 6.1°C and meets the objective of novel design. If we compare to other non-uniformly cooled designs, it operates at 4°C lower or better in uniformity.

The improved smaller model with better thermal contact for cooling individual solar cells improved the uniformity in cooling further to 4.2°C. The price of fabrication of novel low height cooling pipe configuration dropped by a factor of 6. The thermal efficiency increased by 5% due to better thermal contact between tube and fin.

7.2 Recommendations

The prototype BIPV-T is now ready for commercialization. With better production facility following recommendations may be adopted to improve the performance:

1. Use ultrasonic welding for attaching copper cooling pipe to the copper plate. Alternatively, low temperature bracing may be used;
2. Use low height design to assemble copper pipe as explained in paper 3;
3. Laminate the plate and tube at the back of the PV module to ensure uniform contact of copper plate with solar cells;
4. This study was restricted to developing and testing only the BIPV-T module. Further study can be conducted by making large BIPV-T module and make a complete system for field testing;
5. Look for partners who may be willing to commercialize the BIPV-T module with novel uniform cooling system.

BIBLIOGRAPHY

[1] J. W. Stultz, "Thermal and other tests of photovoltaic modules performed in natural sunlight," *Journal of Energy,* vol. 3, no. 6, pp. 363-372, 1979.

[2] M. K. Fuentes, "A simplified thermal model for flat-plate photovoltaic arrays," Sandia National Labs., Albuquerque, NM (USA), 1987.

[3] M. Bakker, H. Zondag, and W. Van Helden, *Design of a dual flow photovoltaic/thermal combipanel*. Stan Ackermans Institute, 2002.

[4] H. A. Zondag, D. d. de Vries, W. Van Helden, R. C. van Zolingen, and A. Van Steenhoven, "The thermal and electrical yield of a PV-thermal collector," *Solar energy,* vol. 72, no. 2, pp. 113-128, 2002.

[5] M. Bosanac, B. Sorensen, K. Ivan, H. Sorensen, N. Bruno, and B. Jamal, "Photovoltaic/thermal solar collectors and their potential in Denmark," *Final Report, EFP Project, www. solenergi. dk/rapporter/PV-Tpotentialindenmark. pdf,* 2003.

[6] P. Charalambous, G. G. Maidment, S. A. Kalogirou, and K. Yiakoumetti, "Photovoltaic thermal (PV-T) collectors: A review," *Applied thermal engineering,* vol. 27, no. 2-3, pp. 275-286, 2007.

[7] A. H. Fanney, M. W. Davis, B. P. Dougherty, D. L. King, W. E. Boyson, and J. A. Kratochvil, "Comparison of photovoltaic module performance measurements," *Journal of solar energy engineering,* vol. 128, no. 2, pp. 152-159, 2006.

[8] I. Katic, "Measurement Report-Test of PV-T Module ‘‘PV-Twin”," Danish Technological Institute, 2006.

[9] Y. Tripanagnostopoulos, "Aspects and improvements of hybrid photovoltaic/thermal solar energy systems," *Solar energy,* vol. 81, no. 9, pp. 1117-1131, 2007.

[10] T. N. Anderson and M. Duke, "Analysis of a photovoltaic/thermal solar collector for building integration," in *SB07 NZ Conference-Transforming our built environment*, 2007.

[11] K. Touafek, M. Haddadi, and A. Malek, "Experimental study on a new hybrid photovoltaic thermal collector," *Applied solar energy,* vol. 45, no. 3, p. 181, 2009.

[12] T. T. Chow, "A review on photovoltaic/thermal hybrid solar technology," *Applied energy,* vol. 87, no. 2, pp. 365-379, 2010.

[13] P. Hofmann, P. Dupeyrat, K. Kramer, M. Hermann, and G. Stryi-Hipp, "Measurements and Benchmark of PV-T collectors according to EN12975 and development of a standardized measurement procedure," in *Proceedings EuroSun*, 2010, pp. 28.9-1.10.

[14] K. Sopian, G. L. Jin, M. Y. Othman, S. H. Zaidi, and M. H. Ruslan, "Advanced absorber design for photovoltaic thermal (PV-T) Collectors," *Recent Researches in Energy, Environment, and Landscape Architecture,* 2011.

[15] C. S. P. López, L. Tenconi, F. L. Castro, S. Brambilasca, and A. Virtuani, "Testing of a cost-effective photovoltaic thermal hybrid solar collector prototype," in *2012 38th IEEE Photovoltaic Specialists Conference*, 2012: IEEE, pp. 000479-000484.

[16] P. Dupeyrat, C. Ménézo, M. Rommel, and H.-M. Henning, "Efficient single glazed flat plate photovoltaic–thermal hybrid collector for domestic hot water system," *Solar Energy*, vol. 85, no. 7, pp. 1457-1468, 2011.

[17] R. Hosseini, N. Hosseini, and H. Khorasanizadeh, "An experimental study of combining a photovoltaic system with a heating system," in *World Renewable Energy Congress-Sweden; 8-13 May; 2011; Linköping; Sweden*, 2011, no. 057: Linköping University Electronic Press, pp. 2993-3000.

[18] "Test Report M1.11.NRG.0319/43724: Volther Powertherm," Eurofins, Italy, 2011.

[19] "Hybrid PV-Thermal Data Sheet," ed: Solimpeks, 2013.

[20] "Test Report M1.11.NRG.0320/43724: Volther Powervolt," Eurofins, Italy, August 2011.

[21] T. Matuska, "Theoretical analysis of solar unglazed hybrid photovoltaic-thermal liquid collector," in *Proceedings of the Eurosun*, 2010.

[22] J. A. Duffie and W. A. Beckman, *Solar engineering of thermal processes*. John Wiley & Sons, 2013.

[23] "Test Report 20131127-DUALSUN-RAP-05: DualSun 250M," Eliosys, 2013. [Online]. Available: www.eliosys.eu/assets/SOLAIRE-2G_id20131127.pdf

[24] G. L. Jin, M. Yusof, H. Othman, H. Ruslan, and K. Sopian, "Photovoltaic Thermal (PV-T) Water Collector Experiment Study," in *Proc. 7th Int. Conf. Renew. Energy Sources*, 2013, pp. 117-124.

[25] A. Popescu, C.-E. Panaite, and O.-V. Stadoleanu, "Combined Photovoltaic and Thermal Solar Panels-Enhanced Energy Conversion and Heat Transfer," *Termotehnica Supliment*, vol. 1, 2013.

[26] S. Dittmann, T. Friesen, F. Frontini, A. Bohren, D. Zenhäusern, and M. Rommel, "Indoor and Outdoor Testing of an Unglazed PV-T Collector," *EU PVSEC*, 2014.

[27] "Test Report 21222892_E: DualSun 250M," TUV Reinland Energie und Umwelt GmbH, November 2013.

[28] L. Brottier, J.-M. Hugo, and R. Bennacer, "An innovative PV-T collector: CFD and experimental results," vol. Research Gate, 2014.

[29] Y. Hu, W. Cao, J. Ma, S. J. Finney, and D. Li, "Identifying PV module mismatch faults by a thermography-based temperature distribution analysis," *IEEE Transactions on Device and Materials Reliability*, vol. 14, no. 4, pp. 951-960, 2014.

[30] A. Ibrahim *et al.*, "Performance of photovoltaic thermal collector (PV-T) with different absorbers design," *WSEAS Transactions on Environment and Development*, vol. 5, no. 3, pp. 321-330, 2009.

[31] I. L. Alboteanu, C. F. Ocoleanu, and C. A. Bulucea, "Cooling system for photovoltaic module," *Recent Researches in Enviromental and Geolegical Sciences*, pp. 133-138, 2012.

[32] A. Fudholi, K. Sopian, M. H. Yazdi, M. H. Ruslan, A. Ibrahim, and H. A. Kazem, "Performance analysis of photovoltaic thermal (PV-T) water collectors," *Energy conversion and management*, vol. 78, pp. 641-651, 2014.

[33] J. Allan, Z. Dehouche, S. Stankovic, and L. Mauricette, "Performance testing of thermal and photovoltaic thermal solar collectors," *Energy Science & Engineering*, vol. 3, no. 4, pp. 310-326, 2015.

[34] A. Buonomano, F. Calise, and M. Vicidomini, "Design, simulation and experimental investigation of a solar system based on PV panels and PV-T collectors," *Energies*, vol. 9, no. 7, p. 497, 2016.

[35] L. Lu, X. Wang, S. Wang, and X. Liu, "A new concept of hybrid photovoltaic thermal (PV-T) collector with natural circulation," *Heat and Mass Transfer*, vol. 53, no. 7, pp. 2331-2339, 2017.

[36] "Best Research-Cell Efficiency Chart." NREL. https://www.nrel.gov/pv/cell-efficiency.html (accessed 2018).

[37] D. Y. Goswami, F. Kreith, and J. F. Kreider, *Principles of solar engineering*. CRC Press, 2000.

[38] Stine, W. B., and G. Michael, "Power from the Sun," ed, 2001.

[39] K. Touafek, M. Haddadi, and A. Mk, "Experimental comparison of two configurations of hybrid photovoltaic thermal collectors," *Applied Solar Energy*, vol. 47, no. 3, pp. 189-194, 2011.

[40] D. A. Redpath, H. Singh, C. Tierney, and P. Dalzell, "An experimental comparison of two solar photovoltaic-thermal (PV-T) energy conversion systems for production of heat and power," *Energy and Power*, vol. 2, no. 4, pp. 46-50, 2012.

[41] C.-Y. Huang, H.-C. Sung, and K.-L. Yen, "Experimental study of photovoltaic/thermal (PV-T) hybrid system," *Int. J. Smart Grid Clean Energy*, vol. 2, no. 2, pp. 147-151, 2013.

[42] V. Tyagi, S. Kaushik, and S. Tyagi, "Advancement in solar photovoltaic/thermal (PV-T) hybrid collector technology," *Renewable and Sustainable Energy Reviews*, vol. 16, no. 3, pp. 1383-1398, 2012.

[43] H. Zondag, D. De Vries, W. Van Helden, R. Van Zolingen, and A. Van Steenhoven, "The yield of different combined PV-thermal collector designs," *Solar energy*, vol. 74, no. 3, pp. 253-269, 2003.

[44] K. A. Moharram, M. Abd-Elhady, H. Kandil, and H. El-Sherif, "Enhancing the performance of photovoltaic panels by water cooling," *Ain Shams Engineering Journal*, vol. 4, no. 4, pp. 869-877, 2013.

[45] A. Ibrahim *et al.*, "Hybrid Photovoltaic Thermal (PV-T) Air and Water Based Solar Collectors Suitable for Building Integrated Applications " *American Journal of Environmental Sciences,* vol. 5, no. 5, pp. 618-624, 2009.

APPENDIX A SORTING OF SOLAR CELLS

The photovoltaic solar cell manufacturers sort the solar cells in different grades based on the its current output. The Table 8.2 shows solar cells grades are separated by only 10mA current output.

Table 7-1 Electrical performance of graded solar cells (Ref.: Tongwei Solar Datasheet 2017)

S.N.	Efficiency Code	Efficiency %	Pmp (W)	Umpp (V)	Impp (A)	Uoc (V)	Isc(A)
1	TW-156.75P-187	≥18.70%	4.55	0.542	8.399	0.639	8.881
2	TW-156.75P-186	18.60%	4.52	0.540	8.389	0.638	8.876
3	TW-156.75P-185	18.50%	4.49	0.539	8.372	0.637	8.859
4	TW-156.75P-184	18.40%	4.47	0.538	8.347	0.636	8.834
5	TW-156.75P-183	18.30%	4.45	0.536	8.327	0.634	8.813
6	TW-156.75P-182	18.20%	4.43	0.535	8.306	0.633	8.795
7	TW-156.75P-181	18.10%	4.4	0.533	8.284	0.632	8.781
8	TW-156.75P-179	18.00%	4.38	0.532	8.261	0.630	8.770
9	TW-156.75P-195	17.90%	4.36	0.531	8.236	0.629	8.762
Measured at STC (Standard Test Conditions): 1000W/m^2, AM1.5, 25°C							
Temperature Coefficients: Uoc(%/K) = -0.36; Isc(%/K) =+0.06; Pmax(%/K) = -0.36							

Table 7-2 Solar cells grading and equivalent temperature manufactured by TW Solar

S.N.	Impp	Current Difference		Equivalent in Temperature
	A	mA		℃
1.	8.399	-	-	-
2.	8.389	10	mA	1.96
3.	8.372	17	mA	3.33
4.	8.347	25	mA	4.89
5.	8.327	20	mA	3.92
6.	8.306	21	mA	4.11
7.	8.284	22	mA	4.31
8.	8.261	23	mA	4.50
9.	8.239	22	mA	4.31

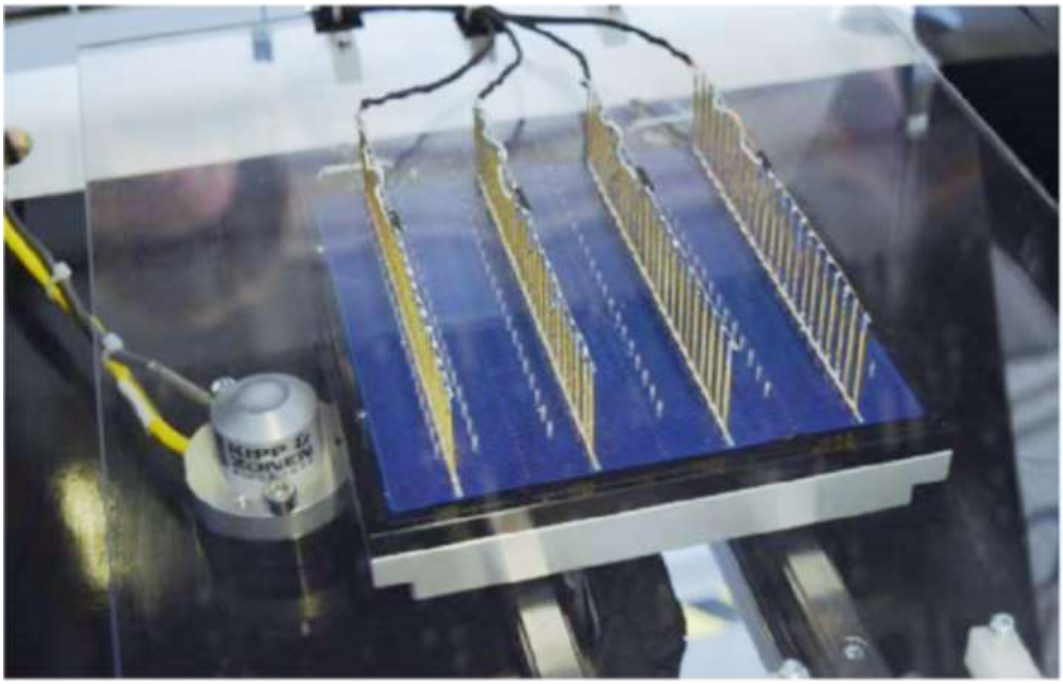

Figure 7-1 Solar cells testing and sorting based on ampere output

Figure 7-2 Automatic solar cells sorting machine

APPENDIX B ELECTRO-LUMINESCENCE (EL) TESTER

EL tester is used to detect following defect in production to prevent mismatching of solar cells in a photovoltaic module:

- Insufficient contact between connecting ribbon and solar cells due to poor soldering
- Show hidden crack in black spot not visible to naked eye
- Current output different due to mix up of two different grades of solar cells
- Process defects (broken grating line, sintering cob webbing, pollution of cells by solder flux etc.)

Figure 7-3 Electro-luminescence tester

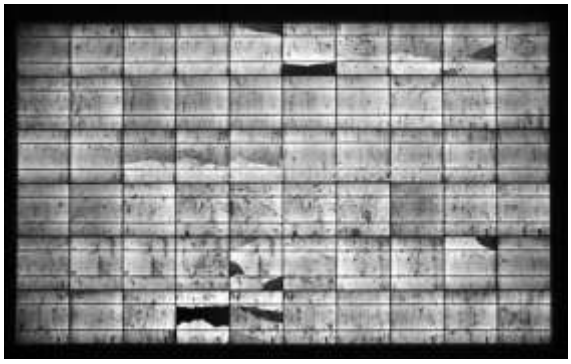

Figure 7-4: Bad solar module

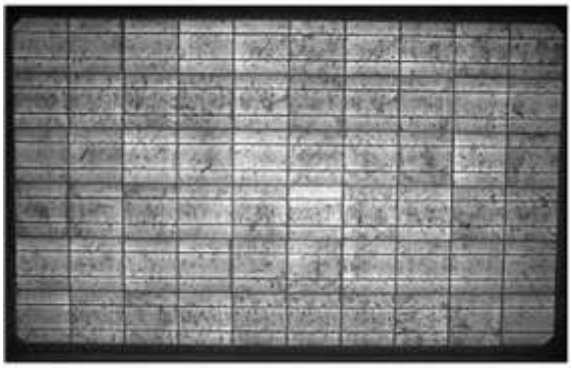

Figure 7-5 Good solar module

APPENDIX C DRONES FOR DETECTING DEFECTIVE SOLAR MODULES

For large solar farms, malfunctioning due to various reasons including mismatching of solar cells and modules are conducted by drones. Described below is information published in solar industry magazine.

REF: Drones fly over 13 million solar modules to discover what affects production: Posted by Betsy Lillian - January 24, 2019.

https://solarindustrymag.com/drones-fly-over-13-million-solar-modules-to-discover-what-affects-production/?utm_medium=email&utm_source=LNH+01-25-2019&utm_campaign=SI+Latest+News+Headlines

Raptor Maps, a Boston-based provider of aerial thermography software, has released a report outlining factors affecting solar production. The company leveraged its data repository of digital photovoltaic systems to query nearly 2,900 MW across 18 countries to help system owners and operators benchmark and improve their portfolios.

The study encompassed 13 million modules across 300 PV systems and showed that, on average, 1.7% of production is affected in some way. Classifications included in the study include equipment (e.g., inverter, combiner and tracker), environmental (e.g., shadowing and soiling), and module-level findings (e.g., cracking, delamination and activated bypass diodes).

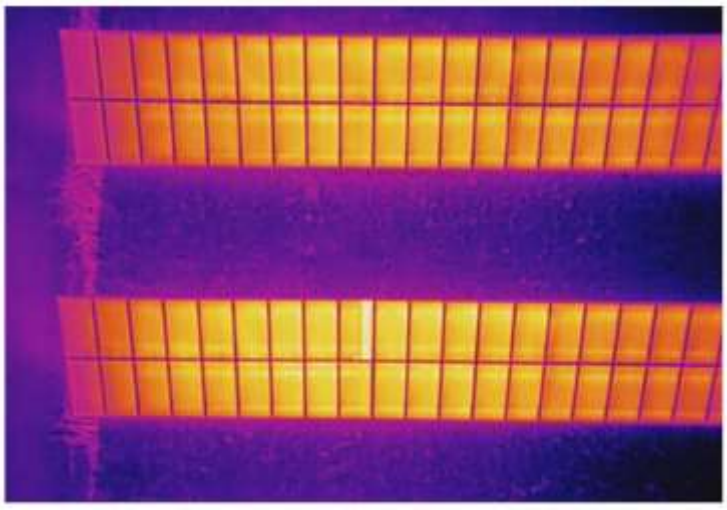

Figure 7-6 Thermography by Drone for large photovoltaic installation

This study encompassed a total of 12,945,747 modules across 292 PV systems with a total nominal capacity of 2,882 MW. Sites ranged from 10 kW to 300 MW across 18 countries and six continents. In total, 276,954 modules contained findings (2.1% of total analyzed), with an affected power of 50.27 MW (1.7% of total analyzed).

Analysis:

The cracking, delamination and activated diodes are mainly result of mismatching of solar cells in a string of solar modules. This is detected by infrared camera fitted on drones.

Taking a conservative approach lets presume solar modules operate for 4 hours of peak sunshine every day. Then 50.27MW is equal to 201,080 kWh per day or loss of US$20,108 per day based on 10 cents/kWh power purchase agreement.

Approximately 40% of this loss is due to mismatching either directly or indirectly.